



National Library  
of Canada

Bibliothèque nationale  
du Canada

Canadian Theses Service

Services des thèses canadiennes

Ottawa, Canada  
K1A 0N4

## CANADIAN THESES

## THÈSES CANADIENNES

### NOTICE

The quality of this microfiche is heavily dependent upon the quality of the original thesis submitted for microfilming. Every effort has been made to ensure the highest quality of reproduction possible.

If pages are missing, contact the university which granted the degree.

Some pages may have indistinct print especially if the original pages were typed with a poor typewriter ribbon or if the university sent us an inferior photocopy.

Previously copyrighted materials (journal articles, published tests, etc.) are not filmed.

Reproduction in full or in part of this film is governed by the Canadian Copyright Act, R.S.C. 1970, c. C-30.

**THIS DISSERTATION  
HAS BEEN MICROFILMED  
EXACTLY AS RECEIVED**

### AVIS

La qualité de cette microfiche dépend grandement de la qualité de la thèse soumise au microfilmage. Nous avons tout fait pour assurer une qualité supérieure de reproduction.

S'il manque des pages, veuillez communiquer avec l'université qui a conféré le grade.

La qualité d'impression de certaines pages peut laisser à désirer, surtout si les pages originales ont été dactylographiées à l'aide d'un ruban usé ou si l'université nous a fait parvenir une photocopie de qualité inférieure.

Les documents qui font déjà l'objet d'un droit d'auteur (articles de revue, examens publiés, etc.) ne sont pas microfilmés.

La reproduction, même partielle, de ce microfilm est soumise à la Loi canadienne sur le droit d'auteur, SRC 1970, c. C-30.

**LA THÈSE A ÉTÉ  
MICROFILMÉE TELLE QUE  
NOUS L'AVONS REÇUE**

THE UNIVERSITY OF ALBERTA

A NEW FAILURE CRITERION FOR FIBRE-REINFORCED COMPOSITE LAMINAE

BY



Pierre LABOSSIERE

A THESIS

SUBMITTED TO THE FACULTY OF GRADUATE STUDIES AND RESEARCH  
IN PARTIAL FULFILMENT OF THE REQUIREMENTS FOR THE DEGREE  
OF DOCTOR OF PHILOSOPHY

DEPARTMENT OF MECHANICAL ENGINEERING

EDMONTON, ALBERTA

SPRING 1987

Permission has been granted to the National Library of Canada to microfilm this thesis and to lend or sell copies of the film.

The author (copyright owner) has reserved other publication rights, and neither the thesis nor extensive extracts from it may be printed or otherwise reproduced without his/her written permission.

L'autorisation a été accordée à la Bibliothèque nationale du Canada de microfilmer cette thèse et de prêter ou de vendre des exemplaires du film.

L'auteur (titulaire du droit d'auteur) se réserve les autres droits de publication; ni la thèse ni de longs extraits de celle-ci ne doivent être imprimés ou autrement reproduits sans son autorisation écrite.

ISBN 0-315-37649-X

THE UNIVERSITY OF ALBERTA

RELEASE FORM

NAME OF AUTHOR: Pierre LABOSSIÈRE

TITLE OF THESIS: A NEW FAILURE CRITERION FOR FIBRE-REINFORCED  
COMPOSITE LAMINAE

DEGREE: Doctor of Philosophy

YEAR THIS DEGREE GRANTED: 1987

Permission is hereby granted to THE UNIVERSITY OF  
ALBERTA LIBRARY to reproduce single copies of this thesis  
and to lend or sell such copies for private, scholarly  
or scientific research purposes only.

The author reserves other publication rights, and  
neither the thesis nor extensive extracts from it may  
be printed or otherwise reproduced without the author's  
written permission.

...*Pierre Labossière*.....

2205 Pagé  
ST. HYACINTHE (Québec)  
J2S 4C8

November 13, 1986



THE UNIVERSITY OF ALBERTA

FACULTY OF GRADUATE STUDIES

The undersigned certify that they have read, and  
recommend to the Faculty of Graduate Studies and Research  
for acceptance, a thesis entitled

A NEW FAILURE CRITERION FOR FIBRE-REINFORCED COMPOSITE LAMINAE

submitted by Pierre LABOSSIERE in partial fulfilment of the  
requirements for the degree of Doctor of Philosophy.

.....  
(Supervisor)

.....  
.....  
.....  
.....  
.....  
(External Examiner)

November 13, 1986

## ABSTRACT

During the last twenty years, our world has undergone considerable transformations; this is especially evident in the areas of transportation and communications. Now, one has easy access to other places in the world, and we have almost reached the "global village" predicted by MacLuhan. Of course, this has only been possible because of the developments of new technologies.

One area where great progress has been made is that of materials science, with the production of new alloys and the introduction of advanced composite materials. Fibre-reinforced composite materials are discussed in this thesis. These are obtained by combining materials with different properties in an original way. The resulting composites often have properties combining those of their constituents. For example, this technique may be used to create a new material with high strength-to-weight ratio.

The analysis of composite materials is a wide and complex matter and one aspect that has attracted researchers is the prediction of their behaviour under multiaxial stress states. Analytical functions known as failure criteria are used to predict the composite's strength under any in-plane loading condition. There are now many failure theories and most of these are generalizations of yield theories for ductile materials. Among all existing theories, the "tensor polynomial criterion" is now the most widely discussed. However, its development seems to have reached a plateau in the recent years, and the need for a new approach to this problem will be identified here.

Similar problems had been faced previously in the area of plasticity and recently, the use of parametric equations was advocated as a means to describe the yield surfaces for ductile materials. It will be hypothesized in this thesis that, following the same rationale as for the other failure theories, this parametric approach can be generalized to write failure criteria for composite materials under plane stress loading conditions. The flexibility of this new approach will be demonstrated by writing parametric failure equations for various materials, for which experimental results have been published in the literature.

## ACKNOWLEDGEMENTS

This thesis was produced under the direction of Dr. Kenneth W. Neale. I wish to thank him gratefully for the help and guidance that he provided during the last three years. This work was initiated during Dr. Neale's short stay at the University of Alberta. Following his departure to the Université de Sherbrooke, contacts were maintained via mail, long distance calls and occasional visits. The complementary direction of Dr. Fernand Ellyin was particularly helpful during this period and is gratefully acknowledged.

Mrs. Lise Dutrisac typed the manuscript and her patience and meticulous work is also gratefully acknowledged.

Enfin, un merci spécial à ma famille: Fabienne, Jean-Marc et France Labossière, pour leurs encouragements constants.

This work was supported by the Natural Sciences and Engineering Research Council of Canada, as well as the Government of Québec (Programme FCAR).

# TABLE OF CONTENTS

CHAPTER	PAGE
1. INTRODUCTION . . . . .	1
2. ANALYTICAL FORMULATIONS . . . . .	11
2.1 Introduction . . . . .	12
2.2 Equations of Elasticity . . . . .	12
2.3 Classical Lamination Theory . . . . .	15
2.4 Progressive Damage Accumulation . . . . .	17
2.5 Conclusion . . . . .	19
3. A REVIEW OF MACROSCOPIC FAILURE CRITERIA FOR FIBRE-REINFORCED COMPOSITE MATERIALS . . . . .	24
3.1 Introduction . . . . .	25
3.2 A Review of Failure Criteria for Isotropic Materials . . . . .	27
3.3 Maximum Stress and Maximum Strain Criteria . . . . .	30
3.4 Hill-Type Criteria . . . . .	31
3.5 Tensor Polynomial Criteria . . . . .	40
3.6 Failure Mode Identification . . . . .	47
3.7 Failure Criteria for Laminates . . . . .	51
3.8 Non-Linear Laminate Analysis . . . . .	53
3.9 Experimental Correlations . . . . .	54
3.9.1 Off-Axis Tests . . . . .	55
3.9.2 Biaxial Tests . . . . .	58
3.9.3 Failure Mode Identification . . . . .	62
3.9.4 Laminate Tests . . . . .	63
3.10 Conclusion . . . . .	65

4.	A NEW FAILURE CRITERION FOR FIBRE-REINFORCED MATERIALS . . .	73
4.1	Introduction . . . . .	74
4.2	Essential Characteristics of a Failure Criterion for Fibre-Reinforced Composites . . . . .	76
4.3	Budiansky's Yield Criterion . . . . .	79
4.4	A New Failure Criterion for Fibre-Reinforced Materials	82
4.5	Generality of the New Failure Surface . . . . .	84
4.6	Alternate Parametric Criteria . . . . .	86
4.6.1	Failure Criterion in Normalized Stress Space .	86
4.6.2	Failure Criteria in Cylindrical Coordinates . .	88
4.6.3	Relationships Between Spherical and Cylindrical-Parametric Criteria . . . . .	89
4.6.4	Summary . . . . .	91
4.7	Guidelines for the Use of the New Failure Criterion in Experimental Studies . . . . .	92
4.8	Conclusion . . . . .	96
5.	APPLICATIONS OF THE NEW FAILURE CRITERION . . . . .	107
5.1	Introduction . . . . .	108
5.2	Experimental-Theoretical Correlations . . . . .	109
5.3	Single Lamina Applications . . . . .	110
5.3.1	Example 1: Transversely Isotropic Graphite . .	110
a)	Material Description . . . . .	110
b)	First Solution for Example 1 . . . . .	112
c)	Second Solution for Example 1 . . . . .	113
d)	Summary of Example 1 . . . . .	116
5.3.2	Example 2: Graphite-Epoxy Fabric . . . . .	117
a)	Material Description . . . . .	117
b)	First Solution for Example 2 . . . . .	119
c)	Second Solution for Example 2 . . . . .	121
d)	Summary of Example 2 . . . . .	124
5.3.3	Example 3: Paperboard . . . . .	125
a)	Material Description . . . . .	125
b)	Parametric Failure Criterion for Example 3	128
c)	Summary of Example 3 . . . . .	131

CHAPTER	PAGE
5.4 Laminate Application: Carbon-Epoxy Laminate . . . . .	132
5.4.1 Material Description . . . . .	132
5.4.2 Parametric Failure Criterion for Example 4 . . . . .	133
5.4.3 Summary of Example 4 . . . . .	137
5.5 Conclusion . . . . .	138
6. CONCLUSION . . . . .	164
REFERENCES . . . . .	169
APPENDIX I: List of Tested Materials in the Literature . . . . .	177
APPENDIX II: Mathematical Relationships Between Budiansky's Criterion and the New Parametric Failure Criterion	179
APPENDIX III: Summary of Examples . . . . .	181
APPENDIX IV: Development of Equation (5-58) . . . . .	185

## LIST OF TABLES

Table	Description	Page
2.1	Relationships Between Tensor and Contracted Notations	20
3.1	Tests on Uniaxial Laminae	68
4.1	Angular Position of Some Experimental Tests	98
5.1	Example 1: Biaxial Stresses in Graphite	141
5.2	Example 2: Biaxial Strength of Graphite-Epoxy Fabric	142
5.3	Example 2: Normalized and Radial Data	143
5.4	Example 2: Average Radial Data for $\tau_{12} \neq 0$	145
5.5	Example 2: Experimental-Theoretical Correlation	145
5.6	Example 3: Biaxial Strength of Paperboard	146
5.7	Example 3: Error Calculation	147
5.8	Example 3: Calculation of Best-Fit for Each $\tau_{12}$ Plane	148
5.9	Example 4: Experimental Results for Carbon-Epoxy	149
5.10	Example 4: Uniaxial Tension of Angle-Ply Laminates	149



## LIST OF FIGURES

Figure		Page
1.1	Fibre-Reinforced Laminae	8
1.2	Failure Modes of Uniaxial Laminae	9
1.3	Laminate Construction	10
2.1	Lamina Orientation	21
2.2	Laminate Analysis	22
2.3	Damage Accumulation Analysis	23
3.1	Typical Hill-Type Criterion with Quadratic Terms	69
3.2	Hill-Type or Tensor Polynomial Criteria with Linear and Quadratic Terms	69
3.3	Typical Tensor Polynomial Criterion with Cubic Terms	70
3.4	Fibre Failure Identification	70
3.5	Lamina Failure Envelope	71
3.6	Off-Axis Tension Test	72
3.7	Off-Axis Shear Test	72
4.1	General Failure Envelope for Transversely Isotropic Materials	99
4.2	Shear Strength Symmetry for Unidirectional Laminae	99
4.3	Isotropic Failure Criteria	100
4.4	Budiansky's Failure Criterion	100
4.5	Parametric Failure Envelope for Fibre-Reinforced Laminae	101

## LIST OF FIGURES (CONT'D)

Figure		Page
4.6	Parametric Failure Envelope in Normalized Coordinates	102
4.7	Plane of Constant Angle $\alpha$	103
4.8	Plane of Constant Angle $\phi$	103
4.9	Parametric Failure Envelope in Cylindrical Coordinates	104
4.10	Parametric Failure Envelope in Normalized and Cylindrical Coordinates	105
4.11	Angular Position of Various Biaxial Failure Strengths	106
5.1	Experimental-Theoretical Correlation	150
5.2	Example 1: Biaxial Stresses in Graphite	151
5.3	Example 1: First Parametric Solution	152
5.4	Example 1: Second Parametric Solution	153
5.5	Example 2: Biaxial Stresses in Graphite Epoxy Fabric	154
5.6	Example 2: First Parametric Solution	155
5.7	Example 2: Second Parametric Solution	156
5.8	Example 2: Fitting of the Second Parametric Solution	157
5.9	Example 2: Additional Sections of the Second Parametric Solution	157
5.10	Example 3: Biaxial Stresses in Paperboard	158
5.11	Example 3: Fitting of the Failure Function	159
5.12	Example 3: Modified Norris Criterion	160

## LIST OF FIGURES (CONT'D)

Figure		Page
5.13	Example 4: Biaxial Stresses in Carbon-Epoxy	161
5.14	Example 4: Angle-Ply Laminate Stresses	162
5.15	Example 4: Quadratic Tensor Polynomial	163
5.16	Example 4: Parametric Failure Envelope	163

# LIST OF SYMBOLS

$A_1, A_2, \dots, A_6$	Geometric parameters of an ellipsoid's equation
$[A], [B], [D]$	Laminate's extensional, coupling, and bending stiffness matrices
$C_{ij}, C_{ijkl}$	Tensor of elastic moduli
$E$	Young's modulus for isotropic materials
$E_t$	Total error between theoretical and experimental data
$E'_t$	Total error in normalized coordinate system
$E_1, E_2$	Young's moduli of an orthotropic material in the two principal directions
$F, G, H, L, M, N$	Constants in Hill's yield criterion
$F_1, F_{1j}, F_{1jk}$	Strength parameters in the tensor polynomial theory
$G_{12}$	Shear modulus
$G_i, G_{ij}$	Strain parameters in the tensor polynomial theory
$K_1, K_2, \dots, K_6$	Strength parameters in the Hoffman, Raghava and Caddell, Marin theories
$K_1$	Parameters depending on total strain energy in the Sandhu theory
$K_{\lambda 12}$	Constant depending on material properties in the Chamis theory
$K'_{\lambda 12\alpha B}$	Theory-experiment correlation coefficient in the Chamis theory
$\{M\}$	Moments applied on the laminate
$\{N\}$	Forces applied on the laminate
$P$	On-axis equal biaxial tensile strength
$P'$	On-axis equal biaxial compressive strength
$[Q]$	Lamina stiffness matrix in material axes of symmetry

# LIST OF SYMBOLS (CONT'D)

$[\bar{Q}]$	Lamina stiffness matrix in any direction
$S$	Shear strength along the material axes of symmetry
$S_c$	Maximum shear at the center of ellipsoidal failure surface
$S_{ij}, S_{ijkl}$	Compliance tensor
$S_{\lambda 1\alpha}, S_{\lambda 2\beta}, S_{\lambda 12}$	Strength parameters in the Chamis theory
$S_T$	Transverse shear strength
$S_\theta$	Positive shear strength of a $\theta$ -degree off-axis lamina
$S'_\theta$	Negative shear strength of a $\theta$ -degree off-axis lamina
$[T]$	Stress transformation matrix
$U_\theta$	Uniaxial tensile strength of a $\theta$ -degree off-axis lamina
$U'_\theta$	Uniaxial compressive strength of a $\theta$ -degree off-axis lamina
$X$	Uniaxial tensile strength in the fibre direction
$X'$	Uniaxial compressive strength in the fibre direction
$Y$	Uniaxial tensile strength perpendicular to the fibre direction
$Y'$	Uniaxial compressive strength perpendicular to the fibre direction
$Z$	Tensile strength perpendicular to the lamina surface
$Z'$	Compressive strength perpendicular to the lamina surface
$a$	Ratio of biaxial stresses $\sigma_x/\sigma_y$
$b$	Ratio of the stresses $\sigma_x/\tau_{xy}$

# LIST OF SYMBOLS (CONT'D)

$f(\cdot), f_1(\cdot), f_2(\cdot)$	Fitting functions of the parametric failure envelope
$g(\beta)$	Parametric failure-envelope for an isotropic material
$t$	Total laminate thickness
$z$	Distance from the laminate mid-plane
$\alpha$	Angular position of the failure point with respect to the $\sigma_1$ -axis
$\alpha'$	Angular position of the failure point with respect to the $\sigma_1/X$ -axis
$\beta$	Angular position of the failure point in Budiansky's criterion
$\gamma_{12}$	Shear strain in material axes of symmetry
$\gamma'$	Interaction factor in the Wu-Scheublein theory
$\Gamma$	Function of the shear stress which controls the area of the failure envelope, in cylindrical coordinates
$\Gamma'$	Same as $\Gamma$ , in normalized coordinates system
$\{\epsilon\}$	Laminate strain
$\{\epsilon^0\}$	Laminate strain at mid-plane
$\epsilon_i$	Strain tensor in contracted notation
$\epsilon_{ij}$	Strain tensor
$\epsilon_p, \epsilon_q, \epsilon_r$	Strain in principal directions
$\epsilon_{1u}^-, \epsilon_{2u}^-, \epsilon_{1u}^+, \epsilon_{2u}^+$	Limit strain in the axes of symmetry
$\theta$	Loading angle with respect to the fibre directions
$\{\kappa\}$	Curvature of the laminate mid-plane
$\lambda, \mu, \kappa$	Power exponents in the Gol'denblat and Kopnov theory

# LIST OF SYMBOLS (CONT'D)

$\phi$	Angular position of the failure point with respect to the $\tau_{12}$ -axis
$\phi'$	Angular position of the failure point with respect to the $\tau_{12}/S$ -axis
$\nu_{12}, \nu_{21}$	Poisson ratios
$E, \Pi, S_{\xi\eta}$	Laminate strengths relative to the principal strength axes in the Wu-Scheublein theory
$\rho$	Radial distance to the failure point in the $\sigma_1 - \sigma_2 - \tau_{12}$ coordinate system
$\rho^T$	Radial distance to the failure point in the $\sigma_1/X - \sigma_2/Y - \tau_{12}/S$ coordinate system
$\{\sigma\}_{12}$	Stress vector in the material axes of symmetry
$\{\sigma\}_{xy}$	Stress vector in any reference system
$\sigma_1, \sigma_2$	Stresses in the material axes of symmetry
$\sigma_1^C, \sigma_2^C$	Centre of ellipsoidal failure surface
$\sigma_1^m$	Matrix load in the fibre direction
$\sigma_{bt}$	Equal biaxial tensile strength of isotropic material
$\sigma_i$	Stress tensor in contracted notation
$\sigma_{ij}$	Stress tensor
$\sigma_{\lambda 1\alpha}, \sigma_{\lambda 2\beta}$	Stresses in principal directions, Chamis theory
$\sigma_p, \sigma_q, \sigma_r$	Stresses in principal directions
$\sigma_s$	Pure shear strength of isotropic material
$\sigma_x, \sigma_y$	Stresses at an angle with the axes of symmetry,
$\sigma_{\xi}, \sigma_{\eta}$	Stresses in laminate strength axes, Wu-Scheublein theory
$\tau_{12}$	Shear stresses in the material axes of symmetry

# LIST OF SYMBOLS (CONT'D)

$\tau_{xy}$	Shear stresses at an angle with axes of symmetry
$\tau_{\xi\eta}$	Shear stresses in the laminate principal strength axes, Wu-Scheublein theory
$T$	Parametric failure envelope for transversely isotropic material, in cylindrical coordinates
$T'$	Same as $T$ , in normalized coordinate system
$\psi$	Radial distance from the $\tau_{12}$ -axis to any point on this plane
$\psi'$	Radial distance from the $\tau_{12}/S$ -axis to any point on this plane



## CHAPTER 1

### INTRODUCTION

## CHAPTER 1

### INTRODUCTION

The word "composite" designates a material consisting of two or more components separated by a distinct interface. These materials are designed in order to obtain better combinations of mechanical properties than their individual components. Among these properties are strength-to-weight ratio, stiffness, toughness, and high temperature performance characteristics.

Different applications require different types of composite materials. For example, reinforced concrete is a composite used successfully in construction. Another type of composite is the variety of fibre-reinforced materials considered here. These are widely used in the aeronautics and aerospace industries. Typical fibres are produced from glass, boron, carbon, and graphite, with diameters in the range of one micron. The fibres are embedded in thin plastic or epoxy layers called "laminae" which have thicknesses of about 0.25 mm. The resulting material combines the low weight of the matrix with the high strength of the fibre. During the last twenty years, these composites with high strength-to-weight ratios have gained an ever-increasing importance in aeronautics.

When all the fibres are embedded in the same direction inside the matrix, the resulting lamina is termed unidirectional; a bidirectional lamina is obtained by embedding a woven fabric in the matrix. Typical laminae are shown schematically in Figure 1.1. For unidirectional laminae, the 1-axis indicates the fibre orientation, and the 2-axis is perpendicular to the fibres in the plane of the lamina. For

a bidirectional lamina, the 1- and 2-axes both indicate a fibre orientation, with the strongest in the 1-direction. The 3-axis is always perpendicular to the plane of the lamina. As a rough estimate, it can be assumed that the stiffness and strength of unidirectional laminae in the fibre direction are of the order of those for the fibre material while these properties in the transverse direction are of the order of those for the matrix alone. Experimental studies have demonstrated that many unidirectional materials show a linear stress-strain relationship up to failure for on-axis loadings. Non-linear curves are obtained for composites with very low fibre volume fraction and with matrices capable of plastic deformation. Shear stress-strain relationships are also generally non-linear up to failure.

Since a lamina is often not continuous and isotropic at the microscopic scale, its behaviour can be rather complex. This is confirmed by the variety of failure modes observed when simple tests are performed on a single fibre-reinforced lamina. Some of the failure modes are shown schematically in Figure 1.2. Three principal failure modes are observed for unidirectional laminae stressed in tension in the fibre direction. When breakage is due to a weak fibre cross-section, it is characterized by a clear-cut fracture surface perpendicular to the fibres. If some fibres have broken prior to total failure, stress concentrations at broken fibre ends may be identified by fibre pull-out along the fracture surface. Cracks perpendicular to the fibres at different cross-sections can also be joined by cracks in the matrix parallel to the fibres. A unidirectional lamina under transverse tensile load usually fails by splitting of the matrix or because of insufficient interfacial bond between fibres and matrix. For a lamina under longitudinal

compressive loading, a possible failure mode is by transverse failure resulting from the Poisson ratio effect. More likely is failure by microbuckling of the fibres, "in-phase" for high fibre content and "out-of-phase" for low fibre content. In-plane shear can also produce debonding of the constituents and matrix shear failure. Combinations of these failure modes are also possible, especially under complex loading conditions.

The strength and stiffness of laminae in the fibre direction can be dramatically reduced by various factors: misorientation of some fibres, discontinuous fibres, fibres of non-uniform strength, interfacial stresses between fibres and matrix, residual stresses resulting from temperature curing, etc. It has indeed been observed that failure of individual fibres in a lamina loaded axially can be initiated at loads much smaller than the composite failure load. The breakage of individual fibres causes stress concentrations at the broken ends and subsequent lamina behaviour depends on the matrix properties. A matrix with good shear capacity would transmit the load from one end of the broken fibre to the other. In the opposite case, the stress concentrations will cause microcracks in the matrix. Propagation of these cracks parallel to the fibres would cause the composite to behave as a bundle of fibres. Crack propagation perpendicular to the fibres would cause stress concentrations in neighbouring filaments and ultimately, total failure of the lamina. The above problems are usually studied from a microscopic approach, which takes into account the behaviour of the individual fibres and their relationship with the surrounding matrix.

The strength, stiffness, failure modes, and overall behaviour of fibre-reinforced laminae are strongly directional. In order to

withstand various load combinations and improve material behaviour under complex loads, laminae are usually stacked together in a specific sequence of orientations  $\theta_i$  to form a "laminate" as illustrated in Figure 1.3. The stacking sequence within a laminate is described by  $(\theta_1, \theta_2, \dots, \theta_n)$  and is determined upon consideration of anticipated loading conditions. All lamina failure modes discussed above could conceivably occur in individual laminae within a laminate. Failure of a complex laminate could furthermore be produced by debonding of the laminae. This phenomenon termed "delamination" is more likely to take place either at a discontinuity in the laminate or at a free edge.

The prediction of laminate behaviour is a complicated matter and some simplifying assumptions are usually made. First, each comprised lamina is viewed as a continuous and anisotropic material. Second, the bond between laminae is considered to be infinitely thin and is neglected in laminate analysis. Nevertheless, the comprised laminae are analyzed as perfectly bonded, and the strain is supposed to be identical throughout the laminate. The equations of elasticity for anisotropic materials are thus the basis for the analysis of laminae and laminates from a macroscopic point of view. These equations will be reviewed briefly in Chapter 2.

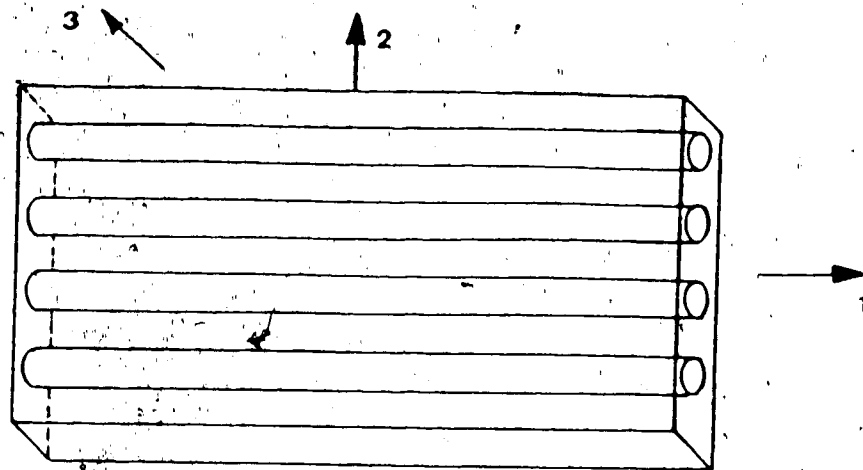
The prediction of the behaviour of fibre-reinforced materials in their axes of physical symmetry is a complex problem, often dealt with using the microscopic approach. Alternatively, material properties in these directions can be measured directly for the given lamina. One major issue in composite materials analysis is the prediction of their behaviour under complex loading conditions. The determination of their

failure surface from simple tests is a task undertaken by many researchers in the last twenty years, and is still widely discussed to this day. This matter is important for single laminae and for complex laminates. Accordingly, a significant number of failure criteria for fibre-reinforced composites have been proposed over the years. A review of these criteria will be presented in Chapter 3. It will be observed that most existing criteria can be grouped in categories sharing common characteristics. The most recent proposals will be discussed and the need for a new approach to this problem will be underlined. This chapter also contains a review of the experimental data available in the literature.

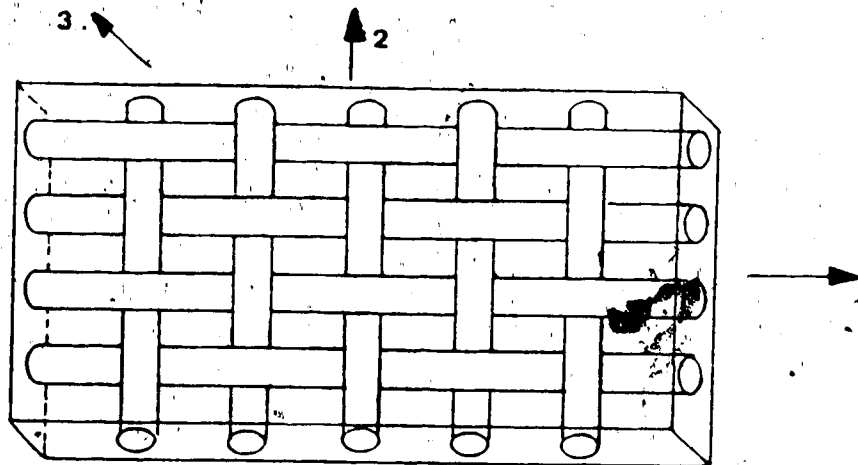
There have been interesting similarities between the development of failure criteria for fibre-reinforced materials and that of yield criteria for anisotropic ductile materials. In recent years, the use of a new parametric expression was proposed as a new way to write yield criteria for anisotropic materials. The advantages of this new approach will be discussed in Chapter 4. As a proposed solution to the need illustrated in Chapter 3 for new composite material failure criteria, a generalization of this technique will be proposed for transversely isotropic materials, and unidirectional fibre-reinforced laminae in particular. It will be shown that a parametric failure criterion can satisfy all conditions required to describe the failure surfaces of fibre-reinforced laminae. Different forms of this new failure criterion will be presented, its generality will be demonstrated, and the discussion will include some guidelines for its use in experimental studies.

A survey of the literature has shown that only a few extensive experimental studies of the failure surface for composite materials have

been conducted. However, some of these results will be used to demonstrate the flexibility of the new parametric failure criterion for transversely isotropic materials. It will be shown that in certain cases, the experimental-theoretical correlation can be greatly improved by using the proposed parametric criterion instead of one of the traditional failure criteria. It will also be shown that a parametric failure envelope can be easily modified to accomodate additional failure results in a way that no other criteria have as yet been able to do. Examples will be given for single laminae and for a laminate.



A - UNIDIRECTIONAL



B - BIDIRECTIONAL

FIGURE 1-1 FIBRE-REINFORCED LAMINAE



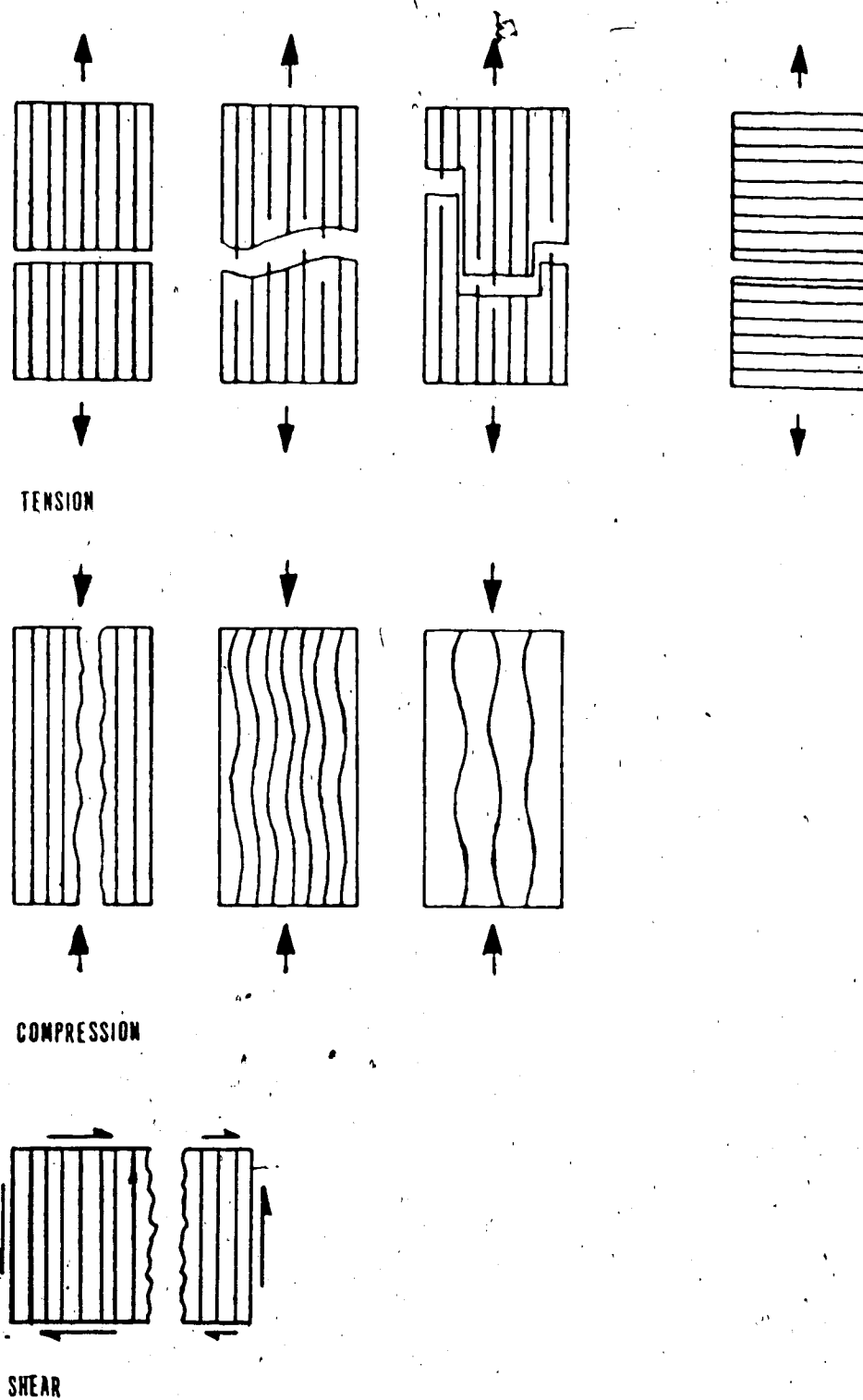
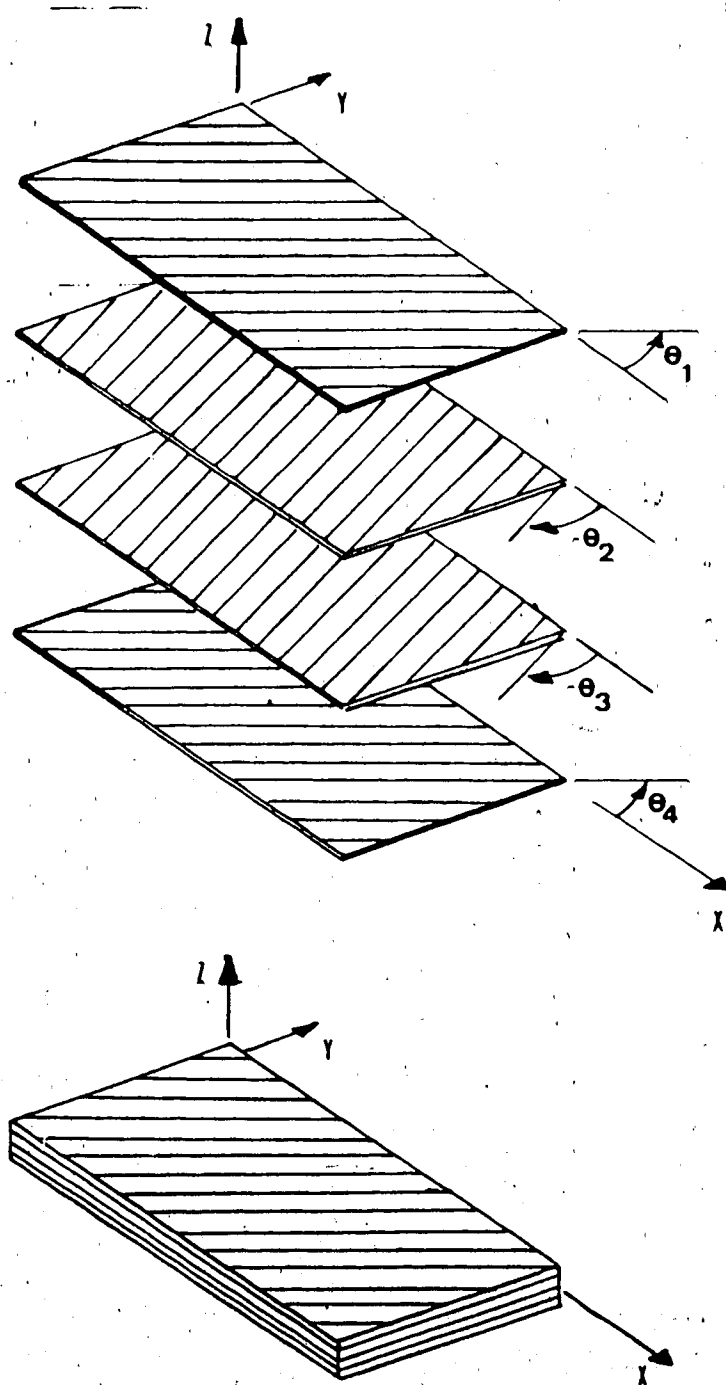


FIGURE 1-2 FAILURE MODES OF UNIAXIAL LAMINAE



$[\theta_1, \theta_2, \theta_3, \theta_4]$

FIGURE 1-3 LAMINATE CONSTRUCTION

## CHAPTER 2

### ANALYTICAL FORMULATIONS

## CHAPTER 2

### ANALYTICAL FORMULATIONS

#### 2.1 INTRODUCTION

As discussed in the introductory chapter, the macromechanical approach to the analysis of fibre-reinforced composite materials is based on the representation of the material by homogeneous, yet anisotropic materials. For a unidirectional lamina, it is generally assumed that it has the same strength in the 2- and 3-directions. The plane perpendicular to the fibre axis is therefore viewed as a plane of isotropy, and the lamina is analyzed as a material transversely isotropic with respect to the 1-axis. For a bidirectional lamina, there are no planes of isotropy, and it is analyzed as an orthotropic material. The corresponding equations of elasticity will be presented here. The analysis of single laminae can be extended to laminates by using classical lamination theory. This theory will be introduced in this chapter. A procedure frequently used to determine whether the failure of a compressed lamina triggers complete laminate failure will also be presented.

#### 2.2 EQUATIONS OF ELASTICITY

The generalized Hooke's law of linear elasticity can be written as (Jones, 1975):

$$\sigma_{ij} = C_{ijkl} \epsilon_{kl} \quad (2-1)$$

or  $\epsilon_{ij} = S_{ijkl} \sigma_{kl}$

where  $\sigma_{ij}$  is the stress tensor,  $\epsilon_{kl}$  is the strain tensor,  $C_{ijkl}$  is

the tensor of elastic moduli and  $S_{ijkl}$  is the compliance tensor. This notation can be contracted to:

$$\sigma_i = C_{ij} \epsilon_j \quad (2-2)$$

or 
$$\epsilon_i = S_{ij} \sigma_j$$

where  $i, j = 1, 2, \dots, 6$ . The relationships between the contracted and tensor notations are summarized in Table 2.1. The matrices  $C_{ij}$  and  $S_{ij}$  contain 36 independent components but because of material symmetries, this can be reduced to nine independent constants for an orthotropic material, and to only five in the case of a transversely isotropic material.

In most structural applications, it is assumed that the fibre-reinforced laminae are under a state of plane stress. Only this case will be examined here. The constitutive equations of an orthotropic or transversely isotropic lamina with its plane of symmetry perpendicular to the 1-direction would in both cases reduce to the following plane stress system of equations (Jones, 1975):

$$\begin{Bmatrix} \sigma_1 \\ \sigma_2 \\ \tau_{12} \end{Bmatrix} = \begin{bmatrix} Q_{11} & Q_{12} & 0 \\ Q_{12} & Q_{22} & 0 \\ 0 & 0 & Q_{66} \end{bmatrix} \begin{Bmatrix} \epsilon_1 \\ \epsilon_2 \\ \gamma_{12} \end{Bmatrix} \quad (2-3)$$

or to 
$$\begin{Bmatrix} \epsilon_1 \\ \epsilon_2 \\ \gamma_{12} \end{Bmatrix} = \begin{bmatrix} S_{11} & S_{12} & 0 \\ S_{12} & S_{22} & 0 \\ 0 & 0 & S_{66} \end{bmatrix} \begin{Bmatrix} \sigma_1 \\ \sigma_2 \\ \tau_{12} \end{Bmatrix} \quad (2-4)$$

where

$$\begin{aligned} S_{11} &= 1/E_1 \\ S_{22} &= 1/E_2 \\ S_{12} &= -\nu_{12}/E_1 \\ S_{66} &= 1/G_{12} \end{aligned} \quad (2-5)$$

and

$$\begin{aligned} Q_{11} &= E_1/(1 - \nu_{12}\nu_{21}) \\ Q_{12} &= \nu_{21}E_1/(1 - \nu_{12}\nu_{21}) \\ Q_{22} &= E_2/(1 - \nu_{12}\nu_{21}) \\ Q_{66} &= G_{12} \end{aligned} \quad (2-6)$$

In these relations,  $E_1$  and  $E_2$  are the Young's moduli in the two principal directions,  $\nu_{12}$  is the major Poisson's ratio, and  $G_{12}$  the shear modulus. These four constants are sufficient to characterize any plane stress condition. The Poisson ratio  $\nu_{21}$  is related to the other constants through

$$\nu_{21} = E_2 \nu_{12}/E_1 \quad (2-7)$$

For a lamina oriented at an angle  $\theta$  with the applied loads  $\sigma_x$ ,  $\sigma_y$  and  $\tau_{xy}$  shown in Figure 2.1, the stresses in the material directions of symmetry are calculated from the following transformation law (Jones, 1975):

$$\text{or} \quad \{\sigma\}_{12} = [T] \{\sigma\}_{xy} \quad (2-8)$$

$$\begin{Bmatrix} \sigma_1 \\ \sigma_2 \\ \tau_{12} \end{Bmatrix} = \begin{bmatrix} \cos^2\theta & \sin^2\theta & 2\sin\theta\cos\theta \\ \sin^2\theta & \cos^2\theta & -2\sin\theta\cos\theta \\ -\sin\theta\cos\theta & \sin\theta\cos\theta & (\cos^2\theta - \sin^2\theta) \end{bmatrix} \begin{Bmatrix} \sigma_x \\ \sigma_y \\ \tau_{xy} \end{Bmatrix} \quad (2-9)$$

It can then be shown that the relationships between the stresses and

strains in the directions  $x$  and  $y$  become:

$$\begin{Bmatrix} \sigma_x \\ \sigma_y \\ \tau_{xy} \end{Bmatrix} = \begin{bmatrix} \bar{Q}_{11} & \bar{Q}_{12} & \bar{Q}_{16} \\ \bar{Q}_{12} & \bar{Q}_{22} & \bar{Q}_{26} \\ \bar{Q}_{16} & \bar{Q}_{26} & \bar{Q}_{66} \end{bmatrix} \begin{Bmatrix} \epsilon_x \\ \epsilon_y \\ \gamma_{xy} \end{Bmatrix} \quad (2-10)$$

where

$$\begin{aligned} \bar{Q}_{11} &= Q_{11} \cos^4 \theta + Q_{22} \sin^4 \theta + 2(Q_{12} + 2Q_{66}) \sin^2 \theta \cos^2 \theta \\ \bar{Q}_{12} &= Q_{12}(\cos^4 \theta + \sin^4 \theta) + (Q_{11} + Q_{22} - 4Q_{66}) \sin^2 \theta \cos^2 \theta \\ \bar{Q}_{16} &= (Q_{11} - Q_{12} - 2Q_{66}) \sin \theta \cos^3 \theta + (Q_{12} - Q_{22} + 2Q_{66}) \sin^3 \theta \cos \theta \\ \bar{Q}_{22} &= Q_{11} \sin^4 \theta + Q_{22} \cos^4 \theta + 2(Q_{12} + 2Q_{66}) \sin^2 \theta \cos^2 \theta \\ \bar{Q}_{26} &= (Q_{11} - Q_{12} - 2Q_{66}) \sin^3 \theta \cos \theta + (Q_{12} - Q_{22} + 2Q_{66}) \sin \theta \cos^3 \theta \\ \bar{Q}_{66} &= (Q_{11} + Q_{22} - 2Q_{12} - 2Q_{66}) \sin^2 \theta \cos^2 \theta + Q_{66} (\sin^4 \theta + \cos^4 \theta) \end{aligned} \quad (2-11)$$

### 2.3 CLASSICAL LAMINATION THEORY

With classical lamination theory, the analysis of single laminae can be extended to complex laminates. This theory is based on the hypothesis that the laminae are perfectly bonded together, that the bonding material is infinitesimally thin, and the laminae cannot slip relative to each other. This implies that plane surfaces remain plane, and that the strain at a distance  $z$  from the laminate midplane is given by the following (Petit and Waddoups, 1969; Jones, 1975):

$$\{\epsilon\} = \{\epsilon^0\} + z \{\kappa\} \quad (2-12)$$

or

$$\begin{Bmatrix} \epsilon_x \\ \epsilon_y \\ \gamma_{xy} \end{Bmatrix} = \begin{Bmatrix} \epsilon_x^0 \\ \epsilon_y^0 \\ \gamma_{xy}^0 \end{Bmatrix} + z \begin{Bmatrix} \kappa_x \\ \kappa_y \\ \kappa_{xy} \end{Bmatrix} \quad (2-13)$$

where the superscript  $(^o)$  identifies the midplane of the laminate and  $\kappa$  is the curvature of the middle-surface. The resultant forces and moments applied on the laminate, as shown in Figure 2.2, are given by (Jones, 1975):

$$\{N\} = \{N_x; N_y; N_{xy}\} = \int_{-t/2}^{t/2} \{\sigma_x; \sigma_y; \tau_{xy}\} dz \quad (2-14)$$

$$\{M\} = \{M_x; M_y; M_{xy}\} = - \int_{-t/2}^{t/2} \{\sigma_x; \sigma_y; \tau_{xy}\} z dz \quad (2-15)$$

where  $t$  is the total laminate thickness.

Combining Equations (2-10), (2-12), (2-14), and (2-15) leads to the following relation:

$$\begin{Bmatrix} N \\ M \end{Bmatrix} = \begin{bmatrix} A & B \\ B & D \end{bmatrix} \begin{Bmatrix} \epsilon^o \\ \kappa \end{Bmatrix} \quad (2-16)$$

where

$$A_{ij} = \int_{-t/2}^{t/2} \bar{Q}_{ij} dz \quad (2-17)$$

$$B_{ij} = \int_{-t/2}^{t/2} \bar{Q}_{ij} z dz \quad (2-18)$$

$$D_{ij} = \int_{-t/2}^{t/2} \bar{Q}_{ij} z^2 dz \quad (2-19)$$

The above submatrices  $A$ ,  $B$  and  $D$  are respectively the extensional stiffness, coupling stiffness, and bending stiffness matrices. Equations (2-16) and (2-18) indicate that in-plane loading would produce bending as well as extension when the submatrix  $[B]$  is non-zero. Also, the application of moments  $\{M\}$  would cause extension as well as bending. These coupling effects can be prevented by constructing laminates symmetrical with respect to the midplane, thus making  $[B]$  vanish. For a given set of applied stresses on a laminate, forces and moments



alike, deformations are found using Equation (2-16). These values are then substituted back into Equations (2-9) and (2-10) to find the internal stresses in each lamina. For laminates submitted to in-plane loads  $\{N\}$  only, the same lamina stresses will be found for any modification of a specific stacking sequence, provided that the entire laminate remains symmetrical. This is contrary to experimental observations, probably because the interlaminar stresses are neglected in the classical lamination theory.

#### (2.4) PROGRESSIVE DAMAGE ACCUMULATION

A large number of load configurations can be applied to a given composite structure. However, it is not a practicable task to submit such a structure to an extensive testing programme that would reproduce all probable loading conditions to which it might be submitted during its lifetime. Instead, analytical functions known as failure criteria are used, that define limiting envelopes in stress or strain space. The structural integrity of the lamina is maintained as long as the loading condition remains inside the failure envelope defined by the assumed criterion. When these limits are exceeded, lamina failure will occur. An extensive survey of existing criteria is the subject of the next chapter.

For multilayered laminates, the problem is complicated by the possibility that a particular lamina may fail without causing failure of the entire laminate. A procedure used to calculate the first lamina failure as well as the ultimate strength of the laminate is summarized in Figure 2.3 (e.g. Tennyson, 1981). It is an iterative procedure in which the applied loads are increased proportionately and monotonically.

It combines classical lamination theory, the assumed failure criterion, and the following hypotheses on the stiffness reduction due to lamina failures.

At a given load, the stresses in each lamina are compared to the assumed failure criterion. If no failure is detected, the loads are increased proportionately until breakage is found. If failure is detected, the failure mode is identified and the lamina stiffness is reduced accordingly. The failure modes generally considered are fibre breakage and matrix failure. For the case of fibre breakage, the matrix  $[Q]$  of Equation (2-3) is reduced to zero in the subsequent calculations. For matrix breakage, the following terms are inserted in the matrix  $[Q]$

$$Q_{12} = Q_{22} = Q_{66} = 0 \quad (2-20)$$

This means that only the stiffness in the fibre direction is kept for the broken lamina. The above procedure is repeated for each lamina, and new stiffness matrices  $[A]$ ,  $[B]$  and  $[D]$  are calculated for the laminate. The same loads are reapplied to the modified laminate until no more damage is detected for this loading condition. The loads are then increased and the entire procedure repeated until complete laminate failure, in which case the matrices  $[A]$  and  $[D]$  become singular.

By joining together the first failure points at different stress ratios for the same laminate, a "first-ply-failure" envelope is obtained. As long as a load applied to the laminate remains inside this envelope, the laminate retains its structural integrity. By joining together the points of ultimate strength at different stress ratios, an "ultimate-ply-failure" is also obtained. Where it is different from the first-ply-failure envelope, the laminate is able to sustain loads higher

than those causing the first structural damage. However, it is observed that the shape of the ultimate ply failure envelope is dependent on the loading history. With the method outlined above, this envelope is obtained under the assumption of proportional loading. Other types of loading could eventually lead to different failure envelopes because the sequence of damage might differ from that obtained from proportional loading.

## 2.5 CONCLUSION

In this chapter, the fundamentals of fibre-reinforced lamina and laminate analysis were introduced. Simplifying assumptions of homogeneity and transversely isotropic behaviour are usually adopted for unidirectional laminae. The theory of elasticity for transversely isotropic materials combined with classical lamination theory forms the basis of the analysis for complex laminates. Both theories were presented in this chapter. The usual methodology for laminate analysis beyond first failure was also briefly summarized.

The problem of modelling failure with appropriate failure criteria was briefly mentioned. This topic will be reviewed extensively in the next chapter.

TABLE 2.1 - Relationships Between Tensor and Contracted Notations

## a) Stress space

tensor	contracted
$\sigma_{11}$	$\sigma_1$
$\sigma_{22}$	$\sigma_2$
$\sigma_{33}$	$\sigma_3$
$\sigma_{23} = \tau_{23}$	$\sigma_4$
$\sigma_{31} = \tau_{31}$	$\sigma_5$
$\sigma_{12} = \tau_{12}$	$\sigma_6$

## b) Strain space

tensor	contracted
$\epsilon_{11}$	$\epsilon_1$
$\epsilon_{22}$	$\epsilon_2$
$\epsilon_{33}$	$\epsilon_3$
$2\epsilon_{23} = \gamma_{23}$	$\epsilon_4$
$2\epsilon_{31} = \gamma_{31}$	$\epsilon_5$
$2\epsilon_{12} = \gamma_{12}$	$\epsilon_6$

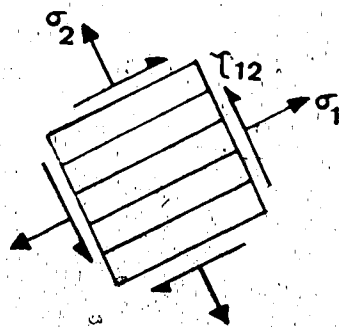
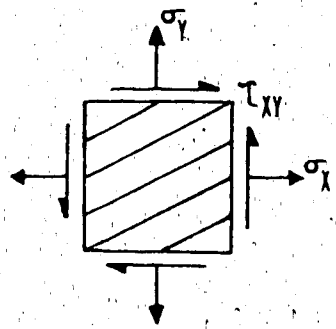
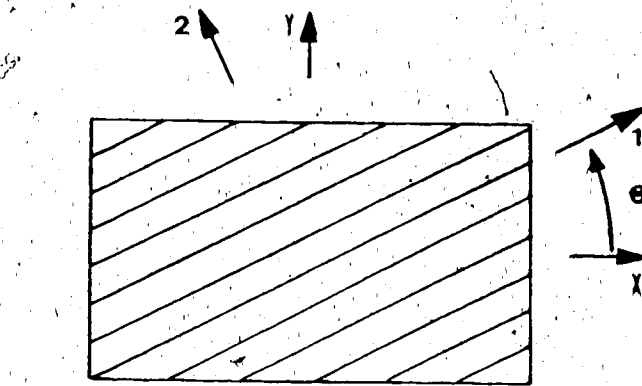


FIGURE 2-1 LAMINA ORIENTATION

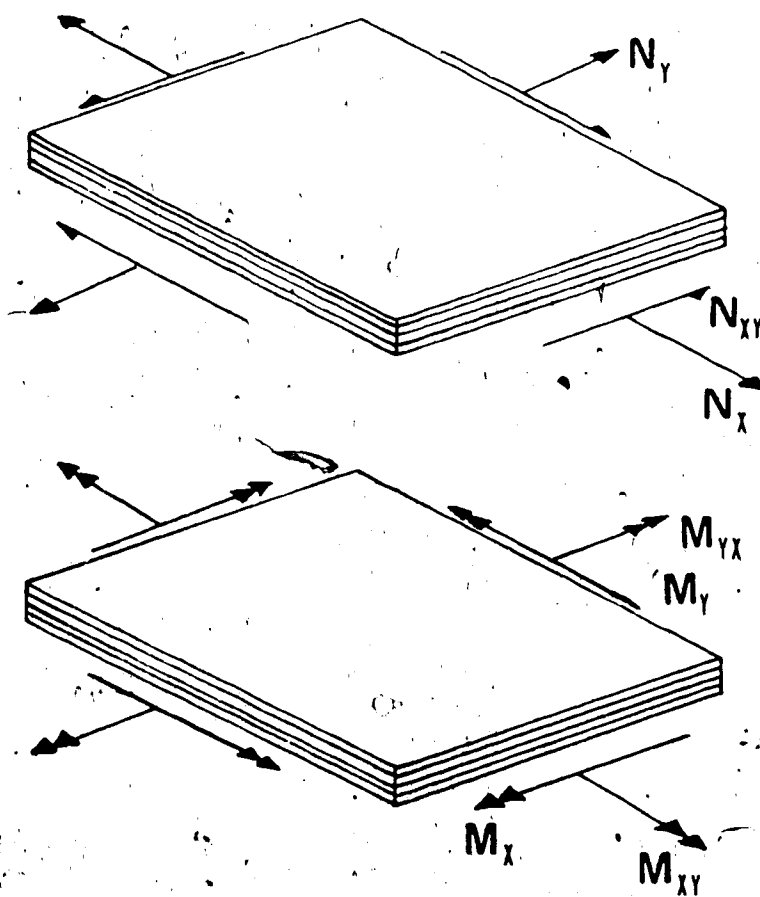
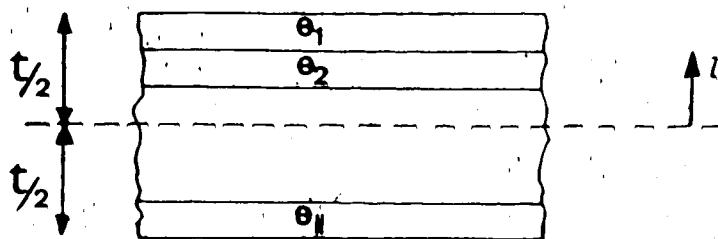


FIGURE 2-2 LAMINATE ANALYSIS

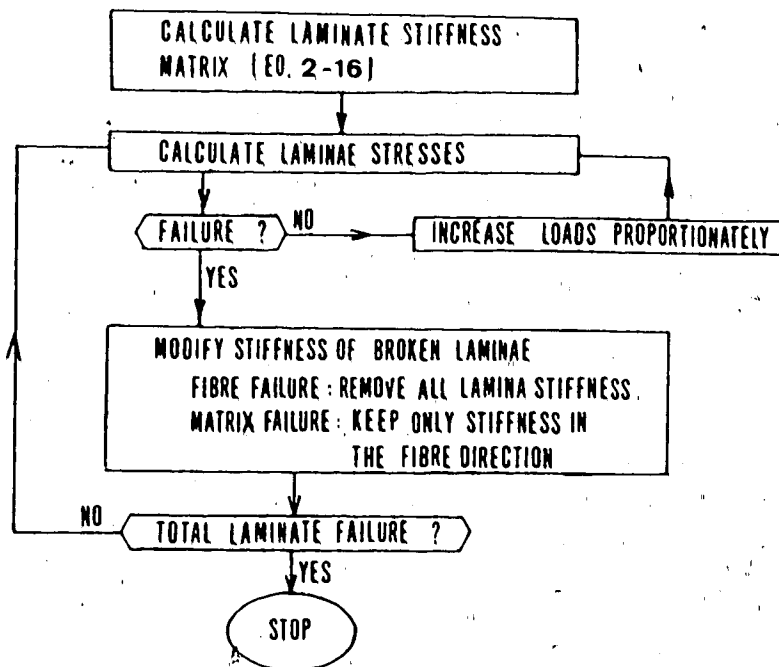


FIGURE 2-3 DAMAGE ACCUMULATION ANALYSIS

## CHAPTER 3

### A REVIEW OF MACROSCOPIC FAILURE CRITERIA FOR FIBRE-REINFORCED COMPOSITE MATERIALS



## CHAPTER 3

### A REVIEW OF MACROSCOPIC FAILURE CRITERIA FOR FIBRE-REINFORCED COMPOSITE MATERIALS

#### 3.1 INTRODUCTION

A failure criterion attempts to predict mathematically whether or not failure will occur for any given loading condition. Its accuracy can only be judged from the agreement between the predicted results and experimental data. Ideally, the number of parameters necessary to define the failure function should be as small as possible. For example, knowing the failure stress of an isotropic material under uniaxial load, a failure criterion might be developed that would predict its strength under any biaxial loading condition. In fact, a single parameter such as uniaxial tensile strength is often sufficient for isotropic materials. In contrast to isotropic materials, the strength properties of fibre-reinforced materials are strongly dependent on the direction of loading. Accordingly, more than one parameter is needed to describe the failure criterion. This chapter will focus on the various failure theories that have been proposed for composite materials. We shall limit attention to quasi-static macroscopic failure and exclude from our discussion phenomena such as fatigue, fracture, creep and microscopic damage.

Material failure can be defined in a number of ways, for example, to be either fracture or a state of excessively large deformation. Many so-called "failure criteria" were first developed to predict the onset of yield or plastic flow in ductile metals. This was the case with the

isotropic failure criteria of von Mises and Tresca, and with the orthotropic failure criterion proposed by Hill (1948). For fibre-reinforced materials, "failure" clearly is not due to plastic yielding. It is associated with a loss of strength or stress-carrying capability. Thus, when a loading condition exceeds those defined by the failure criterion, the material is deemed to have failed in one of among a number of possible modes, possibly one of those described in Chapter 1.

Only a few failure criteria have been proposed for isotropic materials and these are reviewed briefly in the next section. The development of failure criteria for orthotropic and transversely isotropic materials is based on analogous hypotheses. One of the desired characteristics of orthotropic failure criteria is that they reduce to isotropic criteria when identical strength characteristics are present in all directions. Over the last two decades, a significant number of failure criteria for composite materials, or more generally for anisotropic materials, have been proposed. They can be classified into general families and each group will in turn be reviewed in this chapter. Failure criteria that have been proposed to characterize composite laminates are also discussed. In addition, a survey of experimental results published over the last twenty years will be presented.

In most applications, it can be assumed that a lamina of the composite is under a state of plane stress. It is therefore sufficient to describe the failure envelope in the three-dimensional stress space  $\sigma_1 - \sigma_2 - \tau_{12}$  where  $\sigma_1, \sigma_2$  are normal stresses and  $\tau_{12}$  is the shear stress. For transversely isotropic or orthotropic laminae, the 1-axis and 2-axis are taken to coincide with the material axes of symmetry.

Since material behaviour is indifferent to the direction of the shear stress  $\tau_{12}$ , the entire envelope must be symmetrical with respect to the plane  $\tau_{12} = 0$ . Ideally, this envelope should be described by as few terms as possible.

The tensile stresses at failure for uniaxial loading in the directions 1 and 2 are denoted respectively by  $X$  and  $Y$ . The corresponding compressive strengths are  $X'$  and  $Y'$ . The value  $S$  is the failure stress in pure shear. These specific stresses are commonly used to characterize the failure envelope. However, most failure criteria for composites require the use of additional points to define the surface more accurately.

When the principal axes of a lamina are oriented at an angle  $\theta$  with respect to the direction of loading, the specimen is referred to as an "off-axis" lamina. Shear tests  $S_\theta$  or  $S'_\theta$  on off-axis laminae are often suggested in addition to the above uniaxial tests. Most of these are performed at an angle of  $\pm 45^\circ$ , and the strengths obtained are designated as  $S_{45}$  and  $S'_{45}$  respectively. Tensile or compressive strengths under equi-biaxial loading  $P$  and  $P'$  can also be measured to provide more points on the failure envelope. Uniaxial tensile and compressive strengths  $U_\theta$  or  $U'_\theta$  on off-axis laminae oriented at an angle  $\theta$  can also provide useful information on the failure envelope. The various tests performed on uniaxial laminae are summarized in Table 3.1.

### 3.2 A REVIEW OF FAILURE CRITERIA FOR ISOTROPIC MATERIALS

The behaviour of an isotropic material subjected to a set of complex loads is the simplest case which arises. For this case, failure criteria are often based on the additional assumption that their tensile

and compressive strengths are identical. There is not yet a unified theory applicable to all isotropic materials without exception. Indeed, several criteria have often been proposed for the same material.

Since all planes of an isotropic material are planes of material symmetry, it is convenient to transform the applied stresses into their principal values  $\sigma_p$ ,  $\sigma_q$  and  $\sigma_r$ . (The subscripts p, q, r are used here to avoid confusion with the system of axes 1, 2, 3 that identifies the axes of material symmetry for an orthotropic material.) For the plane stress case,  $\sigma_r = 0$ .

The simplest criterion proposed to date for isotropic materials is the maximum stress criterion. It stipulates that failure occurs when one of the following conditions is attained:

$$|\sigma_p| = X \quad \text{or} \quad |\sigma_q| = X \quad (3-1)$$

This criterion can also be written as

$$(\sigma_p^2 - X^2)(\sigma_q^2 - X^2) = 0 \quad (3-2)$$

where  $X$  is the uniaxial tensile strength of the material. This is a non-interactive criterion, in the sense that failure takes place when an individual stress component reaches the critical value  $X$ , regardless of the value of the other. This failure condition is sometimes applied to brittle isotropic materials. From similar hypotheses, a non-interactive failure criterion with principal strains as parameters can be defined in plane stress as:

$$\epsilon_p = X/E, \quad \epsilon_q = X/E, \quad \epsilon_r = X/E \quad (3-3)$$

where  $E$  is the modulus of elasticity. It can be observed by drawing

Equations (3-1) and (3-3) in the same space that these criteria are identical only for the theoretical case of zero Poisson's ratio.

The observation that failure in isotropic materials often occurs by slipping on a plane at  $45^\circ$  from the load axes led Tresca to hypothesize that the shear stress component was the critical cause of failure. This hypothesis leads to the following set of equations:

$$|\sigma_p| = X, \quad |\sigma_q| = X, \quad |\sigma_p - \sigma_q| = X \quad (3-4)$$

This failure condition is most suitable for describing plastic yielding in ductile materials.

Another criterion, the maximum distortion energy criterion, is based on the decomposition of the total elastic energy stored in a material into the sum of the dilatational energy and the distortion energy. Developed originally for the yielding of metals, it assumes that failure is unaffected by the hydrostatic pressure. In terms of principal stresses, this can be expressed as

$$(\sigma_p - \sigma_q)^2 + (\sigma_q - \sigma_r)^2 + (\sigma_r - \sigma_p)^2 = 2X^2 \quad (3-5)$$

Under plane stress conditions,  $\sigma_r = 0$  and the condition (3-5) can be transformed to

$$\left(\frac{\sigma_p}{X}\right)^2 - \left(\frac{\sigma_p \sigma_q}{X^2}\right) + \left(\frac{\sigma_q}{X}\right)^2 = 1 \quad (3-6)$$

This criterion is known as the von Mises or Hencky-von Mises yield criterion. From a theoretical point of view, the use of this criterion is attractive because it is a continuous and interactive function. As with Tresca's failure criterion, this criterion is often used to describe yielding of ductile materials.

### 3.3 MAXIMUM STRESS AND MAXIMUM STRAIN CRITERIA

In view of its inherent directional properties, the strength of an orthotropic fibre-reinforced lamina is strongly dependent on the direction of loading. Also, the different failure mechanisms in tension and compression will cause failure at different values of applied load. The simplest failure criterion for such a material can be obtained from a direct extension of the isotropic maximum stress criterion. It stipulates that failure will occur when any one of the following conditions is exceeded (Tsai, 1983)

$$\begin{aligned} -X' &< \sigma_1 < X \\ -Y' &< \sigma_2 < Y \\ -S &< \tau_{12} < S \end{aligned} \quad (3-7)$$

To apply this, the internal stresses must first be transformed to the material axes of symmetry. This will be the case for all failure criteria considered here. As is the case for its isotropic counterpart, this criterion is non-interactive, since failure is predicted independently by any one of the three of Equations (3-7). A similar extension of the isotropic maximum strain criterion produces the next set of equations (Tsai, 1983)

$$\begin{aligned} \epsilon_{1u}^- &= -X'/E_1 < \epsilon_1 < X/E_1 = \epsilon_{1u}^+ \\ \epsilon_{2u}^- &= -Y'/E_2 < \epsilon_2 < Y/E_2 = \epsilon_{2u}^+ \\ -S/G_{12} &< \gamma_{12} < S/G_{12} \end{aligned} \quad (3-8)$$

where  $E_1$  and  $E_2$  are Young's moduli, and  $G_{12}$  is the shear modulus in the principal material axes. Assuming linearity up to failure and combining (3-8) with Equation (2-3), the failure envelope in stress space becomes

$$\begin{aligned}
\frac{Q_{12}\sigma_2}{Q_{22}} + \epsilon_{1u}^- (Q_{11} - \frac{Q_{12}^2}{Q_{22}}) < \sigma_1 < \frac{Q_{12}\sigma_2}{Q_{22}} + \epsilon_{1u}^+ (Q_{11} - \frac{Q_{12}^2}{Q_{22}}) \\
\frac{Q_{12}\sigma_1}{Q_{11}} + \epsilon_{2u}^- (Q_{22} - \frac{Q_{12}^2}{Q_{11}}) < \sigma_2 < \frac{Q_{12}\sigma_1}{Q_{11}} + \epsilon_{2u}^+ (Q_{22} - \frac{Q_{12}^2}{Q_{11}}) \quad (3-9) \\
-S < \tau_{12} < S
\end{aligned}$$

This failure envelope coincides with the conditions (3-7) only when the Poisson ratios  $\nu_{12} = \nu_{21} = 0$ .

According to a survey by the AIAA composite structures subcommittee (see Soni 1983), the two preceding criteria are the most widely used by designers of composite structures; more than 50% of the respondents surveyed claimed to use one of these. The popularity of these criteria stems from their simplicity rather than their accuracy. When these criteria are used for unidirectional laminae, it is generally assumed that fibre fracture occurs when  $\sigma_1$  exceeds the limiting values and that failure due to  $\sigma_2$  or  $\tau_{12}$  is associated with matrix failure. Experimental results seem to indicate that the maximum stress criterion gives good results only for composites with very low moduli, and that the maximum strain criterion is representative of some composites with low shear moduli.

### 3.4 HILL-TYPE CRITERIA

In 1948, Hill proposed a criterion to describe plastic yielding for anisotropic metals. On the assumption that an analogous criterion can be used to predict failure in fibre-reinforced materials, it has since been adapted to composite materials. Hill's criterion has inspired the development of other failure equations and these also will be presented in this section.

The criterion proposed by Hill (1948) was developed in a general form for orthotropic materials. Hill generalized the von Mises distortional energy criterion to account for anisotropy. Basically, he assumed that such a criterion would have to satisfy the following conditions: First, it should be of quadratic form. Second, supposing that the tensile and compressive strengths would be the same, all the linear terms of the quadratic expression would be equal to zero. Third, the axes of reference would be taken to coincide with the principal axes of orthotropy. To satisfy these conditions, the criterion was postulated as follows:

$$2f(\sigma_{ij}) = F(\sigma_2 - \sigma_3)^2 + G(\sigma_3 - \sigma_1)^2 + H(\sigma_1 - \sigma_2)^2 + 2L \tau_{23}^2 + 2M \tau_{31}^2 + 2N \tau_{12}^2 = 1 \quad (3-10)$$

where  $F$ ,  $G$ ,  $H$ ,  $L$ ,  $M$  and  $N$  are constants characteristic of the material. In Hill's original proposal, these values were obtained from the yield stresses in the principal material directions. The values of the constants  $F$ ,  $G$ ,  $H$ ,  $N$  are then:

$$\begin{aligned} 2N &= 1/S^2 \\ 2F &= 1/Y^2 + 1/Z^2 - 1/X^2 \\ 2G &= 1/X^2 + 1/Z^2 - 1/Y^2 \\ 2H &= 1/X^2 + 1/Y^2 - 1/Z^2 \end{aligned} \quad (3-11)$$

where  $Z$  is the yield strength in the 3-direction.

In plane stress, the constants  $L$  and  $M$  vanish. Substituting (3-11) in (3-10) and assuming plane stress conditions gives:

$$\left(\frac{\sigma_1}{X}\right)^2 + \left(\frac{\sigma_2}{Y}\right)^2 - \left(\frac{1}{X^2} + \frac{1}{Y^2} - \frac{1}{Z^2}\right) \sigma_1 \sigma_2 + \left(\frac{\tau_{12}}{S}\right)^2 = 1 \quad (3-12)$$



For an isotropic medium,  $X = Y = Z = \sqrt{3} S$  and (3-12) reduces further to:

$$\left(\frac{\sigma_1}{X}\right)^2 + \left(\frac{\sigma_2}{X}\right)^2 - \frac{\sigma_1 \sigma_2}{X^2} + \left(\frac{\tau_{12}}{S}\right)^2 = 1 \quad (3-13)$$

This expression is equivalent to the von Mises failure criterion (3-6).

It was observed experimentally that the shapes of failure envelopes for fibre-reinforced materials were similar to those obtained for yielding of orthotropic materials. This led to the use of Hill's criterion (3-12), originally intended as a yield criterion for metals, for the prediction of failure in fibre-reinforced laminae. In this case, the constants  $F$ ,  $G$ ,  $H$  and  $N$  are calculated from the strengths in the principal material directions. This extension of Hill's criterion was first suggested by Azzi and Tsai (1965). Since the criterion (3-12) was not developed specifically for fibre-reinforced materials, it is of limited applicability for them, mainly because of the hypothesis of equal strengths in tension and compression. However, other criteria specially intended for use with fibre-reinforced laminae were obtained from extensions or modifications of (3-12).

For unidirectional composites, Azzi and Tsai (1965) invoked the transverse isotropy condition in the plane perpendicular to the fibre direction to insert the equality  $Z = Y$  in (3-12). This leads to the following:

$$\left(\frac{\sigma_1}{X}\right)^2 - \left(\frac{\sigma_1 \sigma_2}{X^2}\right) + \left(\frac{\sigma_2}{Y}\right)^2 + \left(\frac{\tau_{12}}{S}\right)^2 = 1 \quad (3-14)$$

This criterion is sometimes referred to as the Tsai-Hill criterion. Since there are no provisions for different strengths in tension and compression, some authors use different values of  $X$  and  $Y$ , depending

in which quadrant of the space  $\sigma_1 - \sigma_2$  the load conditions fall. This produces a failure envelope that has discontinuous slopes at the four points where it intersects the  $\sigma_1$  and  $\sigma_2$  axes. These slope discontinuities can be eliminated by multiplying the cross-product term  $\sigma_1 \sigma_2$  by the same coefficient in the four quadrants. This common coefficient is usually taken as  $1/X^2$ , as computed in the first quadrant.

Wood is an example of a natural material with directionally-dependent properties, and it is often assumed to be orthotropic. In plane stress, a failure criterion for wood has been proposed by Norris (1950):

$$\left(\frac{\sigma_1}{X}\right)^2 - \left(\frac{\sigma_1 \sigma_2}{XY}\right) + \left(\frac{\sigma_2}{Y}\right)^2 + \left(\frac{\tau_{12}}{S}\right)^2 = 1 \quad (3-15)$$

This criterion is very similar to the failure criteria proposed by Azzi and Tsai, and by Hill. As for the previous criterion, different values of  $X$  and  $Y$  can be used, depending on the signs of the stresses. To ensure slope continuity where the envelope intersects the  $\sigma_1$  and  $\sigma_2$  axes, the coefficient of the cross-product  $\sigma_1 \sigma_2$  obtained with positive  $X$  and  $Y$  is usually retained for the entire envelope. Norris also postulated the additional condition that the stress values should not exceed the maximum strength in the 1- and 2-directions, that is:

$$X' < \sigma_1 < X, \quad Y' < \sigma_2 < Y \quad (3-16)$$

This produces a failure envelope which is truncated by flat planes perpendicular to the axes at the values of maximum uniaxial strengths in the 1- and 2-directions. The major difference between the three failure criteria above and the maximum stress or strain criteria is that the interaction between the stresses is now taken into account.

The only term that differs in the above criteria (3-13) to (3-15) is that associated with the product  $\sigma_1 \sigma_2$ . The coefficient of this term however depends only on the uniaxial strengths  $X$  and  $Y$ . Ashkenazi (1966) proposed that the value of this interaction parameter be found by performing an additional test. He suggested conducting a uniaxial tensile test on a lamina at  $\theta = 45^\circ$  and using the value of its ultimate strength  $U_{45}$  in the computation of the interaction term. With this new value, Ashkenazi's criterion becomes:

$$\left(\frac{\sigma_1}{X}\right)^2 + \left(\frac{\sigma_2}{Y}\right)^2 + \left(\frac{\tau_{12}}{S}\right)^2 + \left[\frac{4}{U_{45}^2} - \frac{1}{X^2} - \frac{1}{Y^2} - \frac{1}{S^2}\right] \sigma_1 \sigma_2 = 1 \quad (3-17)$$

Other authors have proposed criteria in which the value of the interaction parameter would be a function of the elastic constants of the lamina in the principal directions. A slight modification to Norris' criterion has thus been proposed by Fischer (1967):

$$\left(\frac{\sigma_1}{X}\right)^2 + \left(\frac{\sigma_2}{Y}\right)^2 + \left(\frac{\tau_{12}}{S}\right)^2 - K \frac{\sigma_1 \sigma_2}{XY} = 1 \quad (3-18)$$

where  $K$  is given as:

$$K = \frac{E_1(1 + \nu_{21}) + E_2(1 + \nu_{12})}{2 [E_1 E_2 (1 + \nu_{21})(1 + \nu_{12})]^{1/2}} \quad (3-19)$$

A comparable criterion, proposed by Chamis (1969), that was intended to take into account the properties of the constituent fibre and matrix materials reads as:

$$f(\sigma_x, S_x, K_{x12}) = 1 - \left[ \left(\frac{\sigma_{x1\alpha}}{S_{x1\alpha}}\right)^2 + \left(\frac{\sigma_{x2\beta}}{S_{x2\beta}}\right)^2 + \left(\frac{\sigma_{x12}}{S_{x12}}\right)^2 - K'_{x12\alpha\beta} K_{x12} \frac{\sigma_{x1\alpha}}{S_{x1\alpha}} \frac{\sigma_{x1\beta}}{S_{x1\beta}} \right] \quad (3-20)$$

where  $f(\sigma_x, S_x, K_{x12}) < 0$  indicates failure. In this equation, there are two correlation coefficients:  $K'_{x12\alpha\beta}$  is a theory-experiment correlation coefficient, and  $K_{x12}$  is defined as:

$$K_{x12} = \frac{(1 + 4\nu_{12} - \nu_{13})E_2 + (1 - \nu_{23})E_1}{[E_1E_2(2 + \nu_{12} + \nu_{13})(2 + \nu_{21} + \nu_{23})]^{\frac{1}{2}}} \quad (3-21)$$

In Equation (3-20) the subscripts  $\alpha$  and  $\beta$  differentiate between the tension and compression modes. The values of  $S_{x1\alpha}$ ,  $S_{x1\beta}$ ,  $S_{x2\alpha}$ ,  $S_{x2\beta}$ ,  $S_{x12}$  are the ultimate strengths in tension, compression and shear. Chamis calculates these values using the elastic properties of the constituent materials. However, they could be found experimentally, and would then be equivalent to the values  $X$ ,  $X'$ ,  $Y$ ,  $Y'$ , and  $S$ , respectively. For an isotropic material, this criterion reduces to the von Mises theory. With different strengths in tension and compression, this produces a failure envelope with discontinuous slopes at the four points where it intersects the  $\sigma_1$ - and  $\sigma_2$ -axes.

The failure criteria of Hill (3-12), Azzi and Tsai (3-14), Norris (3-15), Fisher (3-18), Ashkenazi (3-17), and Chamis (3-20) all represent ellipsoids in the stress space  $\sigma_1 - \sigma_2 - \tau_{12}$ . With the hypothesis of unequal strengths in tension and compression, different strength parameters are used in each quadrant, and each portion of the surface is a section of an ellipsoid. All ellipsoids or portions thereof are centered at the origin. Their respective length and orientation are determined by the coefficient of  $\sigma_1 \sigma_2$ . According to these criteria the shape of the failure curve in a plane  $\tau_{12} = \text{constant}$  will remain identical for any shear stress  $\tau_{12}$ . In fact, with increasing  $\tau_{12}$ , the failure curve will shrink towards the point  $(\sigma_1 = 0, \sigma_2 = 0, \tau_{12} = S)$ , as shown

in Figure 3.1. These criteria thus make it impossible for the shear stress to be greater than  $S$ . This is not the case for the stresses  $\sigma_1$  and  $\sigma_2$  which can reach values higher than  $X$  and  $Y$ , except when this is specifically prevented with additional conditions, such as those specified by Norris, Equations (3-16).

The only way to account for different strengths in tension and compression in the above criteria is by using different constants in the equations, depending on whether the stresses are tensile or compressive. The entire failure envelope is therefore defined with four different portions of ellipse, one in each quadrant. Hoffman (1967) tried to improve Hill's failure condition by including more terms to take the possibility of unequal tensile and compressive strengths into account while still describing the failure envelope by a single equation. This was achieved by including linear terms in  $\sigma_1$ ,  $\sigma_2$ ,  $\sigma_3$  in Equation (3-10). His criterion contained nine strength parameters instead of six:

$$C_1(\sigma_2 - \sigma_3)^2 + C_2(\sigma_3 - \sigma_1)^2 + C_3(\sigma_1 - \sigma_2)^2 + C_4\sigma_1 + C_5\sigma_2 + C_6\sigma_3 + C_7\tau_{23}^2 + C_8\tau_{13}^2 + C_9\tau_{12}^2 = 1 \quad (3-22)$$

For plane stress conditions and transverse isotropy with respect to the 1-axis, this reduces to:

$$K_1(\sigma_1^2 - \sigma_1\sigma_2) + K_2\sigma_2^2 + K_3\sigma_1 + K_4\sigma_2 + K_5\tau_{12}^2 = 1 \quad (3-23)$$

where:

$$\begin{aligned} K_1 &= 1/XX' \\ K_2 &= 1/YY' \\ K_3 &= 1/X - 1/X' \\ K_4 &= 1/Y - 1/Y' \\ K_5 &= 1/S^2 \end{aligned} \quad (3-24)$$

Raghava and Caddell (1974) also proposed (3-22) as a failure criterion for an orthotropic polycarbonate. Because of the assumption of orthotropy, that equation becomes, in plane stress:

$$K_1 \sigma_1^2 + K_2 \sigma_2^2 + K_3 \sigma_1 + K_4 \sigma_2 + K_5 \tau_{12}^2 - 2K_6 \sigma_1 \sigma_2 = 1 \quad (3-25)$$

where the constants  $K_1$  to  $K_5$  are given by (3-24) and

$$K_6 = \left( \frac{1}{XX'} + \frac{1}{YY'} - \frac{1}{ZZ'} \right) \quad (3-26)$$

For a material transversely isotropic with respect to the 1-direction  $Y = Z$  and  $Y' = Z'$ , so that  $K_6 = 1/XX'$  and Equation (3-25) becomes identical to (3-23).

A generalization of the von Mises theory to orthotropic materials, taking into account different tensile and compressive strengths, has been proposed by Marin (1957). Assuming the reference axes to coincide with those of material symmetry and principal stress directions, this criterion is given as:

$$K_1 (\sigma_1^2 + \sigma_2^2) + K_2 \sigma_1 + K_3 \sigma_2 + K_4 \sigma_1 \sigma_2 > 1 \quad (3-27)$$

where:

$$\begin{aligned} K_1 &= 1/XX' \\ K_2 &= 1/X - 1/X' \\ K_3 &= 1/Y - Y/XX' \\ K_4 &= \left[ \frac{2}{XX'} - \frac{1}{S^2} + \frac{1}{S} \left( \frac{1}{X} - \frac{1}{X'} - \frac{1}{Y} + \frac{Y}{XX'} \right) \right] \end{aligned} \quad (3-28)$$

This theory has two major disadvantages. First, it does not take into account the compressive strength in the 2-direction. More importantly, the hypothesis of coincidence of principal stress axes and the axes of material symmetry limits the range of applicable stresses since the shear stress  $\tau_{12}$  is ignored. According to this theory,  $\tau_{12}$  has no influence on the strength.

The three failure criteria proposed by Hoffman (3-23), Raghava and Caddell (3-25), and Marin (3-27), can all be written in the form:

$$A_1 \sigma_1^2 + A_2 \sigma_2^2 + A_3 \sigma_1 \sigma_2 + A_4 \sigma_1 + A_5 \sigma_2 + A_6 \tau_{12}^2 = 1 \quad (3-29)$$

This is the ~~general~~ equation for an ellipsoid in the space  $\sigma_1 - \sigma_2 - \tau_{12}$  symmetrical about the plane  $\tau_{12} = 0$ . As shown by Suhling et al. (1985), the center of that ellipsoid will be at  $(\sigma_{1C}, \sigma_{2C}, 0)$  where:

$$\begin{aligned} \sigma_{1C} &= \frac{A_3 A_5 - 2 A_2 A_4}{|A_3^2 - 4 A_1 A_2|} \\ \sigma_{2C} &= \frac{A_3 A_4 - 2 A_1 A_5}{|A_3^2 - 4 A_1 A_2|} \end{aligned} \quad (3-30)$$

These parameters are shown in Figure 3.2. The major axis of the ellipse will be oriented at an angle  $\delta$  with the 1-direction equal to:

$$\delta = \frac{1}{2} \arctan \left( \frac{A_3}{A_1 - A_2} \right) \quad (3-31)$$

The above parameters are shown in Figure 3.2. Like the other Hill-type criteria, increasing the value of  $\tau_{12}$  results in a shrunken ellipse centered about the same axis. Ultimately, these ellipses will converge towards the point  $(\sigma_1^C, \sigma_2^C, S_C)$  where  $S_C$  is given by:

$$S_C = S \left[ 1 + \frac{A_4^2}{4 A_1} + \frac{\left( \frac{A_3 A_4}{2} - A_1 A_5 \right)^2}{4 A_1 \left| \frac{A_3^2}{4} - A_1 A_2 \right|} \right]^{1/2} \quad (3-32)$$

Accordingly, for any ellipse not centered about the origin, the shear stress  $\tau_{12}$  at failure may reach a value  $S_C$  which is higher than the strength  $S$  in pure shear.

In this section, we have shown that all Hill-type failure criteria for plane stress have the shape of an ellipsoid symmetrical about

the plane  $\tau_{12} = 0$ . In some versions, the envelope is given by different portions of ellipsoids in each quadrant. The general form of these criteria can be represented by Equation (3-29). When  $A_4 = A_5 = 0$ , the ellipsoid or portion thereof is centered at the origin and the shear stress cannot exceed  $S$ . When  $A_4 \neq 0$  or  $A_5 \neq 0$ , the center of the ellipsoid is located at the point given by Equation (3-30), and the maximum shear at failure can exceed  $S$ . All criteria assume that the overall shape of the failure envelope is the same at different levels of the shear stress  $\tau_{12}$ , and that it shrinks as a function of  $\tau_{12}^2$ . All the criteria could actually be written as:

$$f(\sigma_1, \sigma_2) = 1 - \left(\frac{\tau_{12}}{S}\right)^2 \quad (3-33)$$

where the parameters of  $f(\sigma_1, \sigma_2)$  are fixed and calculated from the uniaxial strengths of the lamina with respect to its axes of material symmetry. With Ashkenazi's failure equation, one of these values also depends on the uniaxial strength of a lamina oriented at  $\theta = 45^\circ$ .

### 3.5 TENSOR POLYNOMIAL CRITERIA

In the 1960's, the idea that the mathematical model of a failure envelope of fibre-reinforced materials be invariant with respect to the choice of coordinate axes was advanced. It was also suggested that the model should have enough flexibility to describe a failure envelope of any shape. This motivated the use of tensorial notation, the stress state being characterized by a stress tensor, and the strength properties by scalar or tensorial quantities. It was recognized that a criterion of that nature should take into account different tensile and compressive strengths, and the dependence of the ultimate shear strength on



the direction of the applied shear stresses. Finally, it was stipulated that such a criterion should reduce to the well-established failure criteria for isotropic materials when provided with the appropriate strength properties.

A general failure criterion able to satisfy all these conditions was first proposed by Gol'denblat and Kopnov (1966) and was postulated as follows:

$$[F_i \sigma_i]^k + [F_{ij} \sigma_i \sigma_j]^\lambda + [F_{ijk} \sigma_i \sigma_j \sigma_k]^\mu + \dots = 1 \quad (3-34)$$

An infinite number of failure envelopes can be obtained with this criterion. However, the authors restrained their investigations to the special case with  $k = 1$ ,  $\lambda = 1/2$ ,  $\mu = -\infty$ . In plane stress, Equation (3-34) reduces to:

$$[F_1 \sigma_1 + F_2 \sigma_2] + [F_{11} \sigma_1^2 + F_{22} \sigma_2^2 + F_{66} \tau_{12}^2 + 2F_{12} \sigma_1 \sigma_2]^{\frac{1}{2}} = 1 \quad (3-35)$$

From uniaxial tests along the material axes of symmetry, the strength parameters are:

$$\begin{aligned} F_1 &= \frac{1}{2} \left( \frac{1}{X} - \frac{1}{X_T} \right) & F_{11} &= \frac{1}{4} \left( \frac{1}{X} + \frac{1}{X_T} \right)^2 \\ F_2 &= \frac{1}{2} \left( \frac{1}{Y} - \frac{1}{Y_T} \right) & F_{22} &= \frac{1}{4} \left( \frac{1}{Y} + \frac{1}{Y_T} \right)^2 \\ F_{66} &= \frac{1}{S^2} \end{aligned} \quad (3-36)$$

The interaction parameter  $F_{12}$ , found from positive and negative shear stresses applied to a lamina with its fibres at an angle  $\theta = 45^\circ$ , is

$$F_{12} = \frac{1}{8} \left[ \left( \frac{1}{X} + \frac{1}{X_T} \right)^2 + \left( \frac{1}{Y} + \frac{1}{Y_T} \right)^2 - \left( \frac{1}{S_{45}} + \frac{1}{S_{45}^T} \right)^2 \right] \quad (3-37)$$

The failure criterion of Malmeister (1966) can be obtained from (3-34) by simply putting all exponents equal to unity, that is:

$$F_1 \sigma_1 + F_{1j} \sigma_1 \sigma_j + F_{1jk} \sigma_1 \sigma_j \sigma_k + \dots = 1 \quad (3-38)$$

For the specific problem of plane stress, he suggested keeping only the terms up to the second order. This gives the following equation:

$$F_1 \sigma_1 + F_2 \sigma_2 + F_{11} \sigma_1^2 + 2F_{12} \sigma_1 \sigma_2 + F_{22} \sigma_2^2 + F_{66} \tau_{12}^2 = 1 \quad (3-39)$$

where the strength parameters  $F_1$  and  $F_{11}$  are found from uniaxial tests along the material axes of symmetry:

$$\begin{aligned} F_1 &= \left( \frac{1}{X} - \frac{1}{X^T} \right) & F_{11} &= \frac{1}{XX^T} \\ F_2 &= \left( \frac{1}{Y} - \frac{1}{Y^T} \right) & F_{22} &= \frac{1}{YY^T} \\ F_{66} &= \frac{1}{S^2} \end{aligned} \quad (3-40)$$

From a positive shear test on a lamina with fibres at an angle  $\theta = 45^\circ$ , the interaction parameter  $F_{12}$  is calculated as:

$$2F_{12} = \frac{F_1 - F_2}{S_{45}} + F_{11} + F_{22} - \frac{1}{S_{45}^2} \quad (3-41)$$

Among the researchers that have used the failure equation (3-38), some find the strength parameters  $F_i$  and  $F_{ij}$  from best-fitting techniques of experimental data, rather than calculating them from Equations (3-40) and (3-41).

Assuming that Hill's failure condition could be improved by the addition of linear terms and that the interactions between the stresses should not be fixed, Tsai and Wu (1971) proposed a criterion very similar to (3-38):

$$F_i \sigma_i + F_{ij} \sigma_i \sigma_j = 1 \quad (3-42)$$

The linear terms are kept to characterize the different strengths in tension and compression, while the quadratic terms provide an ellipsoid-

shaped surface in stress space. The cubic and higher terms are eliminated on the basis that they could result in an open failure envelope. Also, retaining these terms implies a large amount of experimental work to determine the numerous strength coefficients. Tsai and Wu did not assume a priori that the positive and negative pure shear strengths in the 1-2 plane would be identical. For the case of plane stress and transverse isotropy in the 1-direction, their criterion reduces to

$$F_1\sigma_1 + F_2\sigma_2 + F_6\tau_{12} + F_{11}\sigma_1^2 + F_{22}\sigma_2^2 + F_{66}\tau_{12}^2 + 2F_{12}\sigma_1\sigma_2 = 1 \quad (3-43)$$

where the strength parameters  $F_1$ ,  $F_2$ ,  $F_{11}$ ,  $F_{22}$  are given by (3-40) and

$$F_6 = \frac{1}{S} - \frac{1}{S^*} \quad F_{66} = \frac{1}{SS^*} \quad (3-44)$$

The value of the interaction parameter  $F_{12}$  must be determined from a biaxial test. Furthermore, to ensure that the failure surface is closed, the following relations must be satisfied

$$\begin{aligned} F_{11}F_{22} - F_{12}^2 &> 0 \\ F_{11}F_{66} &> 0 \\ F_{22}F_{66} &> 0 \end{aligned} \quad (3-45)$$

When this is so, the failure envelope is an ellipsoid which can still be more or less elongated and be oriented within a wide range of angles.

Since the tensor polynomial theory has gained wide acceptance, many attempts have been made to properly define the value of the interaction factor  $F_{12}$ . The influence of this parameter on the failure envelope was discussed recently by Suhling et al (1985). Tsai and Hahn (1981) defined an interaction parameter  $F_{12}^*$  as

$$F_{12}^* = F_{12} / \sqrt{F_{11}F_{22}} \quad (3-46)$$

and proposed that it have a fixed value of  $F_{12}^* = -1/2$ . This assumption is not based on physical grounds but is assumed quite arbitrarily and is not applicable to every material. Hoffman's theory (3-23), is a special case of the Tsai-Wu criterion (3-43), in which the interaction parameter is:

$$F_{12} = -1/(2 XX') \quad (3-47)$$

A theory that was first developed by Hankinson in 1921 to predict the strength of wood in compression was reintroduced by Cowin (1979) in order to calculate the coefficient  $F_{12}$ . The compressive strength of wood at an angle  $\theta$  with the grain was found empirically by Hankinson to be:

$$U_{\theta}' = \frac{X'Y'}{X' \sin^2 \theta + Y' \cos^2 \theta} \quad (3-48)$$

Cowin shows that this strength should also be given by:

$$U_{\theta}'^2 = \frac{(X'Y')^2}{(Y' \cos^2 \theta)^2 + (X' \sin^2 \theta)^2 + (X'Y' \cos \theta \sin \theta)^2 [2F_{12} + \frac{1}{S^2}]} \quad (3-49)$$

Equations (3-48) and (3-49) give

$$F_{12} = \frac{1}{XX'} - \frac{1}{2S^2} \quad (3-50)$$

To account for different strengths in tension and compression, Rowlands (1985) modifies Equation (3-50) as follows:

$$F_{12} = \sqrt{\frac{1}{XX'YY'}} - \frac{1}{2S^2} \quad (3-51)$$

In general, the value of  $F_{12}$  has been found to be very sensitive and dependent on the nature of the particular test employed. Estimating its value is still a debated question. Some authors, such as Narayanaswami and Adelman (1977), have suggested that this term be set

equal to zero. Even though good results are sometimes found from this simplifying assumption, no physical argument has been brought forward to explain why this term should vanish. A recent proposal by Wu and Stachursky (1984) puts

$$F_{12} = \frac{-1}{F_{11} + F_{22}} \quad (3-52)$$

Recent studies have suggested that the quadratic form of the tensor polynomial criteria was not flexible enough to describe the failure envelope of a lamina. Consequently, some investigators, (e.g. Tennyson et al. (1978)), have proposed retaining the cubic terms in (3-38). This gives

$$F_i \sigma_i + F_{ij} \sigma_i \sigma_j + F_{ijk} \sigma_i \sigma_j \sigma_k = 1 \quad (3-53)$$

For a lamina under plane stress, the assumption of equal shear strengths for positive and negative shear and tensorial symmetry leads to the following criterion:

$$\begin{aligned} F_1 \sigma_1 + F_2 \sigma_2 + F_{11} \sigma_1^2 + F_{22} \sigma_2^2 + F_{66} \tau_{12}^2 + 2F_{12} \sigma_1 \sigma_2 + 3F_{112} \sigma_1^2 \sigma_2 \\ + 3F_{221} \sigma_1 \sigma_2^2 + 3F_{166} \sigma_1 \tau_{12}^2 + 3F_{266} \sigma_2 \tau_{12}^2 = 1 \end{aligned} \quad (3-54)$$

In this equation, all terms  $F_i$  and  $F_{ij}$  associated with unidirectional loadings have the same values as given by (3-40) for the quadratic form of the polynomial criterion. However, all interaction terms must be recalculated. The determination of  $F_{12}$ ,  $F_{112}$ ,  $F_{221}$ ,  $F_{166}$  and  $F_{266}$  is not a straightforward matter. Tennyson et al. have proposed an iterative procedure involving biaxial strength tests and four constraint equations for each term. Another difficulty with the cubic form is that Equation (3-54) will not necessarily provide a closed failure surface. This criterion entails a great deal of experimental work and involves

five interaction parameters as opposed to the one parameter  $F_{12}$  for the quadratic criterion. Some authors such as Huang (1985) have used best-fitting techniques to find the strength parameters  $F_i$ ,  $F_{ij}$ ,  $F_{ijk}$ .

All the failure criteria discussed so far have been expressed in terms of stresses. If we assume linear elastic behaviour up to failure, they can all be transformed directly into strain space. Tsai and Hahn (1981) postulated the following general failure criterion in strain space analogous to (3-42)

$$G_i \epsilon_i + G_{ij} \epsilon_i \epsilon_j = 1 \quad (3-55)$$

where the strain parameters  $G_i$  and  $G_{ij}$  are obtained from a transformation of the stress strength parameters  $F_i$  and  $F_{ij}$ . This strain tensor criterion is sometimes preferred in analyses of laminates based on classical lamination theory, since the failure surface of a lamina in strain space is not influenced by its thickness.

In this section, failure criteria proposed by Gol'denblat and Kopnov (3-34), Malmeister (3-38), Tsai and Wu (3-42), Tennyson et al. (3-54), and Tsai and Hahn (3-55), were reviewed. Among these, the criteria of Tsai-Wu and Malmeister are those that have gained the widest acceptance to date. However, whether or not the interaction parameter  $F_{12}$  should be dropped is still a debated issue. Its value can be obtained from an appropriate biaxial strength test or by using one of Equations (3-46), (3-47), (3-50), (3-51) or (3-52). These criteria are of the quadratic form (3-29) and have the general shape of an ellipsoid in the space  $\sigma_1 - \sigma_2 - \tau_{12}$ , with the characteristics specified by Equations (3-30), (3-31), and (3-32). In contrast, the shape of the cubic failure envelope in a given plane  $\tau_{12}$  is not necessarily an ellipse and can conceivably be an open surface. All these criteria are symmetrical

with respect to the plane  $\tau_{12} = 0$  in stress space and can be written as:

$$f(\sigma_1, \sigma_2) = C - \left(\frac{\tau_{12}}{S}\right)^2 \quad (3-56)$$

where  $C$  is a constant equal to unity except for the cubic criterion where the value of  $C$  is given by:

$$C = \frac{1}{F_{66} + 3F_{166}\sigma_1 + 3F_{266}\sigma_2} \quad (3-57)$$

It can be seen from this equation that even if symmetry about the plane  $\tau_{12} = 0$  is maintained, the shape of the failure envelope in the direction  $\tau_{12}$  of the failure surface is no longer a unique function of the shear stress, as shown in Figure 3.3.

### 3.6 FAILURE MODE IDENTIFICATION

The failure modes usually considered for fibre-reinforced laminae are fibre breakage and matrix failure. The failure criteria presented in the previous two sections provide no information concerning the mode that causes the failure of the lamina. Figure 3.4 illustrates two procedures that are generally used to distinguish between the two principal modes. One method postulates that fibre breakage is triggered for every point on the failure envelope for which:

$$\sigma_1 > X \quad \text{or} \quad \sigma_1 < -X' \quad (3-58)$$

All other points indicate matrix failure. This procedure seems to be the most commonly used. The second approach postulates that fibre breakage is found for every point on the failure envelope that satisfies one of the conditions:

$$\begin{aligned} -Y'/X &< \sigma_2/\sigma_1 < Y/X \quad (\sigma_1 > 0) \\ -Y/X' &< \sigma_2/\sigma_1 < Y'/X' \quad (\sigma_1 < 0) \end{aligned} \quad (3-59)$$

The relative proportions of matrix failure and fibre damage on a given envelope depend on the particular procedure employed.

Some failure criteria have been proposed that incorporate failure mode identification. Whitney et al. (1982) proposed using a maximum stress criterion to identify fibre failure together with a quadratic criterion in which the terms involving  $\sigma_1$  are deleted to identify matrix failure. This gives the two-fold criterion:

$$\begin{aligned} \sigma_1 &= X && : \text{fibre failure} \\ \left(\frac{1}{Y} - \frac{1}{Y^*}\right) \sigma_2 + \left(\frac{1}{Y^*}\right) \sigma_2^2 + \left(\frac{\tau_{12}}{S}\right)^2 &= 1 && : \text{matrix failure} \end{aligned} \quad (3-60)$$

Hashin and Rotem (1973) also postulated each failure mode to be independent of the other. Observing that for small lamina angles ( $\theta < 2^\circ$ ) the load is carried mainly by the fibres, failure in this direction is taken as a function of fibre strength only. For larger angles, the in-plane and transverse shear stresses increase, causing the growth of cracks parallel to the fibres. A study of experimental results justified the use of a second-order equation for good curve fits, insensitive to the direction of shear stress. This leads to the following criterion:

$$\begin{aligned} \sigma_1 &= X && : \text{fibre failure} \\ \left(\frac{\sigma_2}{Y}\right)^2 + \left(\frac{\tau_{12}}{S}\right)^2 &= 1 && : \text{matrix failure} \end{aligned} \quad (3-61)$$

where different values of  $X$  and  $Y$  are used in different quadrants. In a later publication, Hashin (1980) maintained the hypothesis of non-interactive failure modes and postulated that each mode could be modelled by a quadratic polynomial. Assuming transverse isotropy, with respect to the 1-direction, he specified that the criterion had to be invariant



under any rotation in the plane perpendicular to this axis. In plane stress, this led to the four-fold criterion:

$$\begin{aligned}
 \sigma_1 &= X' && : \text{fibre compressive failure} \\
 \left(\frac{\sigma_1}{X}\right)^2 + \left(\frac{\tau_{12}}{S}\right)^2 &= 1 && : \text{fibre tensile failure} \\
 \left(\frac{\sigma_2}{Y}\right)^2 + \left(\frac{\tau_{12}}{S}\right)^2 &= 1 && : \text{matrix tensile failure} \\
 \left(\frac{1}{Y'}\right)\left[\left(\frac{Y'}{2S_T}\right)^2 + 1\right] \sigma_2 + \left(\frac{\sigma_2}{2S_T}\right)^2 + \left(\frac{\tau_{12}}{S}\right)^2 &= 1 && : \text{matrix compressive failure}
 \end{aligned} \tag{3-62}$$

where  $S_T$  is the shear strength in the plane of isotropy.

Voloshin and Arcan (1980) developed a criterion similar to Equations (3-61) but with a dependence on the sign of shear stress. They also accounted for different tensile and compressive strengths using a single equation. Matrix failure is described by:

$$\frac{\sigma_2^2}{YY'} + \left(\frac{1}{Y} + \frac{1}{Y'}\right) \sigma_2 \tau_{12} + \left(\frac{\tau_{12}}{S}\right)^2 = 1 \tag{3-63}$$

Another criterion based on the Azzi-Tsai failure equation was proposed by Lifshitz (1982). He assumed that when matrix failure occurred, the properties and state of the fibres should not appear in the criterion. He suggested that the matrix load in the fibre direction be given by:

$$\sigma_1^m = \frac{E_1^m}{1 - \nu_{12}\nu_{21}} \epsilon_1 + \frac{\nu_{21} E_2}{1 - \nu_{12}\nu_{21}} \epsilon_2 \tag{3-64}$$

where  $E_1^m$  is the Young's modulus of the matrix in the 1-direction. For matrix failure, Azzi and Tsai's failure criterion is then rewritten as

$$\left(\frac{\sigma_1^m}{X_m}\right)^2 - \frac{\sigma_1^m \sigma_2}{X_m} + \left(\frac{\sigma_2}{Y}\right)^2 + \left(\frac{\tau_{12}}{S}\right)^2 = 1 \tag{3-65}$$

where  $X_m$  is the strength of the matrix in the 1-direction. Fibre breakage is still assumed to occur when  $\sigma_1$  reaches the value  $X$ .

Puck and Schneider (1969) have proposed a failure criterion that attempts to distinguish between three failure modes: fibre failure, matrix failure, and debonding at the fibre-matrix interface. The three modes are given by:

$$\sigma_1 = X_f \quad : \text{fibre failure}$$

$$\left(\frac{\sigma_1}{X_m}\right)^2 + \left(\frac{\sigma_2}{Y_m}\right)^2 - \frac{1}{3} \frac{\sigma_1 \sigma_2}{X_m Y_m} + \left(\frac{\tau_{12}}{S_m}\right)^2 = 1 : \text{matrix failure (3-66)}$$

$$\left(\frac{\sigma_2}{Y_i}\right)^2 + \left(\frac{\tau_{12}}{S_i}\right)^2 = 1 \quad : \text{adhesion failure}$$

where the subscripts f, m, i stand for fibre, matrix, and interface strength, respectively. This is apparently the only criterion that accounts for more than two failure modes.

The need to identify failure modes in the analysis of laminates has long been recognized. One approach to this problem consists of identifying the failure mode on a portion of a continuous envelope by means of expressions such as (3-58) or (3-59). This can also be done by writing new failure criteria that provide direct information concerning the nature of the damage. This is the case with the criteria proposed by Lifshitz (3-65), Whitney et al. (3-60), Hashin (3-61), (3-62), Voloshin and Arcan (3-63), Puck and Schneider (3-66). These criteria consist of piecewise functions where each section of the envelope corresponds to a particular failure mode. This requires that many equations be examined to check for the possible occurrence of failure.

It should be pointed out that for zero shear stress  $\tau_{12}$ , the criteria (3-60) to (3-63) reduce to four straight lines, as does the maximum stress criterion. Thus, no  $\sigma_1 - \sigma_2$  interaction is predicted contrary to experimental evidence. These criteria imply that the

overall shape of the failure envelope does not change as  $\tau_{12}$  varies. They can still be written in the form (3-33).

Both Voloshin's and Puck's failure criterion predict that the shape of the failure envelope changes as  $\tau_{12}$  is increased. With Voloshin's failure criterion, symmetry with respect to the plane  $\tau_{12} = 0$  can be achieved only if the absolute value of the shear is taken in (3-63).

### 3.7 FAILURE CRITERIA FOR LAMINATES

In the previous sections the various macroscopic failure criteria that have been proposed for fibre-reinforced laminae were reviewed. The use of these criteria in conjunction with classical lamination theory sometimes produces theoretical results quite different from experimental data. This is partially due to the fact that certain effects such as interlaminar stresses are neglected with this theory. Thus, although it is well-known that a variation of the stacking sequence can affect the strength of a laminate, classical lamination theory predicts the same strength under in-plane loading if the layers in a symmetric laminate are re-arranged in a symmetric fashion. Sometimes part of the difficulty lies in a poor correlation between experimental and theoretical failure envelopes of the individual laminae comprising the laminate. To counter these difficulties, failure criteria intended for direct application to the laminate as a whole have been developed.

For a general anisotropic lamina or laminate, Puppo and Evensen (1972) defined an interaction factor as follows:

$$Y = \frac{3 S^2}{XY} \quad (3-67)$$

where  $\gamma$  varies from  $\gamma = 0$  for non-interacting materials to  $\gamma = 1$  for isotropic materials. The authors also define the principal strength directions  $\xi$  and  $\eta$  of the material as those for which  $\gamma$  is a relative extremum. These directions do not necessarily coincide with the axes of orthotropy, nor are they required to be orthogonal. The strengths  $\Xi$ ,  $\Pi$ ,  $S_{\xi\eta}$  relative to principal strength axes are then used to define a new interaction factor  $\gamma'$  with respect to the directions  $\xi$ ,  $\eta$ :

$$\gamma' = \frac{3 S_{\xi\eta}^2}{\Xi \Pi} \quad (3-68)$$

This in turn is employed to define the following:

$$\begin{aligned} \left(\frac{\sigma_{\xi}}{\Xi}\right)^2 - \gamma' \left(\frac{\sigma_{\xi} \sigma_{\eta}}{\Pi^2}\right) + \gamma' \left(\frac{\sigma_{\eta}}{\Pi}\right)^2 + \left(\frac{\tau_{\xi\eta}}{S_{\xi\eta}}\right)^2 &= 1 \\ \gamma' \left(\frac{\sigma_{\xi}}{\Xi}\right)^2 - \gamma' \left(\frac{\sigma_{\xi} \sigma_{\eta}}{\Pi^2}\right) + \left(\frac{\sigma_{\eta}}{\Pi}\right)^2 + \left(\frac{\tau_{\xi\eta}}{S_{\xi\eta}}\right)^2 &= 1 \end{aligned} \quad (3-69)$$

These formulas are for  $\gamma' < 1$ . Another set of similar expressions is used when  $\gamma' > 1$ . When  $\gamma' = 1$ , Equations (3-69) reduce to the von Mises criterion for isotropic materials.

A cubic strength criterion similar to Equation (3-54) has also been proposed by Wu and Scheublein (1974) to describe the failure envelope for laminates. For a symmetric laminate with equal positive and negative shear strengths the criterion in plane stress reduces to:

$$\begin{aligned} F_1 \sigma_x + F_2 \sigma_y + F_{11} \sigma_x^2 + F_{22} \sigma_y^2 + F_{66} \tau_{xy}^2 + 2F_{12} \sigma_x \sigma_y \\ + 3F_{112} \sigma_x^2 \sigma_y + 3F_{221} \sigma_x \sigma_y^2 + 3F_{166} \sigma_x \tau_{xy}^2 + 3F_{266} \sigma_y \tau_{xy}^2 = 1 \end{aligned} \quad (3-70)$$

This criterion has the same drawbacks as the cubic criterion proposed for a single lamina, in that complicated iterative procedures are required to evaluate the interaction parameters  $F_{12}$ ,  $F_{112}$ ,  $F_{221}$ ,  $F_{166}$ ,  $F_{266}$ .

The values of  $F_1$ ,  $F_2$ ,  $F_{11}$ ,  $F_{22}$  and  $F_{66}$  can still be obtained from uniaxial strength tests in tension, compression and shear.

The idea of formulating a failure equation for an entire laminate is attractive because it eliminates the need for considering the stresses in each lamina, interlaminar stresses and delamination, as well as all the other effects that are not taken into account with classical lamination theory. On the other hand, with this approach it becomes necessary to perform a specific set of experiments for each possible laminate configuration. This is perhaps the main reason that this approach has been virtually abandoned in recent years.

### 3.8 NONLINEAR LAMINATE ANALYSIS

A number of investigators have tried to improve theoretical-experimental correlations by introducing nonlinear effects. Methods based on the maximum strain theory and on energy principles have been proposed. The first was developed by Petit and Waddoups (1969) and is based on uniaxial stress-strain data in tension and compression of the individual laminae along the axes of orthotropy as well as the shear stress-strain data. It also requires a knowledge of the variation of the Poisson ratio  $\nu_{12}$  with elongation. The procedure is incremental: small stress increments are applied to the laminate and the computed strain increments are added to the previous values. The individual lamina strains are then used to reevaluate the current laminate stiffness and compliance. Failure of a layer is detected using the maximum strain criterion, and the mode of failure identified accordingly. When failure is observed in a lamina, its modulus is set to a negative value until complete unloading of the lamina occurs. It is subsequently

assigned a negligible value to simulate zero stiffness. This permits a gradual load transfer from a failed lamina to its neighbours. The complete failure of a laminate is assumed to occur when its stiffness matrix either becomes singular or when one of its diagonal components becomes negative. This method is generally used in conjunction with classical lamination theory and as such neglects the effects of inter-laminar stresses.

Sandhu (1974) proposed a similar procedure but with a failure criterion based on the total strain energy rather than on maximum strain. This criterion is

$$f(\sigma, \epsilon) = \sum_{i=1,2,6} K_i \left[ \int_0^{\epsilon_{iu}} \sigma_i d\epsilon_i \right]^{m_i} = 1 \quad (3-71)$$

When experimental data is unavailable, the exponent  $m_i$  is usually taken as unity and the factors  $K_i$  are found from the following:

$$K_i = \left[ \int_0^{\epsilon_{iu}} \sigma_i d\epsilon_i \right]^{-1} \quad (\text{no sum on } i) \quad (3-72)$$

where the  $\epsilon_{iu}$ 's are the ultimate strains. Apart from the form of the failure criterion, the procedure suggested by Sandhu is identical to the one suggested by Petit and Waddoups.

### 3.9 EXPERIMENTAL CORRELATIONS

Although a significant number of failure criteria have been proposed to date for fibre-reinforced composites, the number of experimental studies performed to establish the validity of these criteria has been rather limited. This is largely due to the complexity of the biaxial tests that have to be carried out to determine the various strength parameters. The experimental determination of a complete failure envelope in the  $\sigma_1 - \sigma_2 - \tau_{12}$  space is very difficult and the

validity of existing failure criteria has rarely been demonstrated for more than a very limited range of stress combinations. A survey of published experimental results will be presented in this section.

A wide range of anisotropic, orthotropic, and transversely isotropic materials have been investigated over the years. A list of these materials can be found in Appendix 1. It includes various plastics reinforced with a diversity of fibres, as well as bone and derivatives of wood. It should be mentioned that many of the fibre-reinforced materials tested were fabricated by the experimentalist and that some of their properties are often not reported. In the following, we will discuss the different types of tests that were performed on these materials and determine their range of validity. Depending on the type of loading imposed on a single lamina, different portions of the failure envelope are obtained. These are shown in Figure 3.5.

### 3.9.1 Off-axis tests

This type of test is by far the simplest that can be performed on a single lamina. It consists of loading the lamina at an angle with respect to the orientation of the fibres until the failure load is attained (Figure 3.6). When a lamina is loaded at an angle  $\theta = 0^\circ$  or  $\theta = 90^\circ$ , the failure values fall directly on the axes  $\sigma_1$  and  $\sigma_2$ . When the lamina is loaded at any other angle  $\theta$ , the stresses  $\sigma_1$ ,  $\sigma_2$  and  $\tau_{12}$  are

$$\begin{aligned}\sigma_1 &= U_\theta \cos^2 \theta \\ \sigma_2 &= U_\theta \sin^2 \theta \\ \tau_{12} &= -U_\theta \sin \theta \cos \theta\end{aligned}\tag{3-73}$$

where  $U_\theta$  is the applied stress. In general, experimental results are

presented in terms of the maximum applied stress  $U_\theta$  versus the angle  $\theta$ .

Off-axis tests have been performed on a wide variety of materials, both in tension and in compression. They have been discussed in the following references:— Azzi and Tsai (1965), Cowin (1979), Hashin (1980), Pabiot (1970), Sokolov (1979,1978), Stanowsky (1985), Suhling et al. (1985), Tennyson (1981), Tsai and Wu (1971). The results typically show a very high strength in the direction of the fibres which decreases very rapidly with an increase in the angle  $\theta$ . The ultimate strength of the lamina is very sensitive to small changes of orientation  $\theta$  when this angle is small. When  $\theta$  is near  $90^\circ$ , the change of orientation does not have much influence on the maximum strength of the lamina. A theoretical evaluation of the uniaxial strength as a function of  $\theta$  can be found for each failure criterion. With the maximum stress criterion (3-7), failure occurs when one of the following three conditions is met:

$$\begin{aligned} U_\theta &= X/\cos^2\theta \\ U_\theta &= Y/\sin^2\theta \\ U_\theta &= S/(\sin\theta \cos\theta) \end{aligned} \quad (3-74)$$

For the maximum strain criterion (3-8), we have

$$\begin{aligned} U_\theta &= X/(\cos^2\theta - \nu_{12} \sin^2\theta) \\ U_\theta &= Y/(\sin^2\theta - \nu_{21} \cos^2\theta) \\ U_\theta &= S/(\sin\theta \cos\theta) \end{aligned} \quad (3-75)$$

For the Tsai-Hill criterion (3-14), the failure value is given by:

$$U_\theta = \left[ \frac{\cos^4\theta}{X^2} - \frac{\cos^2\theta \sin^2\theta}{X^2} + \frac{\sin^4\theta}{Y^2} + \frac{\sin^2\theta \cos^2\theta}{S^2} \right]^{-\frac{1}{2}} \quad (3-76)$$

The off-axis uniaxial loading of a lamina cannot be used to discriminate between the numerous failure theories as most theories can



accommodate very well all experimental results obtained with this test. This can be verified in the above references. An objection raised against the maximum stress criterion is that the first of Equations (3-74) actually predicts an increase of lamina strength for very small angle  $\theta$ , which in fact has not been observed experimentally. A tension test on an off-axis lamina induces bending and loss of a uniform plane stress condition. When bending is prevented, high stress concentrations are introduced at the corners of the lamina and these often precipitate premature failure. The applicability of this test is therefore of limited value for determining plane stress failure envelopes for laminae. On the failure envelope, the results of uniaxial off-axis tests fall on the lines illustrated in Figure 3.5.

A much less frequently performed test consists of measuring the shear strength of a lamina at different fibre orientations  $\theta$ . This test is more complicated to execute than the uniaxial test. A common procedure for unidirectional laminae consists of winding the filaments in a tube with the desired orientation, and then loading the tubes in torsion. In this case, the stresses in the material directions of symmetry are

$$\begin{aligned}\sigma_1 &= 2S_\theta \sin \theta \cos \theta \\ \sigma_2 &= -2S_\theta \sin \theta \cos \theta \\ \tau_{12} &= S_\theta (\cos^2 \theta - \sin^2 \theta)\end{aligned}\tag{3-77}$$

By substituting these values in a given failure criterion, one can determine the shear strength as a function of the angle  $\theta$ . Results from experiments of that type can be found in the following references: Cowin (1979), Sokolov et al. (1978), Tennyson (1981), Tsai and Wu (1971). In view of the inherent symmetries, a lamina tested from

$\theta = -45^\circ$  to  $\theta = 45^\circ$  under positive shear stresses provides the section of failure envelope shown in Figure 3.5.

The results of Tsai and Wu (1971) show considerable scatter in pure shear and are not well described by their criterion. For his set of results, Tennyson (1981) finds a better agreement when the cubic form of the tensor polynomial criterion is employed. However, some discrepancies between experimental and theoretical results still exist for the higher values of  $\theta$ . The data published by Sokolov et al. (1978) appear to be in better agreement with theory though the number of experimental points is very limited. The parameters of their failure criterion are calculated from a best-fit technique. Cowin (1979) uses results previously published by Ashkenazi for pine wood loaded with a combination of shear stresses and compares these with Hankinson's formula combined with Tsai-Wu's theory. Here again a least-square fit of the experimental data is made.

In short, the uniaxial off-axis test provides useful information but it cannot be utilized to discriminate efficiently between the various failure theories. The existing quadratic failure criteria do not generally provide a satisfactory correlation of the experimental results for the off-axis shear test. The inclusion of third-order terms in the tensor polynomial failure theory leads to an improved correlation.

### 3.9.2 Biaxial tests

Experimental failure envelopes for the portions of the surface that intersect the planes  $\tau_{12} = 0$ ,  $\sigma_1 = 0$ ,  $\sigma_2 = 0$  can be found in the literature. Curves in the plane  $\tau_{12} = 0$  have been obtained from series of biaxial tests on a lamina, with loads applied in the direction

of the principal material axes. This was done on flat specimens and also by means of internal pressure in a cylindrical tube combined with axial tension or compression. Both kinds of tests require sophisticated equipment. In the planes  $\sigma_1 = 0$  or  $\sigma_2 = 0$ , the curves can be obtained by applying torsion to a cylinder combined with axial tension or compression, a test that also requires sophisticated equipment. In most cases, because of the many complications involved with these experiments, only sections of the failure surfaces in these planes have been obtained.

Most results correspond to portions of the failure curve in the plane  $\tau_{12} = 0$ . They can be found in the following references: de Ruvo et al. (1980), Guess (1980), Huang (1985), Jones (1969), Maksimov et al. (1979), Owen et al. (1978,1981,1982), Skudra and Bulavs (1982), and Weng (1968). Weng (1968) has published results of biaxial loadings  $\sigma_1 - \sigma_2$  for a JT-50 graphite particulate, a material that exhibits transverse isotropy. Maksimov et al. (1979) have reported results for biaxial loadings in the plane  $\sigma_1 - \sigma_2$  for a glass-textolite, an organic textolite, and three hybrid composites containing organic fibres and glass fibres. They show results only for uniaxial tension, compression and pure shear at  $\theta = 45^\circ$ . Biaxial tension test results for the organic fibre composite were also reported at two different stress ratios. With this limited number of results, they obtained the parameters of Malmeister's failure criterion by a least-squares technique.

In a series of publications, Owen and co-workers (1978,1981,1982) studied the biaxial strength behaviour of different glass-fabric reinforced resins. They give an extensive comparison of results with ten existing failure criteria. For their materials, they conclude that the

failure criterion of Norris provides the best fit. However, they point out that the limited agreement between predictions and experimental results could only be obtained after a highly subjective selection of data.

The biaxial strength of paper was studied recently by de Ruvo and co-workers (1980). The two types of paper studied are anisotropic and their failure is compared to the maximum stress theory and to Tsai-Wu's tensor polynomial criterion in the biaxial tension quadrant. The latter theory gives the best approximation. Huang (1985) has recently published data for a transversely isotropic graphite of grade AGOT and stress combinations in the  $\sigma_1 - \sigma_2$  plane. His results are compared with the tensor polynomial theory and a reasonable curve fit can only be obtained if the cubic order terms are included.

In addition to the failure surface in the plane  $\tau_{12} = 0$ , some authors have also published experimental failure surfaces for the planes  $\sigma_1 = 0$  or  $\sigma_2 = 0$ . Hütter et al. (1974) compared their results for a glass-epoxy with the criteria of Tsai, Norris and Puck. Puck's criterion seems to give good agreement in the planes  $\sigma_1 - \sigma_2$  and  $\sigma_1 - \tau_{12}$ , but the agreement is not so good in the plane  $\sigma_1 = 0$ , especially when  $\sigma_2$  is compressive. The agreement in this plane is no better with the other two criteria. Plume and Maksimov (1979) reported a fair number of experimental points on the three surfaces for a woven fiberglass. With their curve-fitting technique, their failure criterion provided a good description of the results. The same comment applies to the results published by Sokolov (1979) which, with the exception of one point, all lie directly on the reference axes. Greenwood (1977), and Puck and Schneider (1969) have also published experimental failure surfaces for a

glass-epoxy in the plane  $\sigma_2 - \tau_{12}$ . These results are insufficient to judge the validity of the theoretical failure criteria, but they indicate a very good correlation in the investigated region.

The most popular of all the failure criteria suggested to date for composites is perhaps the tensor polynomial formulation advocated by Tsai and Wu (1971). An extensive experimental investigation using this criterion has been published by Wu (1974). He studied a fibre-reinforced epoxy lamina (Morganite II) by submitting it to uniaxial, biaxial, and uniaxial-shear load combinations with respect to the material directions. He also conducted a series of tests on a lamina under a combination of uniaxial and shear stresses for six different fibre orientations. This permitted a much more complete evaluation of the entire failure surface. In order to simplify the comparison of the failure criterion with experimental results, Wu used a convolution technique that allowed him to represent all the data in the plane  $\sigma_1 - \sigma_2$ . The agreement is very good. This work by Wu is one of the very few that provides an extensive experimental investigation of the failure surface of a lamina. The very good agreement shown in this early publication may explain the scarcity of subsequent experimental research on the problem.

The Tsai-Wu failure criterion is still widely discussed, primarily because of the difficulty encountered in determining the so-called "interaction parameter"  $F_{12}$ . This point has been studied by many authors, including Owen and co-workers (1978, 1981, 1982), Wu and Stachurski (1984), and Suhling et al. (1985). They all indicate that the off-axis uniaxial loading is unreliable for accurately determining  $F_{12}$ , since the strength prediction of a lamina under an off-axis uniaxial loading

is not very sensitive to the value of  $F_{12}$ . Suhling et al. (1985) discuss various methods for determining the value of  $F_{12}$  and illustrate the dramatic influence of this parameter on the shape of the failure envelope for paperboard. They also give a complete set of experimental results for biaxial loading of paperboard, combined with various shear loads.

In summary, there are not many extensive experimental results published for the determination of the failure surface of fibre-reinforced materials in the three-dimensional stress space  $\sigma_1 - \sigma_2 - \tau_{12}$ . The most complete studies in this area are those of Wu (1974a) and Suhling et al. (1985). There are, however, many published results for restricted portions of the failure envelope of a given material, very often limited to a single quadrant.

### 3.9.3 Failure mode identification

In all the references mentioned above, the validity of a given failure criterion was established by comparing experimentally obtained failure envelopes with theoretical criteria. Unfortunately, almost none of them report on the corresponding modes of failure. Although some of the proposed criteria account for the mode of failure (e.g. Puck and Schneider (1969) and Hashin (1980)), these investigators do not indicate whether the actual failure detected in a material corresponded to the predicted mode.

For a glass woven fabric-reinforced plastic, Owen and Rice (1981) indicated that failure occurred in two steps; the first being matrix cracking and the second fabric breakage. They indicate the values of the first failure as well as the ultimate strength of the composite for various load paths.

### 3.9.4 Laminate tests

In addition to experimental data for the failure of various laminates, the following references contain results from the testing of laminates: Francis et al. (1979), Guess (1980), Hütter et al. (1974), Ikegami et al. (1982,1983), Meshkov et al. (1982), Jones (1969), Skudra and Bulavs (1982), Tennyson et al. (1978,1981), Wu and Scheublein (1974).

Jones (1969) published experimental results for the biaxial tension of a glass-reinforced plastic laminate. The tested laminate was a cross-ply ( $0^\circ, 90^\circ$ ) and a maximum stress criterion appeared to give a good approximation for this portion of the laminate failure surface. The same set of results was used by Skudra and Bulavs (1982).

Hütter et al. (1974) gave a series of experimental points for a ( $90^\circ, 30^\circ, -30^\circ, 90^\circ$ ) glass-reinforced plastic laminate. Their results are well represented by Puppo and Evensen's failure criterion, except in the biaxial compression zone. In this region, the poor correlation is apparently due to laminate buckling.

Wu and Scheublein (1974) provided only five experimental points for a ( $0^\circ, 90^\circ$ )<sub>s</sub> graphite-epoxy laminate to verify the validity of their failure criterion. Francis et al. (1979) published experimental biaxial tension results for ( $0^\circ, 90^\circ$ ) cross-ply and ( $\pm 45^\circ$ ) angle-ply graphite-epoxy laminates. The first failure and ultimate strength of these laminates are well beyond the first-ply failure envelope obtained using the maximum strain criterion.

Tennyson et al. (1978,1981) tested ( $\pm \theta$ )<sub>s</sub> glass-epoxy and graphite-epoxy laminates. They published values for the failure pressure of a

laminated cylinder as a function of fibre orientation. Their analysis is complemented by the testing of  $(0^\circ, 60^\circ, -60^\circ)_s$  graphite-epoxy tubes under internal pressure and torsion. The agreement with the quadratic form of the tensor polynomial failure theory is not very good, but the inclusion of third-order terms improves the correlation considerably.

Ikegami and his co-workers (1982, 1983) used Hoffman's and Tsai-Wu's criteria to describe the failure surface of a glass-epoxy, a carbon fibre-reinforced plastic (CFRP), and a kevlar fibre-reinforced plastic (KFRP). In their investigation, they find that these failure criteria give a good representation of the lamina-failure surface in the planes  $\tau_{12} = 0$  and  $\sigma_1 = 0$ . However, the behaviour of different angle-ply laminates is not predicted successfully. For example, the theory predicts the highest tensile strengths of angle-ply laminates to occur when the fibres are oriented at  $\pm 15^\circ$ , which is not observed experimentally. The strength of angle-ply laminates under combined tensile and shear stresses also correlates poorly with theoretical predictions.

Guess (1980) performed tests on  $(30^\circ, -30^\circ, 90^\circ)_s$  cylindrical specimens of three different fibre-epoxy laminates. He compared his results with the maximum stress criterion and Hill's theory. Meshkov et al. (1982) gave a series of points for four different orientations of fibreglass laminates in the planes  $\tau_{12} = 0$  and  $\sigma_2 = 0$ . As is the case in most of the Soviet literature in the area, the parameters of the failure criterion are obtained by a least-squares technique. There are no experimental points given in the biaxial compression area of the failure envelope. In this publication, it is also not possible to relate the layer properties with those of the laminate.



In short, the number of experimental analyses on laminates is quite limited. In three references, Francis et al. (1979), Jones (1969), Meshkov et al. (1982), the layer properties are not given and cannot therefore be related to the laminate properties. In the other cases, the portion of the laminate failure envelope investigated is very limited. Moreover, there are significant discrepancies between experimental results and theoretical predictions of failure based on classical lamination theory. This may be attributed partially to the existence of failure modes that are not taken into account, such as delamination. However, when tubular specimens are tested, this effect should be limited. The discrepancies in this case might be attributed to the fact that: (i) most criteria do not identify clearly the mode responsible for failure and, (ii) the theoretical lamina failure criterion may not describe properly the real failure envelope of a single layer.

### 3.10 CONCLUSION

Over the last twenty years, a great number of failure criteria have been proposed for anisotropic materials, theoretically applicable to many materials including fibre-reinforced composites. They can be grouped under the following categories: maximum stress and maximum strain criteria, Hill-type criteria, tensor polynomial type or Tsai-Wu criteria, and criteria that include failure mode identification.

A recent survey (Soni, 1983) contends that the maximum stress and maximum strain criteria are the most widely used in design. The popularity of this approach seems to be based more on its relative simplicity than on its ability to accurately represent experimental data. In the

biaxial tension region, these criteria generally appear to be conservative. Moreover, the fact that the stress components in the material axes of symmetry are considered to be non-interactive does not corroborate most experimental observations.

The most popular of the interactive failure criteria is the one by Tsai and Wu (1971), Equation (3-42). In their original article, these authors show that the maximum stress and strain criteria, as well as all Hill-type criteria, are special cases of their tensor polynomial formulation. They suggested using terms up to the second order. This criterion can then be represented as an ellipsoid in the space  $\sigma_1 - \sigma_2 - \tau_{12}$ , Equation (3-29). Such an ellipsoid can also represent all Hill-type criteria and is symmetrical about the plane  $\tau_{12} = 0$ . For different values of the shear stress  $\tau_{12}$  the failure curve is an ellipse, but its size decreases as  $\tau_{12}$  increases. It can be represented by Equation (3-56). With criteria of that form, all but one of the strength parameters  $F_1$  and  $F_{ij}$  are usually calculated from the results of uniaxial tensile strength tests in tension, compression, and pure shear, in the principal directions of material symmetry. There is controversy, however, with regard to the calculation of the remaining parameter, the interaction term  $F_{12}$ . To ensure that the failure surface remains closed, this interaction parameter has to fall within the limits given by Equation (3-45).

Due to the very complicated nature of the tests that must be performed, most researchers have conducted experiments only on restricted portions of the entire failure envelope. The most comprehensive study of a graphite-epoxy lamina is the one by Wu (1974) for which the quadratic expansion of the tensor polynomial gives a good description of

the experimental results. A fairly complete experimental failure envelope for paperboard has been published very recently by Suhling et al. (1985) and Rowlands et al. (1985). Owen and his co-workers (1978,1981, 1982) have also presented significant sections of failure surfaces for fabric-reinforced epoxy. The last two investigations demonstrate the highly subjective interpretation of results that is necessary to obtain a good fit of the theoretical criteria with the experimental results.

The results of Ikegami (1982,1983) are also useful, especially when it is necessary to demonstrate the validity of a given failure criterion for laminae and angle-ply laminates. The results of Tennyson et al. (1978,1981) are also interesting contributions to the study of angle-ply laminates and provide useful information on the relation between lamina and laminate behaviour.

TABLE 3.1 - Tests on Uniaxial Laminae

---

$\theta$	: Orientation of the lamina with respect to the principal axis
----------	--

---

$X$	: Uniaxial tensile strength in the fibre direction
$X'$	: Uniaxial compressive strength in the fibre direction
$Y$	: Uniaxial tensile strength perpendicular to the fibres
$Y'$	: Uniaxial compressive strength perpendicular to the fibres
$S$	: Shear strength along the material axes of symmetry
$S_T$	: Transverse shear strength
$S_{45}$	: Positive shear strength of a $45^\circ$ off-axis lamina
$S'_{45}$	: Negative shear strength of a $45^\circ$ off-axis lamina
$P$	: On-axis equal biaxial tensile strength
$P'$	: On-axis equal biaxial compressive strength
$U_{45}$	: Uniaxial tensile strength of a $45^\circ$ off-axis lamina
$U'_{45}$	: Uniaxial compressive strength of a $45^\circ$ off-axis lamina
$U_\theta$	: Uniaxial tensile strength of a $\theta$ -degree off-axis lamina
$U'_\theta$	: Uniaxial compressive strength of a $\theta$ -degree off-axis lamina
$S_\theta$	: Positive shear strength of a $\theta$ -degree off-axis lamina
$S'_\theta$	: Negative shear strength of a $\theta$ -degree off-axis lamina

---

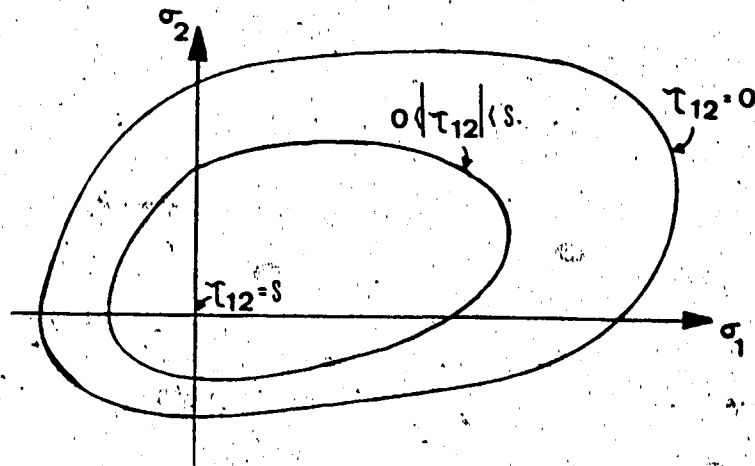


FIGURE 3-1 TYPICAL HILL-TYPE CRITERION WITH QUADRATIC TERMS

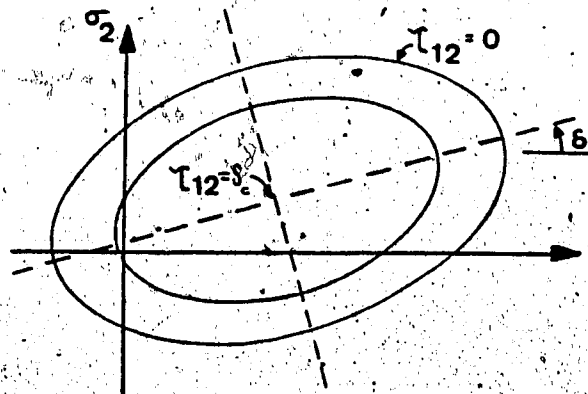


FIGURE 3-2 HILL-TYPE OR TENSOR POLYNOMIAL CRITERIA WITH LINEAR AND QUADRATIC TERMS

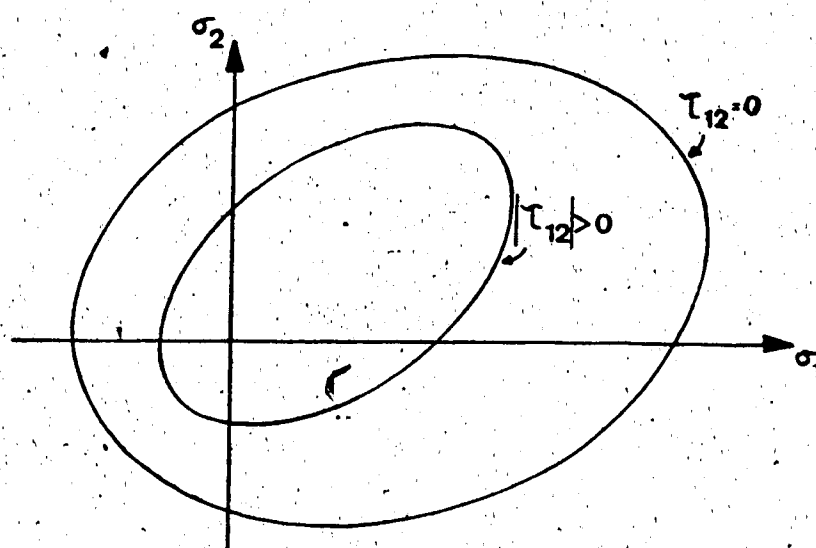


FIGURE 3-3 TYPICAL TENSOR POLYNOMIAL CRITERION WITH CUBIC TERMS

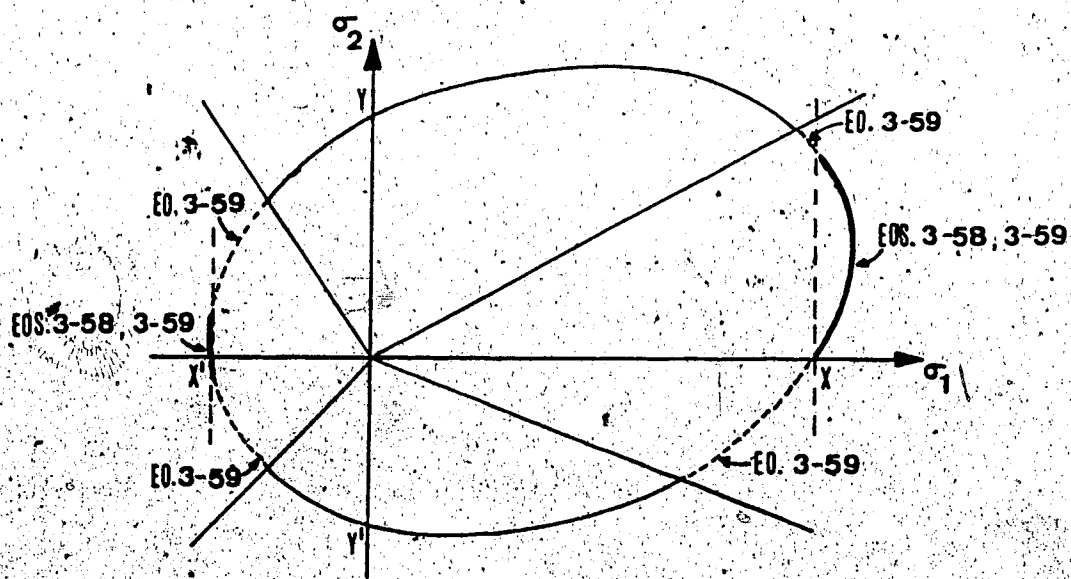
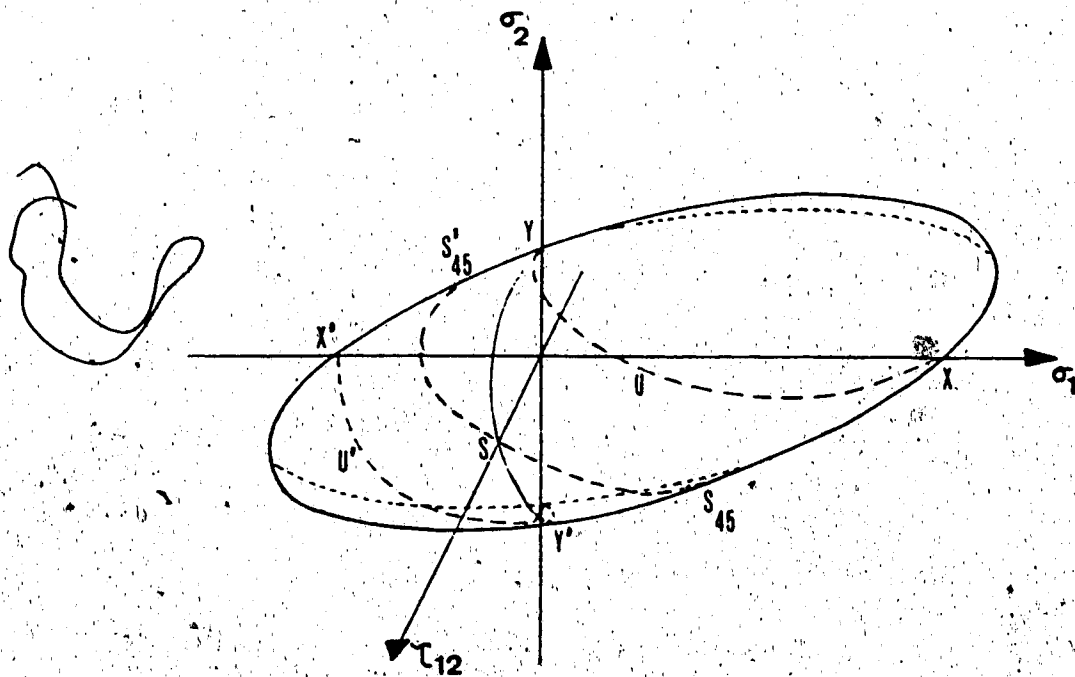


FIGURE 3-4 FIBRE FAILURE IDENTIFICATION



$Y - U - X$  OFF-AXIS TENSION  
 $Y' - U' - X'$  OFF-AXIS COMPRESSION  
 $S_{45} - S - S'_{45}$  OFF-AXIS SHEAR

FIGURE 3-5 LAMINA FAILURE ENVELOPE

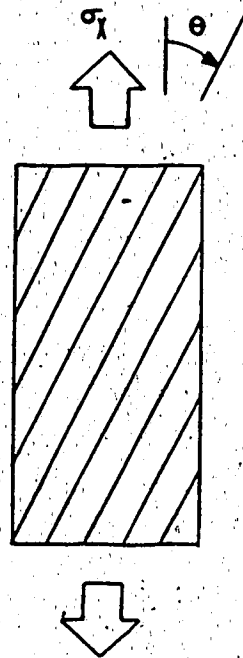


FIGURE 3-6 OFF-AXIS TENSION TEST



FIGURE 3-7 OFF-AXIS SHEAR TEST



## CHAPTER 4

### A NEW FAILURE CRITERION FOR FIBRE-REINFORCED MATERIALS

## CHAPTER 4

## A NEW FAILURE CRITERION FOR FIBRE-REINFORCED MATERIALS

## 4.1 INTRODUCTION

In the last chapter, a review of existing failure criteria for fibre-reinforced materials was presented. Structural components fabricated from these materials are usually thin plates loaded in their plane and failure theories are generally written for plane stress conditions. Among the failure criteria proposed to date for fibre-reinforced composites in plane stress, the maximum stress and maximum strain criteria are still the most widely used. This is mostly because they are relatively simple and easy to use. Also, simple hypotheses concerning failure modes can easily be associated with the failure values. However, more accurate theories are still needed, and among the existing criteria, the tensor polynomial theory has received the widest attention from researchers in recent years. This acceptance is due to the mathematical generality of the tensorial expression which can be manipulated according to well-established rules. Moreover, it has been shown that this form encompasses every failure criterion proposed previously for fibre-reinforced laminae.

The tensor polynomial equation can be expanded to any degree, but the most popular form now is the quadratic expansion. In plane stress, this leads to an ellipsoid-shaped failure envelope in the  $\sigma_1 - \sigma_2 - \tau_{12}$  space, symmetrical about the plane  $\tau_{12} = 0$ . This envelope can be defined from six strength parameters, five of which are calculated from simple tests on a lamina. The remaining parameter, referred to as the interaction term, is responsible for defining the orientation and length

of the major and minor axes of the ellipsoid and is usually calculated from a biaxial test. It has been found experimentally that the value of this interaction term is very dependent on the type of biaxial test performed. Actually, different tests can eventually lead to different values for the interaction parameter, and consequently define different failure envelopes. This suggests that an ellipsoid may not always be the proper way to describe analytically the experimental failure envelopes of a fibre-reinforced lamina.

This observation has led some authors to include the third-order terms of the polynomial in an attempt to obtain a better correlation between the experimental data and the theoretical curve. In that case, however, the gain in precision is obtained at the price of a significantly greater complication in the determination of the additional strength parameters of the failure envelope. In the plane stress case, there is now uncertainty on five interaction parameters instead of one with the quadratic expansion. Despite this serious difficulty, this approach seems to be the one that has received the most attention recently.

With the tensor polynomial theory tending to become increasingly complicated and difficult to handle with the inclusion of higher degree terms, it appears appropriate at this time to develop new and simpler failure theories. It is the purpose of this chapter to introduce a new failure criterion for fibre-reinforced laminae in plane stress. First, the essential conditions that have to be satisfied in developing this new criterion will be identified. Then, the general form of a new yield criterion that was proposed recently by Rudiansky (1984) for sheet

materials transversely isotropic in their plane will be presented. An extension of this criterion to describe failure of fibre-reinforced laminae will then be proposed and the generality of this new failure equation will be demonstrated.

#### 4.2 ESSENTIAL CHARACTERISTICS OF A FAILURE CRITERION FOR FIBRE-REINFORCED COMPOSITES

As explained previously in Sections 2.2 and 3.1, it is generally assumed that the unidirectional and bi-directional laminae considered here are under a state of plane stress. Therefore, they can be submitted in their lifetime to various combinations of in-plane tensile, compressive, and shear loadings. For a lamina that is not isotropic in its plane, not only the value of the applied loads but also their orientation with respect to the axes of maximum strength is important. As a matter of convenience, and also because it is normally expected that the maximum strength will be measured in the fibre directions, the material properties are usually measured with respect to the most easily identifiable axes, that is parallel and perpendicular to the fibre orientations. Also, since we assume homogeneity of the laminae, any arbitrary set of applied loads can easily be transformed into these principal material axes  $\sigma_1$ ,  $\sigma_2$  and  $\tau_{12}$  using Equations (2-9). The failure criterion shall then be written in terms of the stresses  $\sigma_1$ ,  $\sigma_2$  and  $\tau_{12}$ , and it will be represented graphically in this three-dimensional space. To ensure that the ultimate strength for any load combination is finite, this three-dimensional stress failure envelope must be a closed surface.

The distance from the origin of the system of axes to the failure envelope varies for each orientation of the vector  $\sigma_1 - \sigma_2 - \tau_{12}$ .

However, symmetries in the material properties, when there are any, should introduce symmetries in the failure envelope. For example, in the case of isotropic materials, the uniaxial tensile strength must be identical in any direction, and it is also common practice to assume an equal strength in uniaxial tension and compression. These two observations justify the symmetries with respect to the planes  $(\sigma_p + \sigma_q)$  and  $(\sigma_p - \sigma_q)$  for isotropic materials.

With unidirectional composites, the tensile and compressive strengths in the direction parallel to the fibres are normally different from those in the perpendicular direction. This rules out the possibility of symmetry with respect to the axis  $(\sigma_1 + \sigma_2)$  as well as to the planes  $\sigma_1 = 0$  and  $\sigma_2 = 0$ . This is confirmed from pure shear loadings of a lamina oriented at  $\theta = 45^\circ$ . According to the laws of stress transformation (2-9), a lamina with fibres oriented at an angle  $\theta = 45^\circ$  and under pure shear  $S_{45}$  is equivalent to a lamina under a set of combined axial loads  $\sigma_1 = -\sigma_2 = S_{45}$ . When the same lamina is oriented with the fibres at  $\theta = -45^\circ$  and with applied shear stresses  $S'_{45}$ , it is equivalent to the set of loads  $-\sigma_1 = \sigma_2 = S'_{45}$ . Since the strengths  $S_{45}$  and  $S'_{45}$  are generally different, this confirms the absence of symmetry about the plane  $(\sigma_1 + \sigma_2)$ . Similarly, by applying biaxial tension  $\sigma_1 = \sigma_2 = P$  or biaxial compression  $\sigma_1 = \sigma_2 = P'$ , and with the strength  $P$  generally differing from  $P'$ , it is found that there is no inherent symmetry with respect to the plane  $(\sigma_1 - \sigma_2)$ . These operations are illustrated in Figure 4.1. Therefore, for a material transversely isotropic in the 1-direction, all the symmetries that were usual for isotropic materials have been removed. This leads to the conclusion that there are no inherent symmetries of the failure envelope relative to the axes  $\sigma_1$  and  $\sigma_2$ .

As Figure 4.2 indicates, a lamina under pure shear with respect to its principal directions should possess the same strength whether the shear is positive or negative. Also, if a lamina with a positive fibre angle  $\theta$  is submitted to a positive shear stress, and a lamina of the same material with a negative angle  $-\theta$  to negative pure shear, both of them will exhibit the same ultimate strength value. In that case, following the laws of stress transformation to calculate the loads in the principal directions, it is found that they are identical in both cases except for the sign of the shear stress. This implies that the failure envelope must be symmetrical with respect to the plane  $\tau_{12} = 0$ . This is the only symmetry that is inherent to the material and it must be satisfied by any failure equation.

It is also desirable that the parameters of the failure criterion be expressed in terms of easy-to-measure strength characteristics. These are the tensile strengths  $X$ ,  $Y$ ,  $U_\theta$ ; the compressive strengths  $X'$ ,  $Y'$ ,  $U'_\theta$ ; the shear strengths  $S$ ,  $S_\theta$ ,  $S'_\theta$ ; the biaxial strengths  $P$  and  $P'$ . Of all these values, the tensile strengths along the principal material directions are the easiest to measure experimentally. For that reason, it was observed in Chapter 3 that most existing failure criteria are expressed in terms of the strengths  $X$ ,  $Y$ ,  $X'$ ,  $Y'$  and  $S$ . However, it should be pointed out that this is not an absolute requirement, and it may sometimes be more convenient to use other strength characteristics.

Finally, we recall from the previous chapter that the number of complete experimental failure envelopes published in the literature is rather limited. However, from the results published by Wu (1974a) for a graphite-epoxy and by Suhling et al. (1985) for a paperboard, one can assume as a first approximation that the failure envelope keeps the

same overall shape at different levels of constant shear stress  $\tau_{12}$ . This observation can be retained as an hypothesis for some materials and can eventually be included in a simplified failure criterion. Although a formal recognition of this has never been specified in the development of existing failure criteria, this hypothesis is implicitly verified in all non-interactive and all quadratic failure criteria proposed to date since all of them can be written in the form of Equation (3-33).

In summary, any plane stress failure criterion can be written in terms of the stresses  $\sigma_1$ ,  $\sigma_2$  and  $\tau_{12}$ . Its graphical representation in this three-dimensional space should not include in general any inherent symmetry except the one about the plane  $\tau_{12} = 0$ . The criterion parameters could be calculated from any combination of experiments, and not necessarily from uniaxial tensile or compressive tests in the lamina's principal directions. Finally, as a first approximation, the shape of the failure envelope at different levels of constant shear stress  $\tau_{12}$  could be identical but smaller in area than the one in the plane  $\tau_{12} = 0$ .

#### 4.3 BUDIANSKY'S YIELD CRITERION

Previous researchers have observed that the shapes of failure envelopes for fibre-reinforced materials were analogous to yield surfaces for ductile materials. As shown in Chapter 3, this led many to develop failure criteria for composites by extending yield criteria for metals. Among these, the yield criterion for orthotropic metals proposed by Hill has been modified by many authors in an attempt to describe the failure envelope of fibre-reinforced laminae. This was done by

substituting strength values in the lamina principal directions in place of the original yield values. It should then be emphasized that failure envelopes for composite laminae are not yield surfaces but rather strength surfaces. In this section, a recent yield criterion proposed by Budiansky (1984) will be presented, and in the following one, it will be extended in order to describe failure envelopes of fibre-reinforced materials.

In the area of sheet-metal forming, the effects of anisotropy are often important. Some sheets are transversely isotropic, with their plane of isotropy in the plane of the sheet-metal, and limited to plane stress conditions. This has motivated the development of yield criteria especially applicable to these materials and loading conditions. The yield criterion of Hill, Equation (3-10), originally written for anisotropic materials, has been used for that purpose by reducing the appropriate parameters to the transversely isotropic case. Since this original proposal, Hill (1979) has also introduced a set of new yield criteria applicable to anisotropic materials. A new yield criterion for a sheet-metal under in-plane load in its plane of isotropy has also been introduced recently by Budiansky (1984). The latter shows that all the previously proposed criteria are all special cases of his generalized yield surface.

Assuming that the sheet-metal is isotropic in its plane and submitted only to in-plane load, the Budiansky yield criterion is written in terms of the two principal stresses in the plane,  $\sigma_p$  and  $\sigma_q$ . This formulation thus takes into account any possible in-plane shear. A general failure envelope in the normalized stress space  $\sigma_p - \sigma_q$  is illustrated in Figure 4.3. For such a material, there is automatically symmetry with respect to a plane oriented at  $45^\circ$  with the axis



$\sigma_p$ . Budiansky also considers the case of equal strength in tension and in compression. This causes further symmetry of the failure envelope, this time with respect to an axis oriented at  $-45^\circ$  with the reference axis  $\sigma_p$ . The  $45^\circ$  and  $-45^\circ$  axes of symmetry intercept the failure surface at the points of yield under biaxial tension  $\sigma_{bt}$  and under pure shear  $\sigma_s$ , respectively. This allowed Budiansky to postulate that any failure condition can be prescribed parametrically in the following polar coordinate form:

$$\begin{aligned} x &\equiv \frac{\sigma_p + \sigma_q}{2\sigma_{bt}} = g(\beta) \cos \beta \\ y &\equiv \frac{\sigma_q - \sigma_p}{2\sigma_s} = g(\beta) \sin \beta \end{aligned} \quad (4-1)$$

where the yield surface is given in the normalized coordinate system shown in Figure 4.4. In the equations above, the failure criterion  $g = g(\beta)$  is a function of the angle  $\beta$ . In his publication, Budiansky showed that all yield criteria previously proposed for isotropic materials are special cases of Equation (4-1). Moreover, this new parametric form can accommodate any shape of failure envelope, making it theoretically possible to describe precisely any experimental data. For example, he suggests that an experimental yield locus could be fitted with suitable expressions of the form:

$$g(\beta) = \sum_n a_n \cos(2n\beta) \quad (4-2)$$

where the  $a_n$  are constants. In the event that an equation such as the one above were chosen to describe the experimental data, enough terms would have to be included for good curve fitting. It would also be possible to fit different portions of the failure envelope within a range of angles  $\beta$  by different equations.

#### 4.4 A NEW FAILURE CRITERION FOR FIBRE-REINFORCED MATERIALS

In Chapter 3, it was explained that the original "yield" criterion of Hill had been modified to become a "strength" criterion applicable to fibre-reinforced laminae. The justification behind this transformation was that similarly shaped yield or strength surfaces are obtained experimentally for both problems. In this section, a similar operation will be performed on the Budiansky criterion described above with the purpose of extending its use to fibre-reinforced materials. In this case, when a loading condition falls outside the bounds of the envelope, it is assumed that a breakage of the lamina by one of the mechanisms described in Chapter 1 will occur, rather than yield.

In Section 4.2, it was established that the failure envelope of composite laminae under plane stress had to satisfy the two following conditions: (1) it must be a closed surface in the three-dimensional space  $\sigma_1 - \sigma_2 - \tau_{12}$ , and (2), it must be symmetrical with respect to the plane  $\tau_{12} = 0$ . A general failure envelope satisfying these conditions is shown in Figure 4.5. Only the upper half of the entire envelope is pictured, since a mirror image would appear on the negative side of the plane  $\tau_{12} = 0$ . The position of any point on this failure surface can be identified in the spherical coordinates system as:

$$\begin{aligned}\sigma_1 &= \rho(\alpha, \phi) \cos \alpha \sin \phi \\ \sigma_2 &= \rho(\alpha, \phi) \sin \alpha \sin \phi \\ \tau_{12} &= \rho(\alpha, \phi) \cos \phi\end{aligned}\tag{4-3}$$

where  $\rho(\alpha, \phi)$  is the magnitude of the vector going from the origin of the system of axes to the failure point for the given load combination, the angle  $\alpha$  locates the relative position of this vector with respect to the axes  $\sigma_1$  and  $\sigma_2$ , and  $\phi$  indicates its angular position relative

to the  $\tau_{12}$ -axis. These three parameters can be defined separately as functions of the stresses  $\sigma_1$ ,  $\sigma_2$  and  $\tau_{12}$ . The value of angle  $\alpha$  is given by:

$$\alpha = \arctan \left( \frac{\sigma_2}{\sigma_1} \right) \quad (0 < \alpha < 2\pi) \quad (4-4)$$

The angular position of the failure point from  $\tau_{12}$ -axis is given by:

$$\phi = \arccos \left[ \frac{1 + \frac{\sigma_1^2 + \sigma_2^2}{\tau_{12}^2}}{2} \right]^{1/2} \quad (0 < \phi < \pi) \quad (4-5)$$

The length of the vector going from the origin to the failure point is:

$$\rho(\alpha, \phi) = (\sigma_1^2 + \sigma_2^2 + \tau_{12}^2)^{1/2} \quad (4-6)$$

This value must be positive at any angle  $\alpha$  and  $\phi$ .

Since the angles  $\alpha$  and  $\phi$  are sufficient to identify the position of any stress vector  $(\sigma_1, \sigma_2, \tau_{12})$  in this three-dimensional space, the modulus of that vector can be specified as a function of angles  $\alpha$  and  $\phi$ , thus explaining the notation  $\rho(\alpha, \phi)$  above. Geometric consistency and symmetry with respect to the plane  $\tau_{12} = 0$  requires that the following equalities be satisfied for all the points:

$$\begin{aligned} \rho(\alpha, \phi) &= \rho(\alpha + 180^\circ, -\phi) \\ \rho(\alpha, \phi) &= \rho(\alpha, 180^\circ - \phi) \end{aligned} \quad (4-7)$$

The set of Equations (4-3) can therefore be seen as an extension of Budiansky's failure criterion applicable to fibre-reinforced laminae under plane stress. This new parametric failure criterion is given by  $\rho = \rho(\alpha, \phi)$  and is always a closed surface when appropriate functions of the angles  $\alpha$  and  $\phi$  are chosen. Many functions of these angles can be chosen to represent the failure surface. Once the function  $\rho = \rho(\alpha, \phi)$  is determined in the material axes of symmetry, it can be used to find the failure value for any stress combination using Equations (2-9).

#### 4.5 GENERALITY OF THE NEW FAILURE CRITERION

It has been demonstrated by Wu (1974a) that the tensor polynomial criterion, as expressed by Equation (3-38), encompasses all failure criteria suggested previously for fibre-reinforced laminae. It will now be shown that the tensor polynomial criterion is itself a special case of Equations (4-3) when the plane stress terms are retained. The tensor polynomial equation is written as:

$$F_1 \sigma_1 + F_{ij} \sigma_i \sigma_j + F_{ijk} \sigma_i \sigma_j \sigma_k + \dots = 1 \quad (3-38)$$

Substituting in this equation the values  $\sigma_1$ ,  $\sigma_2$  and  $\tau_{12}$  from Equation (4-3), we find that:

$$\sum_{k=1}^n \rho^k(\alpha, \phi) f_k(\alpha, \phi) = 1 \quad (4-8)$$

where  $n$  is the degree of the tensor polynomial expression. The constants  $F_1$ ,  $F_{ij}$ ,  $F_{ijk}$ , etc. are incorporated to the various functions  $f_k(\alpha, \phi)$ . To illustrate this, let's consider the second degree expansion of the tensor polynomial, or Tsai-Wu failure criterion, given as follows:

$$F_1 \sigma_1 + F_2 \sigma_2 + F_{11} \sigma_1^2 + F_{22} \sigma_2^2 + F_{66} \tau_{12}^2 + 2F_{12} \sigma_1 \sigma_2 = 1 \quad (3-43)$$

Substituting the three relations given by Equations (4-3) in this expression, we get

$$\rho(\alpha, \phi) f_1(\alpha, \phi) + \rho^2(\alpha, \phi) f_2(\alpha, \phi) = 1 \quad (4-9)$$

$$\text{where } f_1(\alpha, \phi) = F_1 \cos \alpha \sin \phi + F_2 \sin \alpha \sin \phi \quad (4-10)$$

$$f_2(\alpha, \phi) = F_{11} \cos^2 \alpha \sin^2 \phi + F_{22} \sin^2 \alpha \sin^2 \phi + F_{66} \cos^2 \phi + 2F_{12} \cos \alpha \sin \alpha \sin^2 \phi \quad (4-11)$$

In this case, the failure function is given by the positive value of the equation

$$\rho(\alpha, \phi) = \frac{-f_1(\alpha, \phi) \pm \sqrt{f_1^2(\alpha, \phi) + 4f_2(\alpha, \phi)}}{2f_2(\alpha, \phi)} \quad (4-12)$$

In the same way, the third degree expansion of the tensor polynomial, expressed as Tennyson's failure criterion of Equation (3-54), can be written under the following form:

$$\rho(\alpha, \phi) f_1(\alpha, \phi) + \rho^2(\alpha, \phi) f_2(\alpha, \phi) + \rho^3(\alpha, \phi) f_3(\alpha, \phi) = 1 \quad (4-13)$$

where  $f_1(\alpha, \phi)$  and  $f_2(\alpha, \phi)$  are given by Equations (4-10) and (4-11), and  $f_3(\alpha, \phi)$  is

$$\begin{aligned} f_3(\alpha, \phi) = & 3F_{112} \cos^2 \alpha \sin \alpha \sin^3 \phi + 3F_{221} \sin^2 \alpha \cos \alpha \sin^3 \phi \\ & + 3F_{166} \cos \alpha \sin \phi \cos^2 \phi + 3F_{266} \sin \alpha \sin \phi \cos^2 \phi \end{aligned} \quad (4-14)$$

Once again, it would be possible to write a function  $\rho = \rho(\alpha, \phi)$  that would coincide exactly with the cubic tensor polynomial equation.

Obviously, in the two examples above, the functions  $\rho = \rho(\alpha, \phi)$  are more complicated to write than the original tensor polynomial formulations. For higher than second degree tensor polynomial, the corresponding expression for  $\rho = \rho(\alpha, \phi)$  may not even be explicit. However, these examples were only intended to demonstrate the generality of the parametric function  $\rho(\alpha, \phi)$ , and also to show that the tensor polynomial theory is a particular case of Equations (4-3).

The mathematical relationships between the new failure functions (4-3) and the Budiansky criterion (4-1) are detailed in Appendix II, where it is shown that the latter is a special case of Equations (4-3).

#### 4.6 ALTERNATIVE PARAMETRIC CRITERIA

In Section 4.4, a new failure criterion for transversely isotropic materials was presented. This criterion was written in a parametric form and spherical coordinates were used. Depending on the values of the experimental data, it may be more convenient to use other spaces or coordinate systems. In this section, alternatives to Equations (4-3) will be presented using normalized systems of axes and cylindrical coordinates.

##### 4.6.1 Failure Criterion in Normalized Stress Space

For isotropic materials, it is common practice to represent the failure envelope in non-dimensional form. In that case, the shape of the failure envelope is not modified by this normalization process because the stresses along each axis are divided by the same constant, the ultimate strength in tension. For a transversely isotropic material, the results can be normalized by representing the failure stresses in the system of axes  $\sigma_1/X - \sigma_2/Y - \tau_{12}/S$ , although an effect of this operation is to modify the visual appearance of the failure envelope. This modification will depend on the ratio of the strengths  $X$ ,  $Y$  and  $S$  relative to each other. If the failure criterion is written in the normalized system of axes, the following set of equations, similar to Equations (4-3), are obtained:

$$\begin{aligned}\sigma_1/X &= \rho'(\alpha', \phi') \cos \alpha' \sin \phi' \\ \sigma_2/Y &= \rho'(\alpha', \phi') \sin \alpha' \sin \phi' \\ \tau_{12}/S &= \rho'(\alpha', \phi') \cos \phi'\end{aligned}\tag{4-15}$$

where the parameters  $\alpha'$ ,  $\phi'$  and  $\rho'(\alpha', \phi')$  are illustrated in Figure 4.6.

In terms of applied stresses and strengths  $X$ ,  $Y$  and  $S$ , these parameters are calculated as follows. The angle  $\alpha'$  identifying the position of the vector  $\rho'(\alpha', \phi')$  with respect to the axes  $\sigma_1/X$  and  $\sigma_2/Y$  is given by

$$\alpha' = \arctan \left( \frac{X \sigma_2}{Y \sigma_1} \right) \quad (0 < \alpha' < 2\pi) \quad (4-16)$$

The angular position of the same vector from the  $\tau_{12}/S$ -axis is

$$\phi' = \arccos \left[ 1 + \frac{S^2(Y^2 \sigma_1^2 + X^2 \sigma_2^2)}{X^2 Y^2 \tau_{12}^2} \right]^{-1/2} \quad (0 < \phi' < \pi) \quad (4-17)$$

Finally, the magnitude of the vector  $\rho'(\alpha', \phi')$  is

$$\rho'(\alpha', \phi') = \frac{1}{XYS} \left( \sigma_1^2 Y^2 S^2 + \sigma_2^2 X^2 S^2 + \tau_{12}^2 X^2 Y^2 \right)^{1/2} \quad (4-18)$$

The set of Equations (4-15) to (4-18) is another extension of Budiansky's criterion to the failure analysis of fibre-reinforced laminae in plane stress. As seen earlier for Equation (4-3), it can be shown that these expressions encompass the most general failure equation proposed to date, that is the tensor polynomial theory. Of course, for geometrical consistency, the selected failure equation  $\rho' = \rho'(\alpha', \phi')$  must also satisfy the following equalities:

$$\begin{aligned} \rho'(\alpha', \phi') &= \rho'(\alpha' + 180^\circ, -\phi') \\ \rho'(\alpha', \phi') &= \rho'(\alpha', 180^\circ - \phi') \end{aligned} \quad (4-19)$$

Equations (4-3) and (4-15) are both written in spherical coordinates. When  $\alpha$  is taken as a constant and the angle  $\phi$  varies, all the points lie on the same plane. As shown in Figure 4.7, this plane is perpendicular to the  $\tau_{12} = 0$  plane, passes through the axis  $\tau_{12}$ , and is oriented at an angle  $\alpha$  with respect to the  $\sigma_1$ -axis. In

the normalized space, the angle  $\alpha'$  also describes a similar plane. However, the same is not true of the angles  $\phi$  and  $\phi'$ : by giving a fixed value to the angles  $\phi$  and  $\phi'$ , the set of points obtained do not lie necessarily on the same plane  $\tau_{12}$ , except when  $\phi = 0^\circ$  and when  $\phi = 90^\circ$ . This is illustrated in Figure 4.8.

#### 4.6.2. Failure Criterion in Cylindrical Coordinates

Some authors published experimental failure surfaces at different values of the shear stress  $\tau_{12}$ . Moreover, since it has been suggested in Section 4.2 that the shape of the failure envelope may remain identical at different values of the shear stress  $\tau_{12}$ , it should be easy in that case to isolate "slices" of the failure surface at different shear stress levels. This could be achieved more conveniently if the failure criteria were written in terms of cylindrical, rather than spherical, coordinates. This is illustrated in Figure 4.9, where the failure envelope can be described parametrically in cylindrical coordinates as

$$\begin{aligned}\sigma_1 &= \psi(\alpha) \cos \alpha \\ \sigma_2 &= \psi(\alpha) \sin \alpha \\ \tau_{12} &= \tau_{12}\end{aligned}\tag{4-20}$$

where the new parameter  $\psi(\alpha)$  is the magnitude of the vector going from the  $\tau_{12}$ -axis to the failure point, in the plane of the shear stress  $\tau_{12}$ . The angle  $\alpha$  still indicates the orientation of that vector with respect to the  $\sigma_1$ -axis. In terms of the stresses  $\sigma_1$  and  $\sigma_2$ , the parameters  $\alpha$  and  $\psi(\alpha)$  can be written as follows:

$$\alpha = \arctan(\sigma_2/\sigma_1) \quad (0 < \alpha < 2\pi) \tag{4-4}$$

$$\psi(\alpha) = [\sigma_1^2 + \sigma_2^2]^{1/2} \tag{4-21}$$



The vector joining the origin of the system of axes to the failure point can be written as:

$$T(\alpha, \tau_{12}) = \left( \phi^2(\alpha) + \tau_{12}^2 \right)^{\frac{1}{2}} \quad (4-22)$$

A normalized system of axes could also be set in the space  $\sigma_1/X - \sigma_2/Y - \tau_{12}/S$ , as shown in Figure 4.10, and be described as follows:

$$\begin{aligned} \sigma_1/X &= \phi'(\alpha') \cos \alpha' \\ \sigma_2/Y &= \phi'(\alpha') \sin \alpha' \\ \tau_{12}/S &= \tau_{12}/S \end{aligned} \quad (4-23)$$

where

$$\phi'(\alpha') = \frac{1}{XY} \left( Y^2 \sigma_1^2 + X^2 \sigma_2^2 \right)^{\frac{1}{2}} \quad (4-24)$$

and

$$\alpha' = \arctan \left( \frac{X \sigma_2}{Y \sigma_1} \right) \quad (0 < \alpha' < 2\pi) \quad (4-16)$$

Finally, the equation

$$T'(\alpha', \tau_{12}/S) = \left( \phi'^2(\alpha') + (\tau_{12}/S)^2 \right)^{\frac{1}{2}} \quad (4-25)$$

is an expression of the radius from the origin of the system of axis to the failure point. Equations (4-20) and (4-23) can also be seen as extensions of Budiansky's formulation.

#### 4.6.3 Relationships between Spherical and Cylindrical Parametric Criteria

Since the expressions (4-3) and (4-20), (4-15) and (4-23) are only different mathematical representations of the same failure envelope, the failure surfaces in spherical and cylindrical coordinates are related to each other by means of the following equalities:

$$\phi(\alpha) = \rho(\alpha, \phi) \sin \phi = T(\alpha, \tau_{12}) \sin \phi \quad (4-26)$$

and

$$\phi'(\alpha') = \rho'(\alpha', \phi') \sin \phi' = T'(\alpha', \tau_{12}/S) \sin \phi' \quad (4-27)$$

In this section, it was shown that the failure envelope of a fibre-reinforced lamina can be represented in the three-dimensional space  $\sigma_1 - \sigma_2 - \tau_{12}$  in spherical coordinates with a function of the shape

$$f(\sigma_1, \sigma_2, \tau_{12}) = \rho(\alpha, \phi) \quad (4-28)$$

or in cylindrical coordinates by the function

$$f(\sigma_1, \sigma_2, \tau_{12}) = T(\alpha, \tau_{12}) \quad (4-29)$$

In Section 4.2, it was pointed out that some experimental results can justify the hypothesis that the failure curves keep the same shape at different levels of shear stress  $\tau_{12}$ , but vary in area. This hypothesis has not been taken into account yet in the development of the above expressions. However, when this hypothesis is valid, the following relation can be written:

$$T(\alpha, \tau_{12}) = \phi(\alpha) \Gamma(\tau_{12}) \quad (4-30)$$

where the function  $\phi(\alpha)$  is the radial distance from the  $\tau_{12}$ -axis to the failure point and  $\Gamma(\tau_{12})$  is a function of the shear stress which controls the area of the failure surface at various shear levels.

It can be verified that most of the failure equations presented in Chapter 3 are different expressions of Equation (4-30). The maximum stress and maximum strain criteria, which are non-interactive with the shear  $\tau_{12}$ , are automatically special cases of this new expression. All Hill-type criteria and all those providing failure mode identification, as well as the tensor polynomial up to the second degree, can be written as Equation (3-33), or:

$$f(\sigma_1, \sigma_2) = 1 - g(\tau_{12}) \quad (4-31)$$

where

$$g(\tau_{12}) = (\tau_{12}/S)^2 \quad (4-32)$$

Therefore, it is possible to demonstrate that these criteria are special cases of Equation (4-30). Since each criterion can be written as:

$$h(\sigma_1, \sigma_2, \tau_{12}) = 1 \quad (4-33)$$

and relation (4-31) can be rewritten as:

$$f(\sigma_1, \sigma_2) = 1/j(\tau_{12}) \quad (4-34)$$

$$\text{where } j(\tau_{12}) = 1/(1-g(\tau_{12})) \quad (4-35)$$

Equation (4-33) is then equivalent to:

$$h(\sigma_1, \sigma_2, \tau_{12}) = f(\sigma_1, \sigma_2)j(\tau_{12}) \quad (4-36)$$

which is similar to Equation (4-30) since the value of the angle  $\alpha$  depends only on  $\sigma_1$  and  $\sigma_2$ .

#### 4.6.4 Summary

Equations (4-3), (4-15), (4-20) and (4-23) are four different expressions for a failure criterion which satisfies the conditions defined in Section 4.2. If one assumes further that the overall shape of the failure function is not influenced by the shear stress  $\tau_{12}$ , Equation (4-30) is also an acceptable expression for the failure surface. It has also been shown in this section that most of the failure criteria reviewed in Chapter 3 are already special cases of this equation. In the remaining section of this chapter, it will be shown how these new expressions can be used to represent the experimental data.

#### 4.7 GUIDELINES FOR THE USE OF THE NEW FAILURE CRITERION IN EXPERIMENTAL STUDIES

In this section, it is assumed that the experimentalist has the capability to perform any required test on a given fibre-reinforced lamina. This includes uniaxial and biaxial tests, both tension and compression, as well as pure shear tests. It will be shown here that each type of test occupies a fixed angular position on the failure envelope, whatever the material characteristics. The position of these tests will be identified. From these observations, it will be possible to identify important tests to be performed on a lamina. A chart that can be used as a guideline to experimental studies will also be provided.

One hypothesis presented in Chapter 2 and kept throughout the analysis of fibre-reinforced laminae is to consider these as homogenous. Therefore, any in-plane loading condition can be transformed into components  $\sigma_1$ ,  $\sigma_2$ ,  $\tau_{12}$  in the principal material axes by using the stress transformation law, Equation (2-9). If a lamina with fibres oriented at an angle  $\theta$  is put under biaxial stresses  $\sigma_x$  and  $\sigma_y = a\sigma_x$ , Equations (4-4) to (4-6) can be transformed into

$$\alpha = \arctan \left[ \frac{\sin^2 \theta + a \cos^2 \theta}{\cos^2 \theta + a \sin^2 \theta} \right]^{-\frac{1}{2}} \quad (4-37)$$

$$\phi = \arccos \left[ 1 + \frac{(\sin^2 \theta + a \cos^2 \theta)^2 + (\cos^2 \theta + a \sin^2 \theta)^2}{(a-1)^2 \cos^2 \theta \sin^2 \theta} \right]^{-\frac{1}{2}} \quad (4-38)$$

$$\rho(\alpha, \phi) = \sigma_x \left[ (\cos^4 \theta + \sin^4 \theta)(1+a)^2 + (\sin^2 \theta \cos^2 \theta)(a+1)^2 \right]^{-\frac{1}{2}} \quad (4-39)$$

It can be seen from Equations (4-37) and (4-38) that the value of the angles  $\alpha$  and  $\phi$  is a function of the layer orientation  $\theta$ , and of the ratio between the applied stresses  $a = \sigma_y/\sigma_x$ . Hence, the values of  $\alpha$  and  $\phi$  are independent of the applied stress magnitude. The latter value is required only for the calculation of the function  $\rho = \rho(\alpha, \phi)$ . Since there are no restrictions on the value of  $\theta$  and  $a = \sigma_y/\sigma_x$ , it is possible to find any point on the failure envelope with an appropriate combination of these values. It is also true that any point identified by the parameters  $\alpha$  and  $\phi$  can be found from only one combination of  $a = \sigma_y/\sigma_x$  and  $\theta$ .

In the event that a combination of stresses  $\tau_{xy}$  and  $\sigma_x = b \tau_{xy}$  is applied to the fibre-reinforced lamina, Equations (4-4) to (4-6) can also be written as follows:

$$\alpha = \arctan \left[ \frac{b \sin^2 \theta - 2 \sin \theta \cos \theta}{b \cos^2 \theta + 2 \sin \theta \cos \theta} \right] \quad (4-40)$$

$$\phi = \arccos \left[ 1 + \frac{(b \cos^2 \theta + 2 \sin \theta \cos \theta + (b \sin^2 \theta - 2 \sin \theta \cos \theta)^2)^{1/2}}{(-b \sin \theta \cos \theta + (\cos^2 \theta - \sin^2 \theta))^2} \right]^{-1/2} \quad (4-41)$$

$$\rho(\alpha, \phi) = \tau_{xy} \left[ b^2 + (\cos^4 \theta + \sin^4 \theta + 6 \sin^2 \theta + \cos^2 \theta) + 2b (\sin \theta \cos^3 \theta - \cos \theta \sin^3 \theta) \right]^{1/2} \quad (4-42)$$

Once again, it is observed that the values of  $\alpha$  and  $\phi$  are independent of the applied stress magnitude, which is required only for the calculation of the function  $\rho = \rho(\alpha, \phi)$ . However, some points on the failure surface cannot be found by any combination of  $b = \sigma_x/\tau_{xy}$  and  $\theta$ : these are those of biaxial tension and biaxial compression.

The most frequent plane stress tests performed on a single lamina are summarized in Table 4.1. This table indicates clearly that the angular position of any test on the failure surface is totally independent of the material strength characteristics. It can also be noted that only two points on the failure surface are absolutely independent of the lamina orientation  $\theta$ : these are the equal biaxial tensile strength  $P$  and compressive strength  $P'$ . It seems then that experimentalists who have the capability to perform biaxial tests should try to measure these values because these are theoretically not influenced by a possible misorientation of the lamina with respect to the applied loads.

In order to write the failure function  $\rho = \rho(\alpha, \phi)$  directly in terms of the angles  $\alpha$  and  $\phi$ , one may choose to measure experimental data along planes of constant angles  $\alpha$  and  $\phi$ , as a way to deal with only one variable at a time. To simplify this task, Equations (4-37) and (4-38) can be represented graphically. The result is shown in Figure 4.11. The two axes of this graph are the angle  $\phi$  as abscissa, and the angle  $\alpha$  as ordinate. Plotted on this graph are lines of constant angle  $\theta$  and constant stress ratio  $a = \sigma_y/\sigma_x$ . For simplicity, only a few of these lines are shown. It can be observed that this figure is symmetrical with respect to the axis  $\phi = 0^\circ$ . It should be clearly understood, however, that this symmetry does not indicate any symmetry on the failure envelope itself since  $\rho(\alpha, \phi)$  and  $\rho(\alpha, -\phi)$  are not necessarily identical. This chart indicates only the relative angular position of experimental tests relative to each other. It can be verified that all lines of constant angle  $\theta$  converge towards the points  $P$  and  $P'$ , signifying that the same value of the equal biaxial strength should be measured for any lamina orientation  $\theta$ .

The position of some of the most commonly used tests on the failure surface are indicated in Figure 4.11. Most of them fall on the lines  $\phi = 90^\circ$  or  $\phi = -90^\circ$ , which correspond to zero shear stress  $\tau_{12}$ . For all uniaxial tests  $U_\theta$  or  $U'_\theta$  at various angles  $\theta$ ,  $a = 0$  can be substituted in Equations (4-37) and (4-38). In Figure 4.11, these tests correspond to the lines  $Y - U - X$  in tension and  $Y' - U' - X'$  in compression. Finally, it can also be observed that all the points on the actual failure surface correspond to a single point in Figure 4.9, except for the pure shear stress  $\tau_{12} = S$ . In fact, any value of  $\alpha$  on the vertical axis  $\phi = 0^\circ$  corresponds to this point.

A horizontal line in Figure 4.11 corresponds to a vertical plane containing the  $\tau_{12}$  axis on the failure surface such as the one illustrated in Figure 4.7. It is at an orientation  $\alpha$  relative to the  $\sigma_1$  axis. In Figure 4.11, the axis  $\alpha = 0$  represents the single point  $\tau_{12} = S$  on the actual failure envelope, that is the maximum shear stress in the material axis of symmetry. Any series of failure points on a horizontal line in Figure 4.9 thus lie on the same plane  $\alpha = \text{constant}$ . For example, biaxial tests on a layer with fibres at  $\theta = 45^\circ$  and any stress ratio  $a = \sigma_y/\sigma_x$  would give results on the failure surface along the line  $P' - U' - S - U - P$ . Similarly, pure shear tests on a lamina with any fibre orientation would indicate a failure point on the horizontal line  $S'_{45} - S - S_{45}$ . Besides the two special planes  $\alpha = 45^\circ$  and  $\alpha = -45^\circ$ , there is not any other plane that corresponds to a single layer orientation or a single test type.

An experimentalist who seeks failure points on the same  $\alpha$ -plane can draw a horizontal line at the corresponding value of  $\alpha$  in Figure 4.11 and perform any of the biaxial tests indicated along that line.

For example, if one investigates the failure surface at an angle  $\alpha = 18^\circ$ , the horizontal line at this level indicates that uniaxial tests ( $a=0$ ) on a lamina with fibres at an angle  $\theta = 30^\circ$ ,  $U_{30}$  and  $U'_{30}$ , as well as the pure shear stress  $\tau_{12} = S$  would fall on this surface. Similarly, one can decide to perform tests at constant angle  $\phi$  and therefore, any test along the vertical line corresponding to the chosen  $\phi$  angle could be selected. For example, the uniaxial strengths  $U_{30}$ ,  $U_{60}$ ,  $U'_{30}$  and  $U'_{60}$  could be measured if one chooses to perform tests to obtain details of the failure surface at an angle  $\phi = \pm 61^\circ$ . However, in this case, one should remember that, on the actual failure envelopes, these points do not generally fall on the same plane, as was illustrated in Figure 4.8, except when  $\phi = \pm 90^\circ$ .

A graph of  $\phi'$  and  $\alpha'$  can also be obtained. This figure, however, would be a distorted version of Figure 4.11 because it would also depend on the material characteristics  $X$ ,  $Y$  and  $S$ . Of course, such a chart cannot be of general use because it depends on material properties. It would be observed, however, that planes of constant angle  $\alpha'$  correspond to another plane of constant angle  $\alpha$  in Figure 4.11.

#### 4.8 CONCLUSION

In this chapter, the Budiansky yield criterion, recently proposed to describe plastic flow of transversely isotropic ductile materials, was presented. This criterion was originally developed for sheet metals with their plane of isotropy in the plane of the sheet. Following the same rationale that led to the adoption of Hill's yield criterion to describe failure of composite laminae, a new failure criterion for fibre-reinforced laminae in plane stress, inspired from the Budiansky



criterion, was then proposed. This new parametric criterion satisfies the essential characteristics presented in Section 4.2. It can be written in spherical coordinates, Equations (4-3), or in cylindrical coordinates, Equations (4-20), in the three-dimensional stress space  $\sigma_1 - \sigma_2 - \tau_{12}$ . It can also be represented in normalized stress space by Equations (4-15) or (4-23). When appropriate functions of the angles  $\alpha$  and  $\phi$  in the normal stress space, or  $\alpha'$  and  $\phi'$  in normalized stress space, are chosen, the failure surface is always closed.

It was shown that all failure criteria previously proposed are special cases of this new criterion. Specifically, any failure surface described by the tensor polynomial theory can be transformed to the new parametric criterion. If one assumes that the shape of the failure envelope remains the same but encloses different areas at different values of the shear stress  $\tau_{12}$ , the failure criterion can further be reduced to Equation (4-30).

Finally, it was shown that any point on the failure surface can be found from an appropriate combination of biaxial stresses and lamina orientation. These combinations are illustrated in Figure 4.11, which indicates the angular position of any biaxial test on the failure surface. This chart can be used as a guideline for experiments designed to implement the new failure criterion. Examples of application of the parametric failure criterion will be presented in the next chapter.

TABLE 4.1 - Angular Position of Some Experimental Tests on a Lamina

Equations (4-37) to (4-39)

Type	$a = \sigma_y / \sigma_x$	$\theta(^{\circ})$	$\alpha(^{\circ})$	$\phi(^{\circ})$	Strength
Uniaxial	0	0	0	90	$X$
		0	0	-90	$X'$
		30	18.4	$\pm 61.3$	
		45	45	$\pm 54.7$	$U, U'$
		60	71.6	$\pm 61.3$	
		90	90	90	$Y$
		90	90	-90	$Y'$
Biaxial	1	all	45	90	$P$
		all	45	-90	$P'$
Cylinder with internal pressure	0.5	0	26.6	$\pm 90$	
		30	85.5	$\pm 78.6$	
		45	45	$\pm 76.7$	
		60	54.5	$\pm 78.6$	
		90	63.4	$\pm 90$	
Pure shear	-1	0	-45	$\pm 90$	$S_{45}, S'_{45}$
		30	-45	$\pm 39.2$	
		45	-45	0	$S$
		60	-45	$\pm 39.2$	
		90	-45	$\pm 90$	$S'_{45}, S_{45}$

Equations (4-40) to (4-42)

Type	$b = \tau_{xy} / \sigma_x$	$\theta(^{\circ})$	$\alpha(^{\circ})$	$\phi(^{\circ})$	Strength
Pure shear	1	0	-45	0	$S$
		30	-45	$\pm 67.8$	
		45	-45	$\pm 90$	$S_{45}, S'_{45}$
		60	-45	$\pm 67.8$	
		90	-45	0	$S$

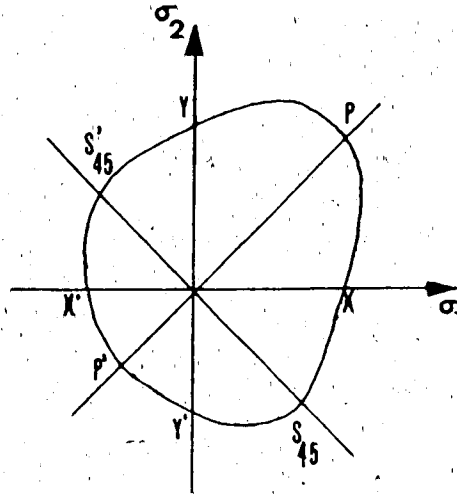


FIGURE 4-1 GENERAL FAILURE ENVELOPE FOR TRANSVERSELY ISOTROPIC MATERIALS ( $\tau_{12}=0$ )

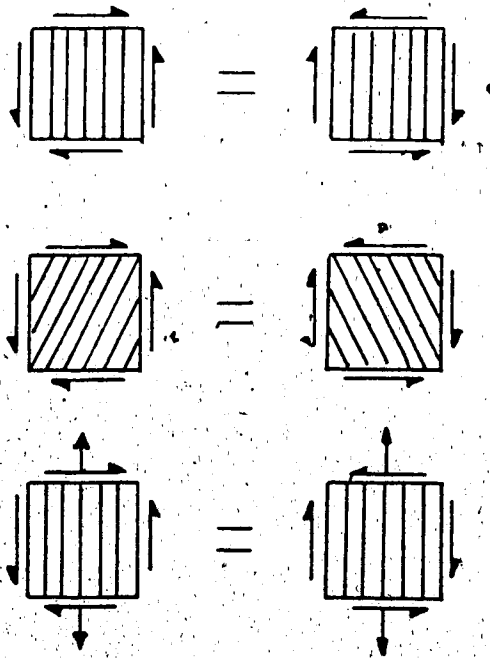


FIGURE 4-2 SHEAR STRENGTH SYMMETRY FOR UNIDIRECTIONAL LAMINAE

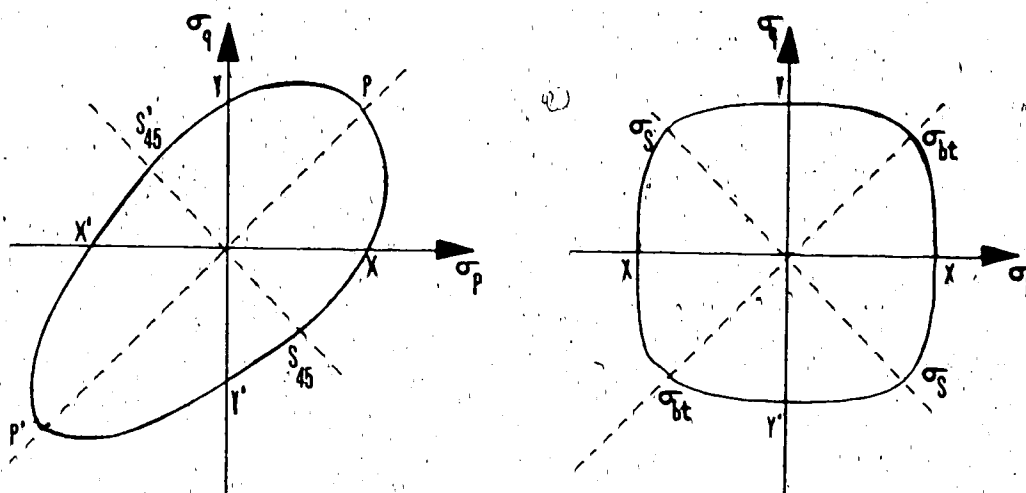


FIGURE 4-3 ISOTROPIC FAILURE CRITERIA

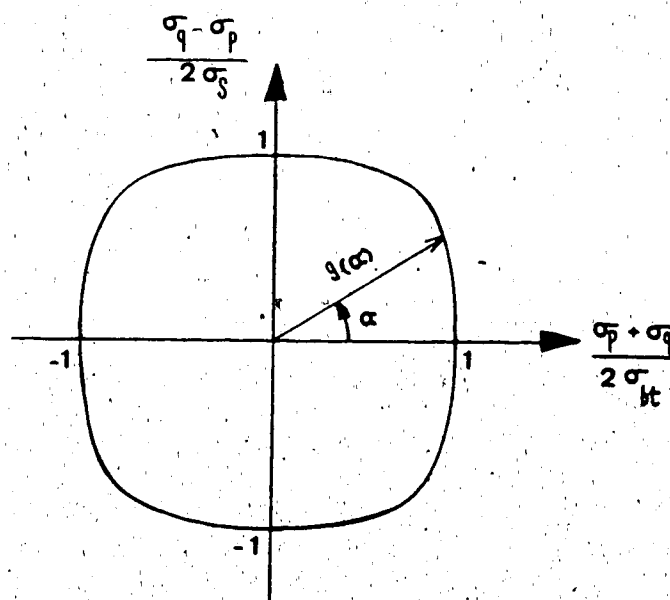


FIGURE 4-4 BUDIANSKY'S FAILURE CRITERION

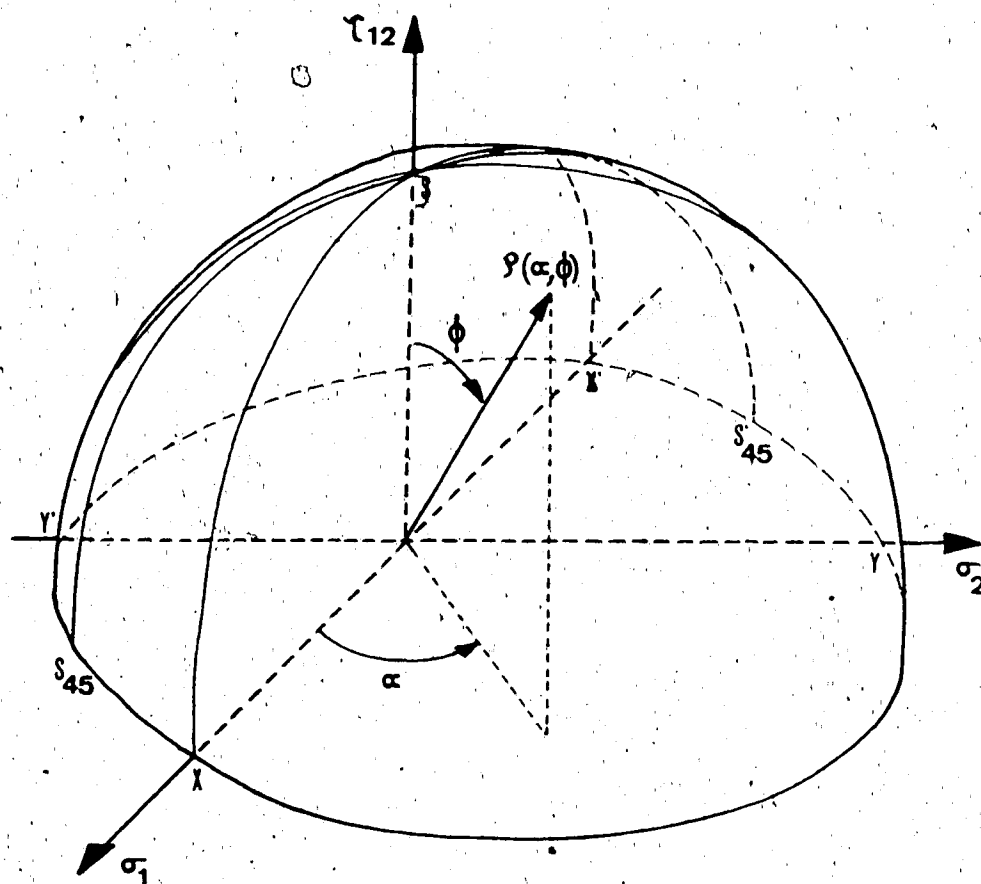


FIGURE 4-5 PARAMETRIC FAILURE ENVELOPE FOR  
FIBRE-REINFORCED MATERIALS

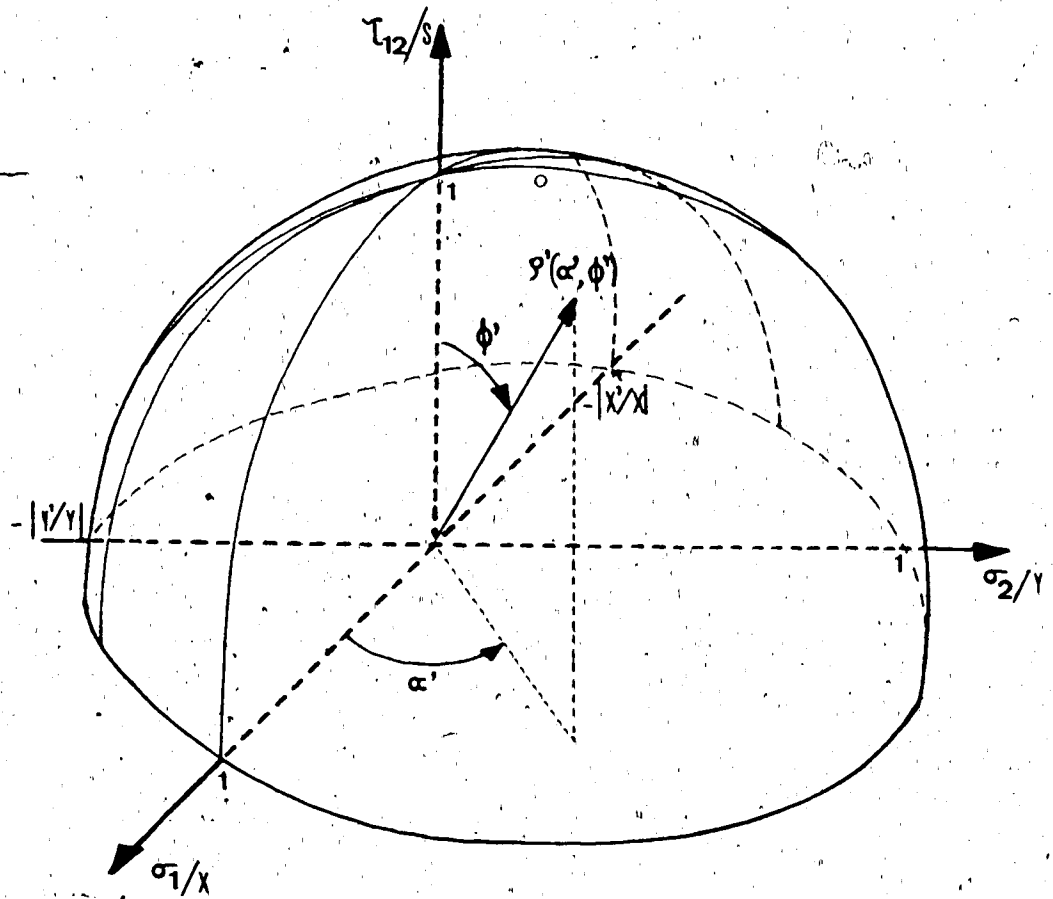
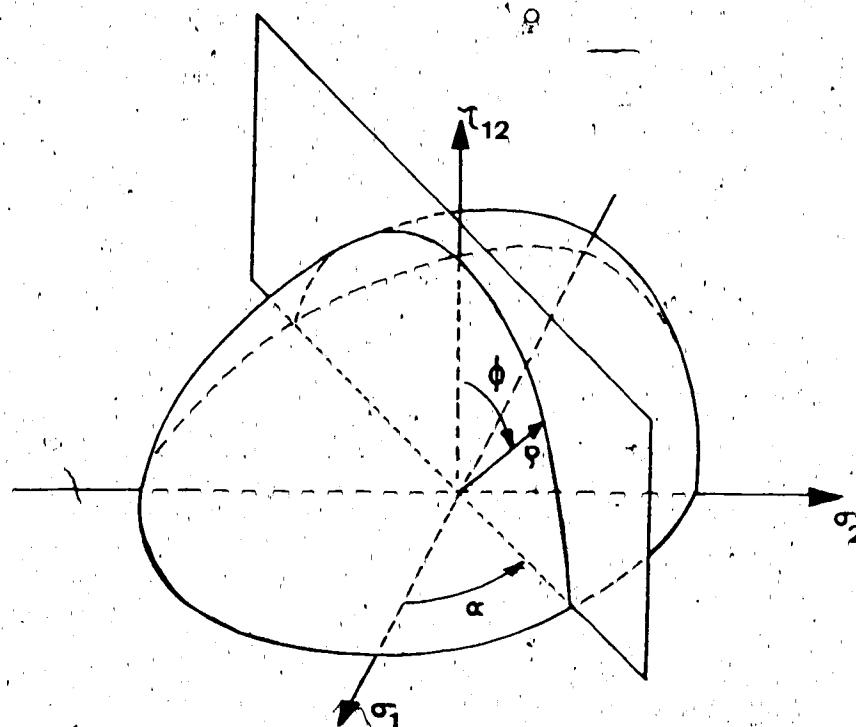
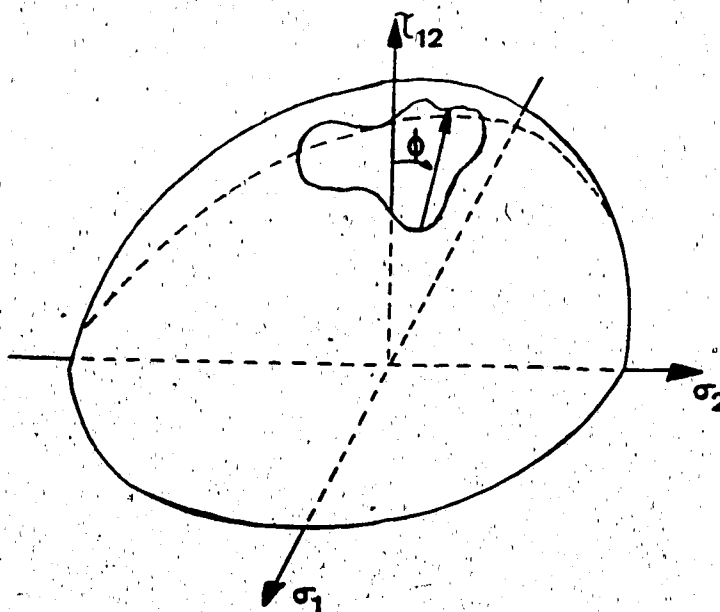


FIGURE 4-6 PARAMETRIC FAILURE ENVELOPE IN  
NORMALIZED COORDINATES

FIGURE 4-7 PLANE OF CONSTANT ANGLE  $\alpha$ FIGURE 4-8 PLANE OF CONSTANT ANGLE  $\phi$

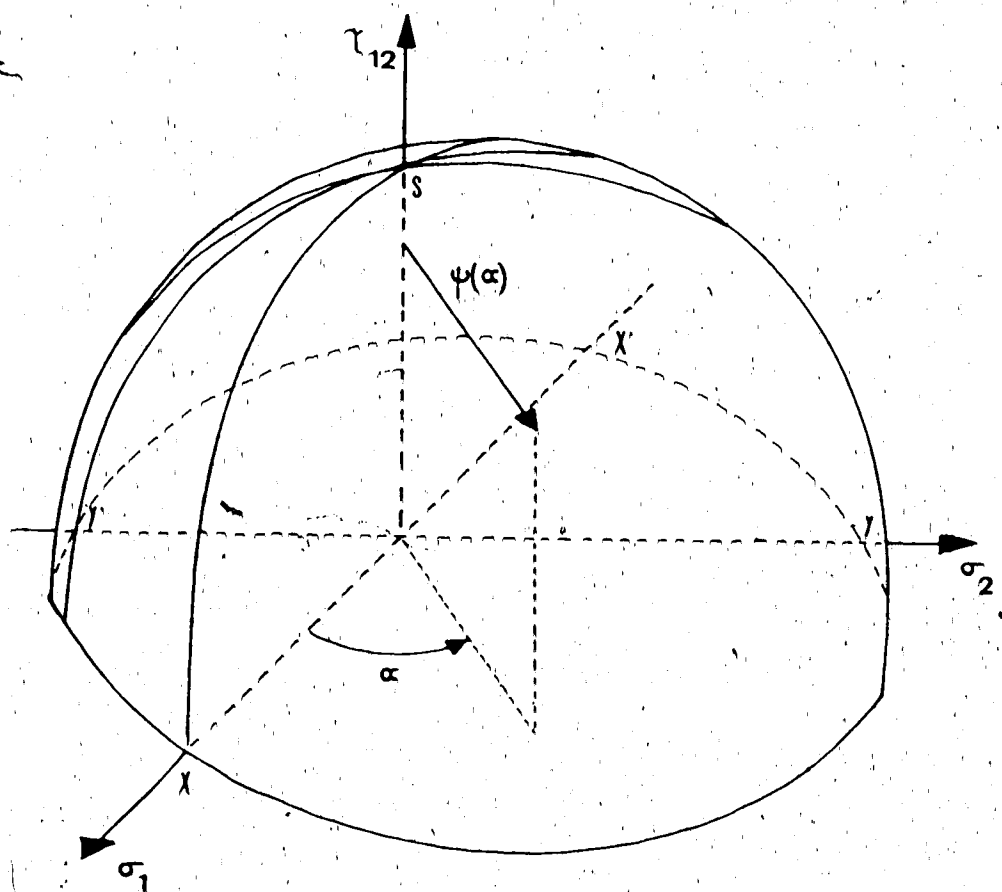


FIGURE 4-9 PARAMETRIC FAILURE ENVELOPE IN  
CYLINDRICAL COORDINATES



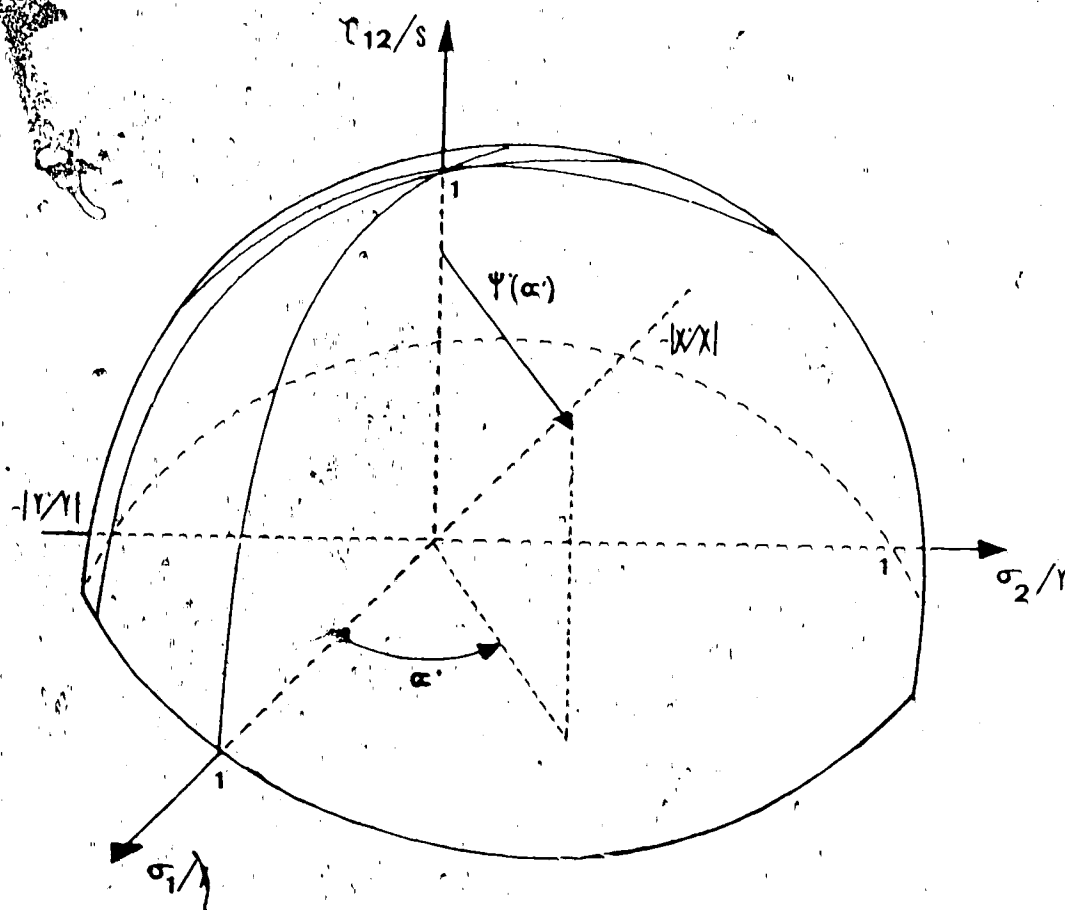
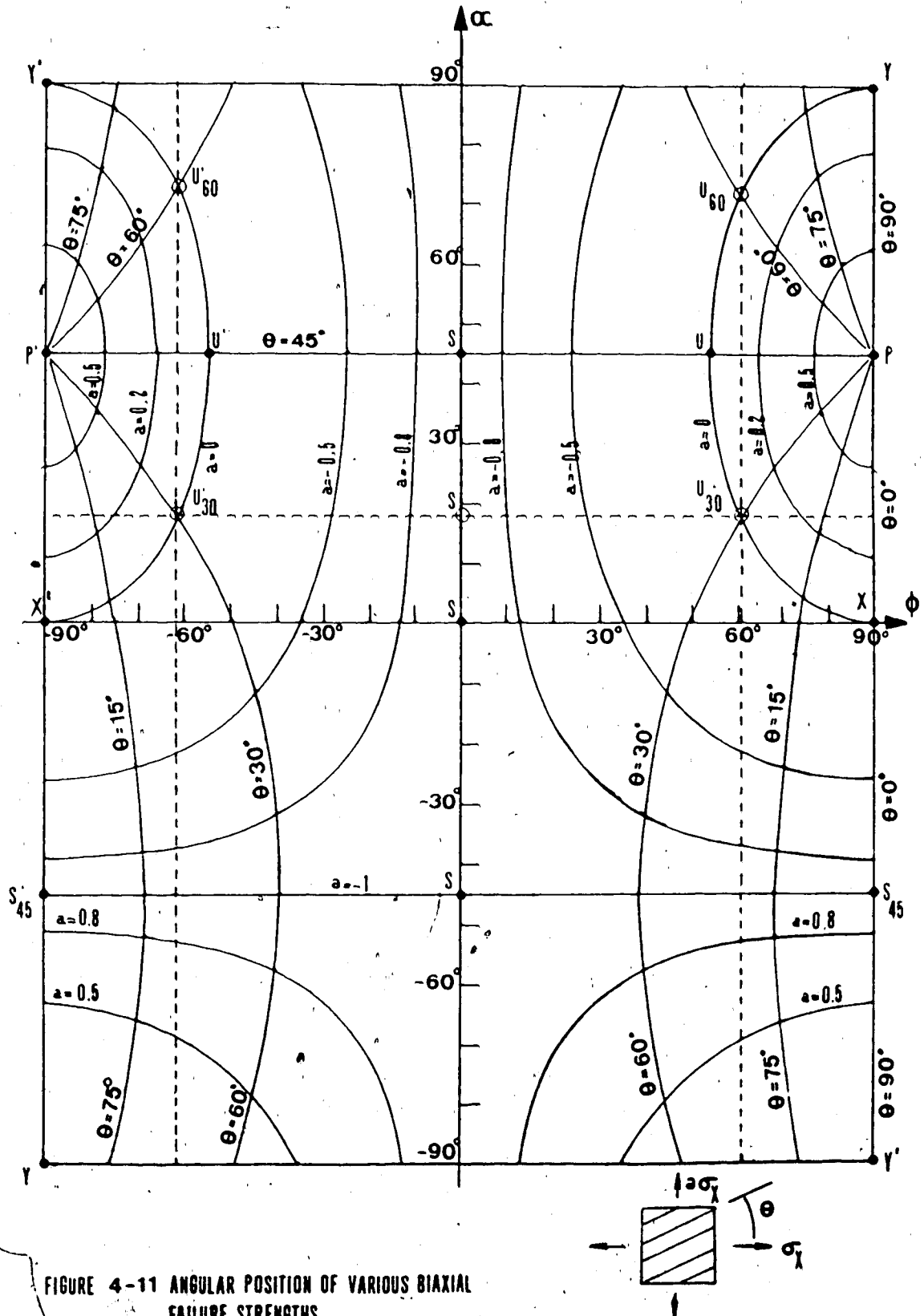


FIGURE 4-10 PARAMETRIC FAILURE ENVELOPE IN  
NORMALIZED AND CYLINDRICAL COORDINATES



## CHAPTER 5

### APPLICATIONS OF THE NEW FAILURE CRITERION

## CHAPTER 5

## APPLICATIONS OF THE NEW FAILURE CRITERION

## 5.1 INTRODUCTION

The validity of an analytical strength criterion can only be judged from the point of view of its ability to predict properly material failure under any loading condition. In this chapter, experimental data published by different authors, for a selection of fibre-reinforced and transversely isotropic materials in plane stress, will be used to demonstrate the applicability of the new failure criterion proposed in the previous chapter.

For most experimental studies published in the literature and discussed in Chapter 3, only small sections of the failure envelope have been investigated. For those experimental data that the quadratic failure criterion fits satisfactorily, there is no immediate need to use the parametric criterion. However, certain researchers who have found the quadratic tensor polynomial criterion inadequate have published data covering significant portions of the failure envelope. This is the case for the studies of Huang (1985), Tennyson and Wharram (1985), and Rowlands et al. (1985). These results will be used here in the section on single lamina examples to demonstrate the flexibility of the new parametric failure criterion. Different approaches to the determination of the failure equation  $\rho = \rho(\alpha, \phi)$  will be shown, depending on the type of experimental results available.

It often happens that a failure criterion appears to provide a good correlation with experimental results for a single lamina. However, when this criterion is combined with classical lamination theory

to predict laminate behaviour, the technique is not always accurate. This was the case in the work of Ikegami and Takahashi (1983). These results will be used in the section on laminate examples. It will be shown how laminate experimental data can be incorporated in the lamina analysis and how the failure criterion can be modified locally to better simulate these additional results.

## 5.2 EXPERIMENTAL-THEORETICAL CORRELATION

With a failure criterion  $\rho = \rho(\alpha, \phi)$ , many functions of the angles  $\alpha$  and  $\phi$  can be written, and the one that provides the best correlation with experimental results has to be selected.

In this chapter, a best-fit technique will sometimes be used to find the value of an undefined parameter in the failure criterion. This value minimizes the error between experimental data and the criterion and is calculated as follows. The error calculation method used is illustrated in Figure 5.1 where, as a matter of convenience, only the plane  $\tau_{12} = 0$  is shown. Considering that a lamina in plane stress would be loaded proportionally from the origin of the system of axes to the failure point, the total error between the experimental data and the parametric curve  $\sigma_1 - \sigma_2 - \tau_{12}$  will be defined as:

$$E_t = \sum_{n=1}^N (\rho_{*n}(\alpha, \phi) - \rho_n(\alpha, \phi))^2 \quad (5-1)$$

where  $N$  is the total number of experimental points,  $\rho_n(\alpha, \phi)$  is the predicted failure strength for the  $n^{\text{th}}$  loading path as calculated from the tested criterion, and  $\rho_{*n}(\alpha, \phi)$  is the radial distance from the origin of the system of axes to the  $n^{\text{th}}$  failure point.

When a failure criterion is written in the normalized space  $\sigma_1/X - \sigma_2/Y - \tau_{12}/S$ , the total error between the experimental data and the theoretical strength surface will be calculated as:

$$E'_t = \sum_{n=1}^N (\rho'_{*n}(\alpha', ') - \rho'_n(\alpha', '))^2 \quad (5-2)$$

where  $N$  is the total number of experimental points,  $\rho'_n(\alpha', ')$  and  $\rho'_{*n}(\alpha', ')$  are the theoretical and experimental failure points, respectively. Since there is no relationship between Equations (5-1) and (5-2), the best-fit of the same failure criterion may be obtained with different parameters, depending on which one of these equations is used to calculate the minimum error.

### 5.3 SINGLE LAMINA APPLICATIONS

#### 5.3.1 Example 1: Transversely Isotropic Graphite

##### a) Material description:

The results used in this section have recently been published by Huang (1985). These are for a porous and brittle graphite, referred to as a grade AGOT graphite. It is compressible and exhibits transversal isotropy in its plane. This material has been tested under a wide range of biaxial tensile and compressive loads. Neither pure shear nor combined shear-tension or shear-compression tests have been performed. The results are entirely in the plane  $\tau_{12} = 0$  and were presented graphically by the author. These results, as tabulated from the original figure, are listed in Table 5.1 and reproduced graphically in Figure 5.2. These data show considerable scatter, particularly in the fourth quadrant in which significantly different failure points along the same loading path have been measured. This observation is common for such

materials but in this case, the results in the fourth quadrant are apparently "disconnected" from the others. In the biaxial compression quadrant, there is also some scatter but it is relatively less important than in the fourth one.

In order to fit the experimental failure data with a single failure equation, Huang suggests using the Gol'denblat and Kopnov (1966) failure criterion with inclusion of cubic order terms:

$$\begin{aligned} (F_1\sigma_1 + F_2\sigma_2)^K + (F_{11}\sigma_1^2 + F_{22}\sigma_2^2 + 2F_{12}\sigma_1\sigma_2 + F_{66}\tau_{12}^2)^\lambda \\ + (F_{111}\sigma_1^3 + F_{222}\sigma_2^3 + F_{112}\sigma_1^2\sigma_2 + F_{122}\sigma_1\sigma_2^2 \\ + F_{266}\sigma_2\tau_{12}^2 + F_{66}\sigma_1\tau_{12}^2)^\mu = 1 \end{aligned} \quad (5-3)$$

Since no shear stress  $\tau_{12}$  is applied, this can be further reduced to the following expression:

$$\begin{aligned} (F_1\sigma_1 + F_2\sigma_2)^K + (F_{11}\sigma_1^2 + F_{22}\sigma_2^2 + 2F_{12}\sigma_1\sigma_2)^\lambda + (F_{111}\sigma_1^3 + F_{222}\sigma_2^3 \\ + F_{112}\sigma_1^2\sigma_2 + F_{122}\sigma_1\sigma_2^2)^\mu = 1 \end{aligned} \quad (5-4)$$

This equation contains twelve constants, but the author gives no indication about the method used to calculate these in order to fit the experimental data. In the work by Huang, two quadratic failure surfaces as well as Equation (5-4) were illustrated and are reproduced here in Figure 5.2. All three curves give a fairly good representation of the experimental data in the first three quadrants. Unfortunately, the expansion of the failure equation to cubic form did not really improve the simulation where it was the most important to obtain a better curve-fit, namely in the fourth quadrant. In view of the considerable amount

of work required to identify the twelve constants in Equation (5-4), we attempted to obtain much simpler and more satisfactory failure envelopes using the previously proposed parametric criterion.

b) First solution for Example 1:

Instead of the above cubic failure criterion, the new failure criterion proposed in Chapter 4 will now be used. Since experimental data are available in the plane  $\tau_{12} = 0$  only, Equation (4-30) will be easier to use:

$$T(\alpha, \tau_{12}) = \psi(\alpha) \Gamma(\tau_{12}) \quad (4-30)$$

A function such as

$$\Gamma(\tau_{12}) = 1 - \left(\frac{\tau_{12}}{S}\right) \quad (3-33)$$

is possible, but no experimental data can confirm the validity of this equation. However, since there are no data available to evaluate the function  $\Gamma = \Gamma(\tau_{12})$ , the following equality will be assumed:

$$\Gamma(\tau_{12}) = 1 \quad (5-5)$$

for all the points on the plane  $\tau_{12} = 0$ . The problem is now reduced to finding an acceptable expression  $\psi = \psi(\alpha)$  able to describe satisfactorily the set of experimental data.

The functions of the angle  $\alpha$  that will be assumed are the trigonometric functions  $\sin \alpha$  and  $\cos \alpha$ . A function that may be attempted is the following:

$$\begin{aligned} \psi(\alpha) = P_1 \cos \alpha + P_2 \sin \alpha + P_3 \cos^2 \alpha \\ + P_4 \sin^2 \alpha + P_5 \sin \alpha \cos \alpha \end{aligned} \quad (5-6)$$

where  $\alpha$  is the angle measured counterclockwise from the  $\sigma_1$ -axis. In this equation, the values  $P_1$  to  $P_5$  are constants to be determined



from experimental results. In order to include the uniaxial strengths in the principal material directions  $\sigma_1$  and  $\sigma_2$ , the following values for the constants are obtained:

$$\begin{aligned} P_1 &= \frac{1}{2} (X - X') & P_2 &= \frac{1}{2} (Y - Y') \\ P_3 &= \frac{1}{2} (X + X') & P_4 &= \frac{1}{2} (Y + Y') \end{aligned} \quad (5-7)$$

In principle, the remaining parameter  $P_5$  can be found from any test involving  $\sigma_1$  and  $\sigma_2$ .

For this case,  $P_5$  was found using the average shear strength  $S_{45}$ ,  $\psi(-45) = \sqrt{2} S_{45} = 3.017 \times 10^3$  psi. The theoretical failure envelope is then given by the following equation:

$$\begin{aligned} \psi(\alpha) &= -1.8665 \cos \alpha - 2.2940 \sin \alpha + 4.0165 \cos^2 \alpha \\ &\quad + 3.4940 \sin^2 \alpha + 2.0811 \sin \alpha \cos \alpha \end{aligned} \quad (5-8)$$

This equation is illustrated in Figure 5.3 together with the experimental data. This parametric failure envelope describes the failure data as efficiently as the quadratic and cubic failure equation shown in Figure 5.2, and only five parameters were required to obtain this result. The results in the fourth quadrant are still slightly overestimated in the region  $-90^\circ < \alpha < -60^\circ$ .

#### c) Second solution for Example 1:

Another possibility to describe the experimental data may be to fit a different failure equation in each quadrant rather than to write a single equation. In that case, the four sections of the failure surface must join together at the points X, X', Y and Y'. For example, a function such as

$$\psi(\alpha) = P |\cos \alpha|^E + R |\sin \alpha|^E \quad (5-9)$$

can be fitted to experimental data in each quadrant where  $P$  and  $R$  are uniaxial strengths bounding the quadrant and  $\xi$  is a real value to be determined in each quadrant. This produces the following set of equations:

$$\psi(\alpha) = X \cos^{\xi} \alpha + Y \sin^{\xi} \alpha \quad (0 < \alpha < \pi/2) \quad (5-10)$$

$$\begin{aligned} \psi(\alpha) &= Y \cos^{\xi}(\alpha - \pi/2) + X' \sin^{\xi}(\alpha - \pi/2) \\ &= Y \sin^{\xi} \alpha + X' (\cos \alpha)^{\xi} \quad (\pi/2 < \alpha < \pi) \end{aligned} \quad (5-11)$$

$$\begin{aligned} \psi(\alpha) &= X' \cos^{\xi}(\alpha - \pi) + Y' \sin^{\xi}(\alpha - \pi) \\ &= X' (-\cos \alpha)^{\xi} + Y' (-\sin \alpha)^{\xi} \quad (\pi < \alpha < 3\pi/2) \end{aligned} \quad (5-12)$$

$$\begin{aligned} \psi(\alpha) &= Y' \cos^{\xi}(\alpha - 3\pi/2) + X \sin^{\xi}(\alpha - 3\pi/2) \\ &= Y' (-\sin \alpha)^{\xi} + X \cos^{\xi} \alpha \quad (3\pi/2 < \alpha < 2\pi) \end{aligned} \quad (5-13)$$

For the graphite material discussed above, a different value for the exponent  $\xi$  has been found to best-fit the experimental data in each quadrant by using Equation (5-1). Substituting these values and those of  $X$ ,  $X'$ ,  $Y$  and  $Y'$  in the equations above, we obtain the following failure surface in four distinct regions:

$$\psi(\alpha) = 2.15 \cos^{1.844} \alpha + 1.2 \sin^{1.844} \alpha \quad (0 < \alpha < \pi/2) \quad (5-14)$$

$$\psi(\alpha) = 1.2 \sin^{3.430} \alpha + 5.8833 (-\cos \alpha)^{3.430} \quad (\pi/2 < \alpha < \pi) \quad (5-15)$$

$$\psi(\alpha) = 5.8833 (-\cos \alpha)^{1.190} + 5.7875 (-\sin \alpha)^{1.190} \quad (\pi < \alpha < 3\pi/2) \quad (5-16)$$

$$\psi(\alpha) = 5.7875 (-\sin \alpha)^{3.65} + 2.15 \cos^{3.65} \alpha \quad (3\pi/2 < \alpha < 2\pi) \quad (5-17)$$

These equations and the experimental data of Table 5.1 are reproduced in Figure 5.4. A very good curve fit has been obtained in the first three quadrants. In the third quadrant, the failure surface given by Equation

(5-16) is practically the same as the one obtained with the cubic Equation (5-4). The curve fit of the fourth quadrant with Equation (5-17) is, however, still unsatisfactory. This is due mainly to the very significant scatter of the experimental results along similar loading paths.

An alternate solution for the failure surface in the fourth quadrant can be obtained by supposing a linear relationship between the  $\sigma_1$  and  $\sigma_2$  stresses in the fourth quadrant only. Assuming that this failure equation should include the point  $\sigma_2 = -Y'$ , it would be written as follows:

$$\sigma_2 = -Y' + P\sigma_1 \quad (5-18)$$

For best-fitting of the points in the region where  $\alpha$  is comprised within the bounds  $3\pi/2 < \alpha < 2\pi$ , the minimum error, as calculated from Equation (5-1), is obtained when

$$\sigma_2 = -5.7875 + 1.968 \sigma_1 \quad (5-19)$$

In terms of  $\alpha$  and  $\psi(\alpha)$ , it can be verified that this equation can also be written as:

$$\psi(\alpha) = \frac{-5.7875}{\sin \alpha - 1.968 \cos \alpha} \quad (3\pi/2 < \alpha < 2\pi) \quad (5-20)$$

Finally, to provide continuity of the failure envelope between the first and fourth quadrants, the following equation can be added:

$$\psi(\alpha) < X/\cos \alpha = 2.15/\cos \alpha \quad (3\pi/2 < \alpha < 2\pi) \quad (5-21)$$

The entire failure envelope will therefore be represented by Equations (5-21) in the remaining section where  $1.801 \pi < \alpha < 2\pi$ . This new envelope is illustrated in Figure 5.4, and is visually more appropriate than the previous one.

It can be speculated that different failure equations in each quadrant may account for different failure modes. In quadrant I, the graphite fails in tension, and compression failure is found in quadrant IV. In both quadrants, the shape of the failure surface resembles that of an ellipse. In the two remaining quadrants, the irregular shape of the envelope may indicate some transition mode between tensile and compressive failure modes. Unfortunately, experimental observations are not available to confirm these conjectures.

d) Summary of Example 1:

With this example, it was demonstrated that it is possible with the new failure criterion proposed here to obtain strength surfaces more variable in shape than with previous criteria. This can even be achieved with fewer parameters. Moreover, despite the complicated shape of the failure surfaces such as those shown in Figures 5.3 and 5.4, the calculation of the theoretical strength value for a given loading path is simpler than using the traditional criteria such as the tensor polynomial because it depends only on the value of the angle  $\alpha$ . It can thus be calculated straightforwardly instead of solving for the roots of a quadratic, cubic, or even higher order equation. It can also be added that this new criterion does not require the verification of additional equations to insure that the failure surface is closed, because this condition can always be satisfied automatically with the use of appropriate trigonometric functions.

One advantage of this new failure criterion is that the number of parameters can easily be adjusted as a function of the number of experimental data available and the desired degree of accuracy. A simple equation can usually be "tailored" to fit almost perfectly with the

experimental data, as it is demonstrated in Figure 5.3. For this example, it was also shown that it is possible to fit properly portions of envelopes in each quadrant with a different equation. This is illustrated in Figure 5.4. A tensor polynomial equation may be more elegant mathematically but a parametric equation will be more calculation-efficient for complicated envelopes. Finally, it can be observed that the curve-fit of the data with the new failure criterion has been obtained from five or eight parameters with results visually comparable to the cubic Equation (5-4) which contained twelve constants (nine if  $\kappa = \lambda = \mu = 1$ ).

### 5.3.2 Example 2: Graphite-Epoxy Fabric

#### a) Material description:

For the second example, the results published by Tennyson and Wharram (1985) will be used. These are for an orthotropic graphite-epoxy composite. Here, the epoxy matrix is reinforced by a graphite fabric. The lamina is identified as a NARMCO Rigidite 5208-WT300, a plain weave (over 1, under 1) of UCC Thornel 300 graphite fibres impregnated with Narmco 5208 Resin. Tension and compression tests were performed on flat coupons, and torsion tests were performed on tubular specimens which were also used for biaxial loading tests. The results of the tests are listed in Table 5.2, which also indicates the calculated maximum strengths in tension, compression, and shear in the principal material directions. These results show a very good consistency for all loading paths. There is, however, some scatter for the uniaxial compressive tests in the directions of reinforcement.

It can be observed that the maximum strengths in tension and compression in the two material axes of symmetry are essentially identical. This makes it an ideal case to demonstrate the use of the new failure criterion in the normalized space  $\sigma_1/X - \sigma_2/Y - \tau_{12}/S$ . In Table 5.3 the experimental results obtained by Tennyson and Wharram (1985), as expressed in the normalized system are listed. Also indicated in the same table are the angles  $\alpha'$  and  $\phi'$ , and the radial distance  $\rho'(\alpha', \phi')$  from the origin of the system of axes to the measured failure point. The failure equation proposed for this material was the cubic expansion of the tensor polynomial, Equation (3-54). In the plane  $\tau_{12} = 0$ , the quadratic form was found to be the best, and the constants  $F_{12}$ ,  $F_{122}$ ,  $F_{112}$  were set equal to zero. The value of the remaining constants  $F_{166}$  and  $F_{266}$  was determined by using the failure results for cylinders submitted to internal pressure. The failure equation was then given by the following:

$$\begin{aligned} 9.183 \times 10^{-8} \sigma_1 - 6.174 \times 10^{-7} \sigma_2 + 2.296 \times 10^{-10} \sigma_1^2 + 2.129 \times 10^{-10} \sigma_2^2 \\ + 3.380 \times 10^{-9} \tau_{12}^2 + 3(-1.097 \times 10^{-14}) \sigma_1 \tau_{12}^2 \\ + 3(-8.845 \times 10^{-15}) \sigma_2 \tau_{12}^2 = 1 \end{aligned} \quad (5-22)$$

This equation is that of an ellipse in any plane  $\tau_{12} = \text{const.}$  The position of the ellipse's centre varies with the level of shear stress  $\tau_{12}$ , but all ellipses have their axes in the direction of the  $\sigma_1 - \sigma_2$  axes since there are no interaction terms between  $\sigma_1$  and  $\sigma_2$ . The normalized data of Table 5.3 and the failure Equation (5-22) are shown graphically in Figure 5.5. In the plane  $\tau_{12}/S = 0$ , the failure surface is circular but is slightly off center from the origin of the system of axes. Slices of the failure envelope at various angles  $\alpha'$  are also

shown. It can be verified that this failure surface gives an accurate representation of the experimental results for most points. It can also be observed that the failure envelope slightly overestimates the lamina strength in the plane  $\tau_{12}/S = 0$  and underestimates it everywhere else, but these errors are not very important. The biggest problem actually encountered with Equation (5-22) is actually to find the theoretical strength value for a given ratio between the stresses  $\sigma_1 - \sigma_2 - \tau_{12}$ , which must be found by solving for the roots of the cubic equation. This process could be greatly simplified by using a failure equation of the form proposed in Chapter 4.

b) First solution for Example 2:

It will now be assumed that the failure equation has the theoretical form given by:

$$\rho'(\alpha', \phi') = T'(\alpha', \tau_{12}/S) = \psi'(\alpha') \Gamma'(\tau_{12}/S) \quad (5-23)$$

This equation indicates that the shape of the failure surface will remain identical in all the planes  $\tau_{12}/S$ , but its size will be controlled by the function  $\Gamma'(\tau_{12}/S)$ . In the plane  $\tau_{12}/S = 0$ , the following equality will have to be satisfied:

$$\Gamma'(\tau_{12}/S) = \Gamma'(0) = 1 \quad (5-24)$$

Since the failure strengths in tension and compression appear to be identical in the principal material directions, a possible function  $\psi' = \psi'(\alpha')$  can be taken as:

$$\psi'(\alpha') = 1.0 \quad (5-25)$$

This represents a circle in the plane  $\tau_{12}/S = 0$  and provides an accurate description of the experimental data in this plane. Above this plane, the function  $\Gamma' = \Gamma'(\tau_{12}/S)$  should control the area of this circle in

different planes in such a way that it would reproduce as accurately as possible the failure data listed in Table 5.2. Therefore, at any level of shear stress  $\tau_{12}$ , it is assumed that the failure function is a circle centered on the  $\tau_{12}$  axis. It can then be written that

$$\Gamma'(\tau_{12}/S) = \psi'(\alpha', \tau_{12}/S) / \psi'(\alpha', 0) = \text{constant} \quad (5-26)$$

Since  $\Gamma'(\tau_{12}/S)$  is a constant value at any constant level of shear  $\tau_{12}$ , the following equality can be substituted in Equation (5-23):

$$\Gamma'(\tau_{12}/S) = \Gamma'(\phi') \quad (5-27)$$

One can observe that for any value of  $\alpha'$  and  $\phi'$  that does not lie on the plane  $\tau_{12}/S = 0$  or on the axis  $\tau_{12}$ , the experimental radius  $\rho'(\alpha', \phi')$  is always greater than unity. For that reason, the following function  $\Gamma' = \Gamma'(\phi')$  among many others can be suggested:

$$\Gamma'(\phi') = 1.0 + P(\sin \phi' \cos \phi')^2 \quad (5-28)$$

for which the conditions  $\Gamma'(0^\circ) = \Gamma'(90^\circ) = 1.0$  are satisfied, and  $P$  is a parameter to be determined. By minimizing the error obtained with Equation (5-1), the best value of the constant  $P$ , for the available data, has been found to be  $P = 1.17$ . Therefore, the failure equation can be written as follows:

$$\rho'(\alpha', \phi') = (1.0)(1.0 + 1.17 [\cos \phi' \sin \phi']^2) \quad (5-29)$$

This is shown in Figure 5.6 with the experimental data. In the plane  $\tau_{12}/S = 0$ , the failure surface still overestimates slightly the strength at most of the points, except on the axes. Above that plane, Equation (5-29) produces a "crown-shaped" failure surface that is identical for any plane at an angle  $\alpha'$ . It can be observed that this shape tends to follow more closely the experimental results above the plane  $\tau_{12} = 0$ .



Since no data are available for negative values of the angle  $\phi'$ , the superiority of the tensor polynomial criterion or of the new criterion given by Equation (5-29) in this area cannot really be assessed.

Since many points are available in the plane  $\tau_{12}/S = 0$  and since they seem to define a circular area, a slight improvement of the theoretical-experimental correlation could be obtained in this case by defining the function  $\psi'(\alpha')$  as

$$\psi'(\alpha') = 0.96845 \quad (5-30)$$

which is the average radius from the origin of the system of axis to the experimental failure points on this plane. Accordingly, the entire strength surface can also be rewritten as follows:

$$\rho'(\alpha', \phi') = 1.00125 \cos^2 \phi' + 0.96845 \sin^2 \phi' + P \sin^2 \phi' \cos^2 \phi' \quad (5-31)$$

where a new value of constant  $P$  has to be determined. By minimizing the error given with the experimental data, the value  $P = 1.24$  is found. The failure criterion can therefore be written as:

$$\rho'(\alpha', \phi') = 1.00125 \cos^2 \phi' + 0.96845 \sin^2 \phi' + 1.24 \sin^2 \phi' \cos^2 \phi' \quad (5-32)$$

This equation is also reproduced in Figure 5.6. It can be observed that a significant improvement over Equation (5-29) has been obtained in the plane  $\tau_{12}/S = 0$ , but that the error has slightly increased for the points above that plane.

#### c) Second solution for Example 2:

In the previous solution, it was assumed that the failure envelope would be circular in each plane  $\tau_{12}/S$ , and centered on the  $\tau_{12}/S$  axis. In that case, it was easier to write a failure equation in cylindrical coordinates. The resulting failure envelope differed

considerably from the one obtained with the cubic tensor polynomial theory. In both cases, the available experimental data are described as well, although the portions of the failure surface where no experimental points were measured are represented very differently. To demonstrate the flexibility of the parametric approach, an alternate failure envelope will now be written for the same experimental data.

It will now be assumed that the failure equation has the form given by Equation (4-16) in spherical coordinates. As for the previous solution, the normalized system of axes will be used. Also, the following equalities must be satisfied:

$$\rho'(\alpha', 90) = 1.0 \quad \text{and} \quad \rho'(\alpha', 0) = 1.0 \quad (5-33)$$

For any value of  $\alpha'$  and  $\phi'$  not on the plane  $\tau_{12}/S = 0$ , or on the axis  $\tau_{12}/S$ , the experimental radius  $\rho_*(\alpha', \phi')$  is always greater than unity. For that reason, the following function  $\rho' = \rho'(\alpha', \phi')$  is advanced:

$$\rho'(\alpha', \phi') = 1 + f(\alpha') \sin \phi' |\cos \phi'| \quad (5-34)$$

which satisfies the conditions (5-33). This equation differs from (5-29) as it is no longer symmetrical with respect to the angle  $\phi'$ . The absolute value of  $\cos \phi'$  is taken here to ensure symmetry of the failure envelope with respect to the plane  $\tau_{12}/S = 0$ . This will cause slope discontinuity of the surface at this plane.

The experimental data to be used with Equation (5-34) are summarized in Table 5.4. All data fall on the planes  $\alpha' = 0^\circ$ ,  $\alpha' = 44^\circ$ ,  $\alpha' = 68^\circ$ ,  $\alpha' = 90^\circ$ . The value of the function  $f(\alpha')$  to fit each point is also given in the table. Assuming that the function  $f(\alpha')$  will include the four average points on each  $\alpha'$ -planes listed in Table 5.4, the failure function on these four planes is shown in Figure 5.7. The shape

of this failure function differs considerably from the first solution and from the cubic tensor polynomial theory.

A function  $f = f(\alpha')$  now has to be written. Many equations can actually be suggested. If a single equation is written for the entire surface, it has to satisfy the following condition:

$$\rho'(\alpha', \phi') = \rho'(\alpha' + 180, -\phi') \quad (4-19)$$

Considering Equation (5-34), this leads to the restraint given by

$$f(\alpha') = -f(\alpha' + 180) \quad (5-35)$$

Accordingly, this function can be written as a series of sines and cosines, such as:

$$f(\alpha') = \sum_m b_m \sin^{2m-1} \alpha' + \sum_n a_n \cos^{2n-1} \alpha' + \sum_s c_s \sin^p \alpha' \cos^q \alpha' \quad (5-36)$$

where the sum  $p + q$  must be odd. Since four points must be fitted, four terms of this equation must be kept. A first solution can be obtained with

$$f(\alpha') = f_1(\alpha') = a_1 \cos \alpha' + b_1 \sin \alpha' + a_2 \cos^2 \alpha' + c_1 \cos \alpha' \sin^2 \alpha' \quad (5-37)$$

Substituting the average values from Table 5.4, this becomes

$$f_1(\alpha') = 0.419 \cos \alpha' + 0.344 \sin \alpha' - 0.322 \cos^2 \alpha' + 0.598 \cos \alpha' \sin^2 \alpha' \quad (5-38)$$

Alternatively, the function  $f = f(\alpha')$  could be given by:

$$f(\alpha') = f_2(\alpha') = a_1 \cos \alpha' + b_1 \sin \alpha' + a_2 \cos^3 \alpha' + a_3 \cos^5 \alpha' \quad (5-39)$$

which becomes the following function after substitution of the experimental data:

$$f_2(\alpha') = 0.967 \cos \alpha' + 0.344 \sin \alpha' - 1.097 \cos^3 \alpha' + 0.549 \cos^5 \alpha' \quad (5-40)$$

The two functions  $f_1(\alpha')$  and  $f_2(\alpha')$  are shown in Figure 5.8. It is difficult to decide which one of these functions would give the best result when substituted back into Equation (5-34) since both of them include the average experimental points listed in Table 5.4. However, since the function  $f(\alpha') = f_2(\alpha')$  has a more regular shape, it will be expected to produce better results. Therefore, the failure envelope for the graphite-epoxy fabric studied here is given by the combination of Equations (5-34) and (5-40)

$$\rho'(\alpha', \phi') = 1.0 + f_2(\alpha') \sin \phi' |\cos \phi'| \quad (5-41)$$

This failure surface has the irregular shape shown in Figure 5.7 and in the additional angular "slices" shown in Figure 5.9.

d) Summary of Example 2:

A quantitative assessment of the error (Equation (5-2)) obtained by comparing the experimental data with the failure surfaces of Tennyson (Eq.(5-22)) and with the new parametric failure criteria, as given by Equations (5-29), (5-32) or (5-41), is available in Table 5.5. It can be observed that all equations produce approximately the same total error. In the plane  $\tau_{12}/S = 0$  only, Tennyson's criterion produces a smaller error than by taking simply  $\psi'(\alpha') = 1.0$  or  $\rho'(\alpha', \phi') = 1.0$  but slightly greater than with  $\phi'(\alpha') = 0.96845$  which is the average radius in this plane. Above the plane  $\tau_{12}/S = 0$ , however, the error has been reduced almost by one half with the failure Equation (5-29), and to almost nothing with Equation (5-41). Overall, it is difficult to claim that one of these criteria gives a more accurate result than the others, and more experimental data would be useful to assess the accuracy of the criteria in the portions of failure envelope where data are missing. In

any case, the calculation of theoretical values is much simpler with the new parametric criteria than with the tensor polynomial. Moreover, for this very specific case, the tensor polynomial theory required that seven parameters be known; on the other hand, Equation (5-29) required that only the parameters  $X$ ,  $Y$ ,  $S$  and  $R$  be used. For this very specific case, there is therefore a definite advantage to use the parametric failure criterion since it can simplify the subsequent analysis. Finally, in the event that experimental data would be available in other regions of the failure surface and would not correspond to the analytical function, that one could easily be rewritten as was shown by writing two parametric solutions for this example. For the tensor polynomial formulation, on the other hand, new values for the strength parameters  $F_{ij}$  and  $F_{ijk}$  would have to be found, and this has been shown to be relatively complicated.

### 5.3.3 Example 3: Paperboard

#### a) Material description:

The results published by Rowlands et al. (1985) will be used in the following example. The material tested is described as a machine made 100 percent Lake State Softwood, unbleached kraft paper, of basis weight  $205 \text{ g/m}^2$  and mass density of  $670 \text{ kg/m}^3$ . This is a unidirectionally-reinforced material. Uniaxial coupons, cylinders and cruciform specimens of this paperboard were subjected to various in-plane combinations of axial stresses and shear stresses. The results are given at four values of the shear stress  $\tau_{12}$ , which was kept constant while the  $\sigma_1$  and  $\sigma_2$  stresses were varied. In the plane  $\tau_{12} = 0$  alone, there are 68 experimental points. At the four stress levels  $\tau_{12} = 0, 6.9, 10.3$  and

15.9 MPa, there is a total of 143 points. These results, listed in Table 5.6, cover a very substantial portion of the failure envelope in the  $\sigma_1 - \sigma_2 - \tau_{12}$  space. The calculated strengths in tension, compression, and shear in the principal directions are also listed in this table, as well as the equal biaxial tensile and compressive strengths, and the shear strength at the lamina angle  $\theta = \pm 45^\circ$ .

The results of Table 5.6 for paperboard are shown in Figure 5.10. It can be observed that the experimental results show a very good consistency along similar loading paths. A well-defined failure surface is obtained at all levels of shear stress  $\tau_{12}$ . The hypothesis that the same shape of failure envelope is obtained at all shear levels can be justified from these results. There are relatively more results in the biaxial compression quadrant than in the others, and the failure envelope is very well identified in that area, especially at the  $\tau_{12} = 0$  level.

Rowlands et al. (1985) compared the above experimental results with many Hill-type failure criteria: the Tsai-Hill criterion (3-14), Norris criterion (3-15) and Ashkenazi criterion (3-17). Also, the value of the interaction parameter  $F_{12}$  has been calculated in each quadrant from the strengths  $P, P', S_{45}, S'_{45}$ . This is referred to as "Rowlands' theory" in this section. It was found that the Ashkenazi failure criterion produced an open failure surface, and was consequently unacceptable for this material. For the other three theories tested, the correlation was very good in quadrants 2, 3, 4 and the value of  $F_{12}$  was found not to influence greatly the failure envelope in this area. The first quadrant, however, is poorly described by these criteria. The Tsai-Hill theory, especially, underestimates the strength in this quadrant. The

best correlation was obtained with Norris's equation, and it was observed that this theory could predict reasonably well the strength of paperboard for  $\tau_{12}/S < 0.65$ . This failure theory is also represented in Figure 5.10.

One disadvantage of the above theories is that they do not permit values of the shear stress  $\tau_{12}$  to reach values higher than the shear strength  $S$  in the principal material directions. However, a few experimental results where  $\tau_{12} > S$  were reported by the authors. This inconvenience can be overcome by using tensorial strength equations. Rowlands et al. (1985) also published an analysis on the use of the quadratic tensor polynomial to describe the paperboard experimental results. In a second article, Suhling et al. (1985) compare various methods for obtaining the value of the interaction parameter  $F_{12}$  in Equation (3-39). Theoretically, this value can be obtained from any biaxial loading. It was indicated in Chapter 3, however, that various authors have advocated the use of one specific test among many others in order to obtain that value. In the above reference, no less than twenty-nine different tests were performed to calculate  $F_{12}$ . Each one of these tests produced a different  $F_{12}$  value. The degree of correlation with the experimental data varied from very good for some values of  $F_{12}$  to very poor for some others. With the uniaxial strengths listed in Table 5.6, the conditions (3-45) for closure of the failure surface forced the value of the interaction parameter to be comprised within the bounds:

$$-1.496 \times 10^{-3} \text{ MPa}^{-2} < F_{12} < 1.496 \times 10^{-3} \text{ MPa}^{-2} \quad (5-42)$$

However, some tests led to a value of  $F_{12}$  that would not satisfy the above condition. It was found that the value  $F_{12} = 0$  would provide the

best representation of the experimental data with this theory.

In order to compare the failure theories discussed above with the experimental data obtained for paperboard, the total error between the theoretical and experimental results of Table 5.6 was calculated. These error values were calculated according to the method outlined in Section 5.2. The error between the experimental data and the theories of Tsai-Hill, Norris, Rowlands, and the quadratic tensor polynomial with  $F_{12} = 0$  and  $F_{12} = -2.017 \times 10^{-4} \text{ MPa}^{-2}$  are listed in Table 5.7. The error on the plane  $\tau_{12} = 0$ , and for the data on all four  $\tau_{12}$  planes are given. It can be observed that the tensor polynomial with  $F_{12} = 0$  is the one that causes the least error when all experimental points are considered. However, when only the results in the plane  $\tau_{12} = 0$  are taken into account, three of the other failure theories listed in the plane  $\tau_{12} = 0$  produce significantly better results.

b) Failure criterion for paperboard:

As commented above, the experimental results justify the assumption that the shape of the failure envelope is the same at all shear levels, but reduces in size as  $\tau_{12}$  increases. Also, since all criteria discussed above could be written as

$$f(\sigma_1, \sigma_2) = 1 - \left(\frac{\tau_{12}}{S}\right)^2 = 1 - g(\tau_{12}) \quad (4-31)$$

which corresponds to

$$T(\alpha, \tau_{12}) = \psi(\alpha) \Gamma(\tau_{12}) \quad (4-30)$$

it can be speculated that a different function  $g = g(\tau_{12})$  or  $\Gamma = \Gamma(\tau_{12})$  could produce a better data representation. It will now be shown how the new failure criterion (4-30) can lead to an improved analytical-experimental correlation than the theories discussed above.



With the five above theories, we shall attempt to find an as yet unknown function  $g = g(\tau_{12})$  that will produce the best curve-fit at all shear levels  $\tau_{12}$ . This function will be obtained by minimizing the error between the experimental data and the failure theory considered at each level of constant shear  $\tau_{12}$ . The error is defined as Equation (5-2). The best-fitting values of the function  $g = g(\tau_{12})$  at the four shear levels are listed in Table 5.8 for the five failure theories. The error measured in each case is also indicated. If a function  $g = g(\tau_{12})$  could be found that equals the best-fit value obtained at each shear level, the total error for each theory would be the one in the last column of Table 5.8. This total error is the lowest that can be found for each theory. When these values are compared with the corresponding ones in Table 5.7, it can be observed how much an appropriate function  $g = g(\tau_{12})$  could do to improve the experimental-theoretical correlation.

For the Tsai-Hill, Norris, and Rowlands theories, the improvement would be very good. In the case of the tensor polynomial theory, the gain in precision would hardly be worth the energy spent in finding the best function  $g = g(\tau_{12})$ . This is especially true for the  $F_{12} = 0$  case, for which the total error in Tables 5.7 and 5.8 is approximately the same. However, since the Norris theory, with an idealized function  $g = g(\tau_{12})$  would give a significantly better result than the other theories, a function  $g = g(\tau_{12})$  will be found for this case. Accordingly, an "improved Norris equation" will be written for this material.

Figure 5.11 shows the five values  $\tau_{12}$  and the corresponding  $g(\tau_{12})$  that would produce the best curve fitting of the experimental data. Also depicted on this figure is the standard function  $g(\tau_{12}) = (\tau_{12}/S)^2$ . As observed by Rowlands et al. (1985), the Norris

theory gives a good representation of the failure envelope for  $\tau_{12}/S < 0.65$ , and this is clearly illustrated in Figure 5.11. On the other hand, the value of  $g(\tau_{12})$  at  $\tau_{12} = 15.9$  is poorly represented by this function.

Alternate functions  $g = g(\tau_{12})$  can be written that will comprise all points in Figure 5.11 and therefore produce the lowest error between experimental and theoretical failure values. For example, a polynomial function such as

$$g(\tau_{12}) = -5.331 \times 10^{-1} |\tau_{12}| + 1.745 \times 10^{-1} \tau_{12}^2 - 1.689 \times 10^{-2} |\tau_{12}|^3 + 5.136 \times 10^{-4} \tau_{12}^4 \quad (5-43)$$

would be perfectly appropriate. However, a look at this function, also shown in Figure 5.11, clearly indicates that it will not provide good representation of the data at other  $\tau_{12}$  shear values. In fact, it appears that simple linear functions of the shear stress would give good results.

It can easily be found that the linear function of  $\tau_{12}$  that includes the point  $g(0) = 0$  and best fits the points  $g(6.9)$  and  $g(10.3)$  is given by:

$$g(\tau_{12}) = 0.035 \tau_{12} \quad (5-44)$$

Another linear function can also fit the points  $g(15.9)$  and  $g(16.6)$ , that is:

$$f_2(\tau_{12}) = 0.058 \tau_{12} - 8.628 \quad (5-45)$$

The "improved Norris criterion", as fitted for this paperboard only, can therefore be written as follows:

$$\left(\frac{\sigma_1}{X}\right)^2 - \left(\frac{\sigma_1 \sigma_2}{XY}\right) + \left(\frac{\sigma_2}{Y}\right)^2 + 0.035 \tau_{12} = 1 \quad (0 < \tau_{12} < 15.8 \text{ MPa}) \quad (5-46)$$

$$\left(\frac{\sigma_1}{X}\right)^2 - \left(\frac{\sigma_1 \sigma_2}{XY}\right) + \left(\frac{\sigma_2}{Y}\right)^2 + 0.058 \tau_{12} - 8.628 = 1 \quad (15.8 < \tau_{12} < 16.6 \text{ MPa})$$

where the values of  $X$  and  $Y$  change in each quadrant, except for the interaction term that is always computed from the tensile uniaxial strengths. These equations can also be written in the form of Equation (4-30)

$$T(\sigma, \tau_{12}) = \phi(\alpha) \Gamma(\tau_{12}) \quad (4-30)$$

as follows:

$$T(\alpha, \tau_{12}) = \left[ \frac{1}{\sqrt{\frac{\cos^2 \alpha}{X^2} + \frac{\sin \alpha \cos \alpha}{XY} + \frac{\sin^2 \alpha}{Y^2}}} \right] \left( \frac{1}{1 - g(\tau_{12})} \right) \quad (5-47)$$

where  $g(\tau_{12})$  is given alternatively by Equation (5-44) if  $\tau_{12} < 15.8$  MPa or by Equation (5-45) otherwise.

### c) Summary of Example 3:

The failure equations (5-46) or (5-47) are shown in Figure 5.12 with the experimental data. Comparing this figure with Figure 5.10, it is observed that a less conservative representation of the results have been obtained at high level of the shear stress  $\tau_{12}$ . However, the portion of the failure envelope with compressive  $\sigma_1$  is now overestimated. Also, despite an overall improvement in theoretical-experimental correlation, the tensor polynomial theory with  $F_{12} = 0$  still produces a better curve fit on the plane  $\tau_{12} = 15.9$  MPa, as can be observed in Tables 5.7 and 5.8. The "improved Norris equation" does not allow any shear stress value to be higher than the maximum shear value

S.

## 5.4 LAMINATE APPLICATION: CARBON-EPOXY

### 5.4.1 Material description

The experimental results published by Ikegami and Takahashi (1983) will now be used to demonstrate how experimental results for laminates can be used to define more precisely the failure envelope. These researchers have tested carbon fibre-reinforced plastics using filament wound tubes which they fabricated. Details on the specimen fabrication were included in their article. Single laminae were tested under various combinations of in-plane loads, and results are given in the planes  $\tau_{12} = 0$  and  $\sigma_1 = 0$  of the failure envelope. These are listed in Table 5.9. The compressive strength in the fibre direction is given as 809 MPa, although this point was not measured experimentally. Details are not given on the method used to calculate this value. Angle-ply laminates  $(\pm\theta)_s$  were also tested in uniaxial tension and compression. Laminate strengths for these cases are listed in Table 5.10. This table also indicates the corresponding failure stresses in the comprised laminae, as calculated from classical lamination theory. Since all layers of the laminate are subjected to the same stresses, they failed simultaneously under uniaxial loads.

The failure equations tested for this material were Hoffman's theory, Equation (3-23), and the quadratic tensor polynomial, Equation (3-39). In both cases, the calculated value  $X' = 809$  MPa was used as a strength parameter. The strength under biaxial loads with  $\sigma_1/\sigma_2 = -10$  was used to calculate the interaction term  $F_{12} = 7.47 \times 10^{-6} \text{ MPa}^{-2}$  in the quadratic tensor polynomial. Hoffman's failure criterion underestimated the strength very significantly and will not be discussed here. The quadratic failure surface proposed by Ikegami is given by Equation

(3-39) with the following strength parameters:

$$X = 1360 \quad X' = 809 \quad Y = 28 \quad Y' = 123.5 \quad S = 62.6 \text{ (MPa)}$$

In the planes  $\sigma_1 = 0$  and  $\tau_{12} = 0$  of the failure surface, the representation of the experimental data is very good. However, when one takes into account the laminate failure strengths in Table 5.10, it is observed that this criterion does not predict the failure of angle-ply laminates with low  $\theta$ -values very well. In fact, it predicts the highest strength under uniaxial load when the laminae are oriented at  $\pm 13^\circ$ . This has clearly not been observed experimentally.

#### 5.4.2 Proposed Failure Criterion

The first step undertaken here to improve the above solution was to use only the available experimental results, and not use the point  $X' = 809$  MPa in the strength parameter calculation. A failure envelope that best fits the experimental points in the plane  $\tau_{12} = 0$  is given by

$$\frac{\sigma_1^2}{455\,581} + \frac{\sigma_2^2}{3\,458} - \frac{\sigma_1}{444.4} + \frac{\sigma_2}{36.2} + \frac{\sigma_1 \sigma_2}{57\,817} + \frac{\tau_{12}^2}{3918.8} = 1 \quad (5-48)$$

In the plane  $\sigma_1 = 0$ , this envelope is identical to the one suggested by Ikegami and Takahashi. It can be observed in Figure 5.13 that this equation provides an excellent correlation with the available experimental data in the planes  $\sigma_1 = 0$  and  $\tau_{12} = 0$ . However, angle-ply laminate strength under uniaxial loads is still poorly predicted in the range of  $\theta < 30^\circ$ . Figure 5.14 shows the uniaxial strength versus ply angle for criterion (5-48) and the corresponding experimental results. An idealized relationship is also represented. It will now be shown how

Equation (5-48) can be modified in order to provide the same curve fit in the planes  $\sigma_1 = 0$  and  $\tau_{12} = 0$ , and also the idealized failure surface in Figure 5.14. The new parametric failure equation will be used.

Since the quadratic tensor polynomial provides a satisfactory correlation with experimental data in the planes  $\tau_{12} = 0$  and  $\sigma_1 = 0$ , it is desirable that the parametric criterion coincide with the quadratic expression on those planes. In parametric form, this criterion is written as

$$\rho(\alpha, \phi) = \frac{f_1(\alpha, \phi) + \sqrt{f_1^2(\alpha, \phi) + 4 f_2(\alpha, \phi)}}{2 f_2(\alpha, \phi)} \quad (4-12)$$

where

$$f_1(\alpha, \phi) = \left[ \frac{\sin \phi \sin \alpha}{36.2} - \frac{\sin \phi \cos \alpha}{444.4} \right] \quad (5-49)$$

$$f_2(\alpha, \phi) = \left[ \frac{\sin^2 \phi \cos^2 \alpha}{455.581} + \frac{\sin^2 \alpha \sin^2 \phi}{3.458} + \frac{\sin^2 \phi \cos \alpha \sin \alpha}{57.817} + \frac{\cos^2 \phi}{3918.8} \right] \quad (5-50)$$

The above failure equation in the planes  $\sigma_1 = 0$  and  $\tau_{12} = 0$  is shown in Figure 5.13. Now, "slices" of the failure envelope can be taken at  $\alpha$ -angles. Three of them are shown in Figure 5.15, where the experimental points illustrated are those for angle-ply laminate failure under uniaxial loadings. It is observed that the point with the lowest value of the angle  $\alpha$  is overestimated by the criterion, while the failure point at  $\alpha = -5.3^\circ$  is underestimated by the failure equation. The failure equation must therefore be modified in order to follow more closely the experimental failure data in the portion of the failure envelope where  $-14^\circ < \alpha < 0^\circ$ . The lower limit for  $\alpha$  has been set

arbitrarily because no data are available in this region. Outside these bounds, it is assumed that Equations (4-12), (5-49) and (5-50) are appropriate, since the laminate strength is well predicted.

In order to modify the failure envelope in the area  $-14^\circ < \alpha < 0^\circ$ , the following modification to Equation (5-50) is suggested

$$f_2(\alpha, \phi) = \frac{\sin^2 \phi \cos^2 \alpha}{455 \ 581} + \frac{\sin^2 \alpha \sin^2 \phi}{3 \ 458} + \frac{\sin^2 \phi \cos \alpha \sin \alpha}{57 \ 817} + \frac{\cos^2 \phi}{3918.8} + f(\alpha, \phi) \quad (5-51)$$

where the function  $f(\alpha, \phi)$  must equal zero on the planes  $\sigma_1 = 0$ ,  $\sigma_2 = 0$ ,  $\tau_{12} = 0$  in order to coincide with the quadratic tensor polynomial on these planes. The following function can be taken:

$$f(\alpha, \phi) = g(\alpha, \phi) \cos \alpha \sin \alpha \cos \phi \sin \phi \quad (5-52)$$

where  $g = g(\alpha, \phi)$  has still to be determined. The sines and cosines in the above equation force the failure surface to follow the quadratic failure surface on the planes of the system of axes. A function  $g = g(\alpha, \phi)$  can now be determined by using the experimental results for the laminate that were ill-represented with the quadratic criterion.

For the two concerned points, the following values are calculated:

$$\begin{aligned} p(-1.8, 87.8) &= 1 \ 262 & \text{and} & & g(-1.8, 87.8) &= - \ 1/1 \ 530 \\ p(-3.5, 85.5) &= 653 & & & g(-3.5, 85.5) &= - \ 1/1 \ 040 \end{aligned} \quad (5-53)$$

Also, since it is desired that the failure function return to the quadratic polynomial at  $\alpha = -14^\circ$ , the next equation must be satisfied

$$g(-14, \phi) = 0 \quad (5-54)$$

for all angles  $\phi$ .

Many functions  $g = g(\alpha, \phi)$  can be written that would satisfy Equations (5-53) and (5-54). With only three known values for this function, it can be assumed that  $g = g(\alpha, \phi)$  will be a function of the angle  $\alpha$  alone. The following one is therefore suggested:

$$g(\alpha, \phi) = A \cos^2 \alpha + B \sin^2 \alpha + C \sin \alpha \cos \alpha \quad (5-55)$$

When the values in (5-53) and (5-54) are substituted in (5-46), the following constants are found:

$$\begin{aligned} A &= -1/792 \\ B &= -1/15 \\ C &= -1/47 \end{aligned} \quad (5-56)$$

The new failure criterion is therefore given by

$$\rho(\alpha, \phi) = \frac{-f_1(\alpha, \phi) + \sqrt{f_1^2(\alpha, \phi) + 4 f_2(\alpha, \phi)}}{2 f_2(\alpha, \phi)} \quad (4-12)$$

where

$$f_1(\alpha, \phi) = \left[ \frac{\sin \phi \sin \alpha}{36.2} - \frac{\sin \phi \sin \alpha}{444.4} \right] \quad (5-49)$$

$$\begin{aligned} f_2(\alpha, \phi) = & \left[ \frac{\sin^2 \phi \cos^2 \alpha}{455.581} + \frac{\sin^2 \alpha \sin^2 \phi}{3.458} + \frac{\sin^2 \phi \cos \alpha \sin \alpha}{57.817} + \frac{\cos^2 \phi}{3918.8} \right. \\ & \left. + W \cos \alpha \sin \alpha \cos \phi \sin \phi \left( -\frac{\cos^2 \alpha}{792} - \frac{\sin^2 \alpha}{15} - \frac{\sin \alpha \cos \alpha}{47} \right) \right] \end{aligned} \quad (5-57)$$

In Equation (5-57),  $W = 1$  for  $-14^\circ < \alpha < 0^\circ$ , and zero otherwise.

The effect of using the new failure criterion is illustrated in Figure 5.16. It can be observed that the failure envelope is now much more complicated than an ellipsoid. On the planes  $\sigma_1 = 0$ ,  $\sigma_2 = 0$ ,  $\tau_{12} = 0$ , it coincides with the quadratic failure envelope, as shown in Figure 5.16. With Equation (5-41), the ellipsoid is then modified in



the fourth quadrant. As the angle  $\alpha$  varies from  $0^\circ$  to  $-2^\circ$ , the ellipsoid is gradually shrunk in order to include the failure point at  $\alpha = -1.8^\circ$ . Following that, the ellipsoid now expands and includes the failure point at  $\alpha = -5.3^\circ$ , which was originally above the failure surface. Finally, the failure envelope decreases again to join with the quadratic failure envelope at  $\alpha = -14^\circ$ . The quadratic tensor polynomial is still used for the remainder of the failure envelope because it provides a good representation of the failure data available. The effect of the new failure envelope is also shown in Figure 5.14.

#### 5.4.3 Summary of Example 4

This was a typical example where the quadratic tensor polynomial seems to provide good correlation between theoretical and experimental results, at least in the planes  $\sigma_1 = 0$  and  $\tau_{12} = 0$ . Therefore, it was appropriate to use this criterion in these planes. However, it was observed that some angle-ply laminate results could not be accurately compared with this criterion. It was then shown that the quadratic tensor polynomial, when written parametrically in terms of angles  $\alpha$  and  $\phi$ , could easily be modified to include these failure data. It was possible to write a failure function  $p = p(\alpha, \phi)$  that includes these points yet still coincides with the quadratic failure criterion in the planes where it was shown to be satisfactory. The shape of the failure envelope then became much more complicated than an ellipsoid in the  $\sigma_1 - \sigma_2 - \tau_{12}$  space, but only three additional constants were required. This parametric criterion is more flexible than cubic or higher expansions of the tensor polynomial. With the cubic expansion, for example, it would be impossible to maintain the elliptic shape of the failure

function in both the planes  $\sigma_1 = 0$  and  $\tau_{12} = 0$  simultaneously. The value of the strength under any loading condition is also easy to calculate with the parametric criterion by substituting the appropriate values of the angles  $\alpha$  and  $\phi$  in Equation (4-12). Finally, if additional experimental results were obtained and required further modification of the failure surface, this could be achieved straightforwardly by following the same procedure as above.

## 5.5 CONCLUSION

Different applications of the new parametric failure criterion introduced in Chapter 4 were presented in this chapter. Examples with single laminae and one laminate were considered, and a different feature of the parametric failure criterion was demonstrated for each case. The hypotheses that led to each of these parametric functions are summarized in Appendix III. The analytical-experimental correlation was improved over the original solution for all examples discussed.

It was demonstrated that the main advantage of this parametric approach is its great flexibility. It is possible to write new failure equations or even to modify existing criteria when this is found necessary to describe complicated experimental failure surfaces. For all cases discussed here, the improved correlation was obtained without using an excessive number of parameters, and in all cases less parameters than with the tensor polynomial theory. The flexibility of this approach was also shown by writing different parametric solutions for a single example.

Among the parametric solutions discussed, the following possibilities were advanced: use of high order equations, use of non-integer

exponents in the failure equation, fitting of different portions of the failure surface with different equations and local improvement of Hill-type or tensor polynomial criteria. The possibilities are endless. However, when a new criterion has to be written for a set of experimental results, it seems best to attempt using primarily trigonometric functions.

Using trigonometric functions has two major advantages over the previous theories. First, the failure surface will always be closed for an appropriate choice of trigonometric functions. In fact, ensuring closure of the failure surface has always been a problem in the previous theories, and this difficulty can now be eliminated when using parametric equations. The second advantage of a parametric equation is its facility of use once defined. In fact, material strength under any proportional loading condition can be obtained directly by substituting the appropriate values of  $\alpha$  and  $\phi$  in the failure equation. This is considerably simpler than solving for the roots of quadratic or cubic equations as in previous theories. Finally, a secondary feature of this parametric approach is the possibility of providing concavity in localized areas of the failure surface. Although the physical meaning of this can be debated, there are some instances where this was observed experimentally. A possible explanation of this may be related to the loading path dependency of the failure surface and to the sequence of damage occurrence in a lamina.

In this thesis, a single parametric equation valid for all fibre-reinforced laminae was not written. A new failure equation must consequently be written for each case. This is a disadvantage in comparison with Hill-type and tensor polynomial theories. For these, the strength

parameters are defined directly from specific experimental results such as uniaxial strengths in the axis of symmetry. The result, however, is that all failure envelopes described with one of the above theories have the same shape. For example, all quadratic tensor polynomials are ellipsoids. This raises the question as to whether or not it is feasible to derive a single equation to represent all possible failure envelopes for fibre-reinforced laminae. It would certainly be useful if such an equation were available, and this was one feature of the tensor polynomial theory. However, this point has not been investigated in detail here. There is some reason to believe that such a general equation, if it indeed does exist, might be easier to obtain in parametric form than with the tensor polynomial. The reason is that series of closed trigonometric functions can now be used. This is more likely to generate the general failure surface than the higher degrees of the tensor polynomial, which are not necessarily closed over the second order.

It can actually be shown that the following series satisfies all requirements discussed in Chapter 4:

$$\rho(\alpha, \phi) = \sum_m \sum_n B_{mn} \sin [(2n-1)\alpha] \sin [(2m-1)\phi] \quad (5-58)$$

The development of this equation is discussed in Appendix IV. This equation can theoretically describe any failure surface symmetrical about the plane  $\rho(\alpha, 90^\circ)$ , but a high number of terms must be generated to converge toward the real failure surface. It can be hypothesized that other functions requiring less terms can be written. This could be an area to explore more closely in future developments of the parametric approach. This eventual equation would be more useful for design purposes than the general equation proposed above.

TABLE 5.1 - Example 1: Biaxial Stresses in Graphite Grade AGOT

(all units:  $10^3$  psi)

$\sigma_1$	$\sigma_2$	$\sigma_1$	$\sigma_2$	$\sigma_1$	$\sigma_2$	$\sigma_1$	$\sigma_2$
1.7	0.0	-5.5	0.0	-3.6	-6.3	0.0	-5.6
1.9	0.0	-5.3	0.0	-3.4	-5.9	0.0	-5.5
2.3	0.0	-6.25	-1.7	-3.2	-6.1	0.0	-5.4
2.7	0.0	-6.9	-3.2	-3.1	-5.4	0.8	-4.8
1.25	1.25	-6.5	-3.1	-2.8	-6.8	0.73	-4.4
0.0	1.4	-6.8	-4.2	-2.5	-6.4	0.72	-4.3
0.0	1.2	-6.9	-4.1	-1.55	-7.3	0.7	-4.2
0.0	1.4	-7.3	-4.3	-1.55	-7.2	0.67	-4.0
-1.3	1.4	-6.3	-4.9	-1.55	-7.1	0.6	-3.6
-1.4	1.4	-5.9	-5.5	-1.4	-6.2	0.57	-3.4
-1.5	1.5	-5.3	-5.4	-1.2	-5.8	0.52	-3.1
-1.6	1.7	-4.9	-5.8	-0.5	-6.4	1.75	-3.5
-1.8	1.7	-4.8	-6.5	-0.5	-6.0	1.7	-3.4
-4.2	1.4	-4.4	-5.5	-0.0	-6.2	1.55	-3.1
-6.5	0.0	-4.2	-5.7	0.0	-6.1	1.4	-2.8
-6.2	0.0	-4.1	-5.6	0.0	-6.0	2.4	-2.4
-6.0	0.0	-4.0	-6.7	0.0	-5.8	2.3	-2.3
-5.8	0.0	-3.7	-6.6	0.0	-5.7	1.7	-1.7

$$X = 2.15 \times 10^3 \text{ psi}$$

$$X' = 5.8833 \times 10^3 \text{ psi}$$

$$Y = 1.2 \times 10^3 \text{ psi}$$

$$Y' = 5.7875 \times 10^3 \text{ psi}$$

TABLE 5.2 - Example 2: Biaxial Strength of Graphite-Epoxy Fabric

(all units:  $10^3$  psi)

$\sigma_1$	$\sigma_2$	$\tau_{12}$	$\sigma_1$	$\sigma_2$	$\tau_{12}$	$\sigma_1$	$\sigma_2$	$\tau_{12}$
70.6	0.0	0.0	-73.3	0.0	0.0	29.1	58.1	0.0
66.4	0.0	0.0	0.0	-51.4	0.0	0.0	43.1	16.8
59.0	0.0	0.0	0.0	-82.3	0.0	35.1	0.0	17.5
65.0	0.0	0.0	0.0	-57.3	0.0	33.6	0.0	18.4
66.9	0.0	0.0	0.0	-68.1	0.0	45.6	46.9	15.4
66.6	0.0	0.0	0.0	-76.3	0.0	45.8	47.0	15.5
0.0	69.7	0.0	0.0	0.0	17.5	27.2	73.2	6.1
0.0	71.7	0.0	0.0	0.0	16.6	29.6	59.3	0.0
0.0	71.8	0.0	0.0	0.0	17.1	29.5	59.0	0.0
0.0	65.4	0.0	0.0	0.0	17.5	27.9	55.8	0.0
0.0	71.5	0.0	0.0	0.0	-17.6	58.8	29.4	0.0
0.0	70.0	0.0	0.0	0.0	-17.6	57.5	28.8	0.0
-65.3	0.0	0.0	0.0	0.0	-17.2	45.4	46.6	15.3
-42.5	0.0	0.0	0.0	0.0	-16.7	-26.8	57.5	0.0
-58.5	0.0	0.0	57.3	28.6	0.0	-	-	-
-67.5	0.0	0.0	58.2	29.1	0.0	-	-	-

$$X = 65.8 \times 10^3 \text{ psi}$$

$$X' = 66.2 \times 10^3 \text{ psi}$$

$$Y = 70.0 \times 10^3 \text{ psi}$$

$$Y' = 67.1 \times 10^3 \text{ psi}$$

$$S = 17.2 \times 10^3 \text{ psi}$$

TABLE 5.3 - Example 2: Normalized and Radial Data

$\sigma_1/X$	$\sigma_2/Y$	$\tau_{12}/S$	$\alpha'$ (°)	$\phi'$ (°)	$\rho'(\alpha', \phi')$
1.073	0.0	0.0	0.0	90.0	1.073
1.009	0.0	0.0	0.0	90.0	1.009
0.897	0.0	0.0	0.0	90.0	0.897
0.988	0.0	0.0	0.0	90.0	0.988
1.017	0.0	0.0	0.0	90.0	1.017
1.012	0.0	0.0	0.0	90.0	1.012
0.0	0.996	0.0	90.0	90.0	0.996
0.0	1.024	0.0	90.0	90.0	1.024
0.0	1.026	0.0	90.0	90.0	1.026
0.0	0.934	0.0	90.0	90.0	0.934
0.0	1.021	0.0	90.0	90.0	1.021
0.0	1.000	0.0	90.0	90.0	1.000
-0.992	0.0	0.0	0.0	-90.0	0.992
-0.646	0.0	0.0	0.0	-90.0	0.646
-0.889	0.0	0.0	0.0	-90.0	0.889
-1.026	0.0	0.0	0.0	-90.0	1.026
-1.114	0.0	0.0	0.0	-90.0	1.114
0.0	-0.734	0.0	90.0	-90.0	0.734
0.0	-1.176	0.0	90.0	-90.0	1.176
0.0	-0.819	0.0	90.0	-90.0	0.819
0.0	-0.973	0.0	90.0	-90.0	0.973
0.0	-1.090	0.0	90.0	-90.0	1.090
0.0	0.0	1.017	all	0.0	1.017
0.0	0.0	0.965	all	0.0	0.965
0.0	0.0	0.994	all	0.0	0.994
0.0	0.0	1.017	all	0.0	1.017
0.0	0.0	-1.023	all	0.0	1.023
0.0	0.0	-1.023	all	0.0	1.023
0.0	0.0	-1.000	all	0.0	1.000
0.0	0.0	-0.971	all	0.0	0.971

TABLE 5.3. - Example 2: Normalized and Radial Data (cont'd)

$\sigma_1/X$	$\sigma_2/Y$	$\tau_{12}/S$	$\alpha'$ (°)	$\phi'$ (°)	$\rho'(\alpha', \phi')$
0.871	0.409	0.0	25.154	90.0	0.962
0.884	0.416	0.0	25.201	90.0	0.977
0.442	0.830	0.0	61.963	90.0	0.940
0.0	0.616	0.977	90.0	32.231	1.155
0.533	0.0	1.017	0.0	27.659	1.148
0.511	0.0	1.070	0.0	25.528	1.186
0.693	0.670	0.895	44.033	47.123	1.315
0.696	0.671	0.901	43.952	47.017	1.322
0.413	1.046	0.355	68.454	72.481	1.179
0.450	0.847	0.0	62.019	90.0	0.959
0.448	0.843	0.0	62.012	90.0	0.955
0.424	0.797	0.0	61.987	90.0	0.903
0.984	0.420	0.0	25.164	90.0	0.988
0.874	0.411	0.0	25.185	90.0	0.966
0.690	0.666	0.890	43.986	47.137	1.308
-0.407	0.821	0.0	116.369	90.0	0.916



TABLE 5.4 - Example 2: Average Radial Data for  $\tau_{12} \neq 0$ 

$\rho_*(\alpha', \phi')$	$\alpha'$ ( $^\circ$ )	$\phi'$ ( $^\circ$ )	$\rho_{avg}$	$\alpha'_{avg}$	$f(\sigma')$	$f_{avg}(\alpha')$
1.148	0	27.659	1.167	0	0.360	0.419
1.186	0	25.528			0.478	
1.322	43.952	47.017			0.646	
1.308	43.986	47.137	1.315	44	0.618	0.632
1.315	44.033	47.123			0.632	
1.179	68.454	72.481	1.179	68.45	0.624	0.624
1.155	0	32.231	1.155	90	0.344	0.344

TABLE 5.5 - Example 2: Experimental-Theoretical Correlation

Failure Equation	Error on the plane $\tau_{12} = 0$ (31 pts)	Error for $\tau_{12} \neq 0$ (15 pts)	Total Error (46 pts)
Tennyson's Cubic Equation Eq. (5-22)	0.31673	0.04068	0.35741
Eq. (5-29)	0.34437	0.02189	0.36626
Eq. (5-32)	0.31351	0.02766	0.34117
Eq. (5-41)	0.34437	0.00491	0.34928

TABLE 5.6 - Example 3: Biaxial Strength of Paperboard (all units: MPa)

$\sigma_1$	$\sigma_2$	$\sigma_1$	$\sigma_2$	$\sigma_1$	$\sigma_2$	$\sigma_1$	$\sigma_2$	$\sigma_1$	$\sigma_2$
$\tau_{12} = 0$ :									
-22.3	7.6	-15.3	22.9	-6.4	-12.7	-20.3	8.5	-15.0	-8.7
-4.8	-13.7	-19.6	11.4	-15.0	22.7	-4.8	-12.5	-19.4	4.0
-12.4	-11.4	-2.0	-12.9	-19.3	-2.5	-12.1	-11.7	0	-12.2
-18.5	16.1	-11.5	-12.6	7.2	-13.1	-18.1	-6.7	-11.4	26.4
11.8	-14.3	-17.9	-5.2	-9.4	-13.1	16.2	-13.4	-17.7	-21.5
-9.3	-12.7	23.1	-13.2	-16.8	-8.0	-8.2	13.6	27.3	-13.3
-15.4	24.4	-8.1	-13.0	27.9	-12.5	6.3	32.1	45.8	35.7
53.0	25.6	6.4	32.5	51.7	6.5	54.3	6.4	16.7	34.8
52.9	24.6	54.5	25.4	17.9	37.0	-13.8	-13.8	-12.1	-12.1
35.5	35.5	-13.4	-13.4	-12.1	-12.1	35.9	35.9	-13.1	-13.1
-11.7	-11.7	35.9	35.9	-13.1	-13.1	34.5	34.5	35.9	35.9
-13.1	-13.1	34.5	34.5	36.5	36.5	-12.4	-12.4	35.2	35.2
36.5	36.5	-12.1	-12.1	35.5	35.5	36.5	36.5		
$\tau_{12} = 6.9$ :									
-16.6	19.0	44.5	21.3	50.2	6.2	6.4	30.5	45.9	0
52.7	5.9	6.9	32.1	46.0	21.4	55.2	25.7	38.5	32.3
-20.3	3.1	-3.5	-11.4	34.1	31.7	-17.9	-1.4	5.9	-11.0
34.1	34.1	-13.1	-5.5	12.4	29.0	37.9	30.0	-14.7	9.7
24.1	32.4	44.8	28.3	-11.4	-11.4	25.5	-12.1	48.3	24.1
-8.3	-11.0	30.7	33.1	50.0	12.4	-16.6	19.0	6.9	31.1
$\tau_{12} = 10.3$ :									
6.3	26.3	29.3	27.8	48.3	23.1	6.3	28.3	45.5	21.2
49.1	0.0	20.5	32.8	46.9	21.8	52.6	6.6	-15.9	-9.3
-0.7	23.4	31.0	31.0	-11.4	0.3	2.8	-9.3	31.4	27.9
-9.3	-5.5	17.6	29.7	37.9	25.9	-9.0	-9.0	19.7	-5.5
48.6	23.8	-5.2	-8.6	26.2	30.6	50.3	14.5		
$\tau_{12} = 15.9$ :									
19.5	25.9	33.6	16.1	38.5	17.9	19.8	23.3	36.8	17.1
39.9	13.4	22.1	22.4	38.4	18.4	40.5	13.1	-3.8	13.8
2.8	21.0	26.2	20.7	-3.5	2.1	13.4	-4.8	34.5	16.6
-1.4	-1.4	17.2	23.1	44.1	6.9	1.0	-4.1	23.1	23.1
48.6	11.7								

$X = 55.9$  ,  $X' = 20.5$  ,  $Y = 30.8$  ,  $Y' = 13.1$  ,  
 $P = 35.7$  ,  $P' = 12.1$  ,  $S_{45} = 13.6$  ,  $S'_{45} = 17.9$  ,  $S = 16.6$

TABLE 5.7 - Example 3: Error Calculation

(all units: MPa<sup>2</sup>)

Theory	Error $\tau_{12} = 0$	Error $\tau_{12} > 0$	Total Error
Tsa1-Wu, $F_{12}=0.0$	1046.3	802.2	1848.5
Tsa1-Wu, $F_{12}=-2.017 \times 10^{-4}$	588.4	1708.4	2296.8
Tsa1-Hill	1005.7	10585.3	11591.0
Norris	579.0	8204.4	8783.4
Rowlands	403.1	8316.5	8719.6

TABLE 5.8 - Paperboard Calculation of Best-fit for Each Plane

Theory	$\tau_{12}$	$g(\tau_{12})$	Error	Total Error
Tsai-Wu $F_{12} = 0$	0	0	1046.3	1821.6
	6.9	0.174	363.3	
	10.3	0.447	301.9	
	15.9	0.957	110.1	
Tsai-Wu $F_{12} = -2.017 \times 10^{-4}$	0	0	588.4	1741.0
	6.9	0.350	473.3	
	10.3	0.594	241.8	
	15.9	1.0	437.6	
Tsai-Hill	0	0	1005.7	2177.4
	6.9	0.061	398.7	
	10.3	0.173	328.2	
	15.9	0.486	444.8	
Norris	0	0	579.0	1495.1
	6.9	0.247	388.2	
	10.3	0.352	187.6	
	15.9	0.594	340.4	
Rowlands	0	0	403.1	1639.0
	6.9	0.269	299.2	
	10.3	0.369	448.4	
	15.9	0.618	488.3	

TABLE 5.9 - Example 4: Experimental Results for Carbon-Epoxy

$\sigma_1$ (MPa)	$\sigma_2$ (MPa)	$\tau_{12}$ (MPa)	$\alpha$ (°)	$\phi$ (°)	$\rho(\alpha, \phi)$ (MPa)
1360	0	0	0	90	1360
0	28	0	90	90	28
0	-123.5	0	-90	90	123.5
0	0	62.6	90	0	62.6
1673	-167	0	-5.7	90	1681
688	-172	0	-14	90	709
648	-162	0	-14	90	668
0	9.2	16.1	90	29.7	18.5
0	12.0	43.8	90	15.3	45.4
0	-48.3	83.6	-90	30	96.5
0	-92.8	62.6	-90	56	111.9

TABLE 5.10 - Example 4: Uniaxial Tension of Angle-Ply Laminates

$\sigma_x$ (MPa)	$\theta$ (°)	$\sigma_1$ (MPa)	$\sigma_2$ (MPa)	$\tau_{12}$ (MPa)	$\alpha$ (°)	$\phi$ (°)	$\rho(\alpha, \phi)$ (MPa)
1220	$\pm 12.5$	1260	-40	$\pm 49$	-1.8	87.8	1262
610	$\pm 28.75$	673	-63	$\pm 127$	-5.3	79.4	688
53	$\pm 49.7$	41	12	$\pm 29$	16.3	55.8	51.6
41	$\pm 61.5$	16	24	$\pm 22$	56.3	52.7	36.3
23	$\pm 78.75$	1	22	$\pm 6$	87.4	74.8	22.8
-135	$\pm 49.4$	-105.4	-29.2	$\pm 74.0$	15.5	-55.9	132.1
-108	$\pm 61.5$	-43.2	-64.5	$\pm 57.3$	56.2	-53.6	96.5
-135	$\pm 79.5$	-6.8	-128.6	$\pm 30.4$	87.0	-76.7	132.2

$$E_1 = 122\,011 \text{ MPa}$$

$$E_2 = 9\,141 \text{ MPa}$$

$$\nu_{12} = 0.3975$$

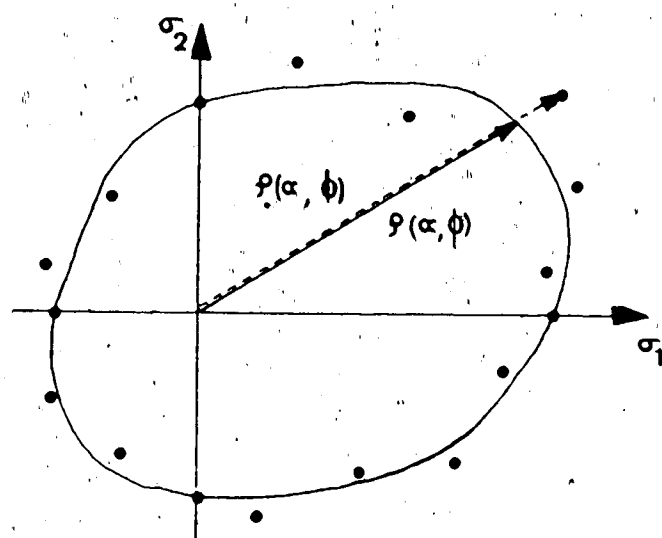
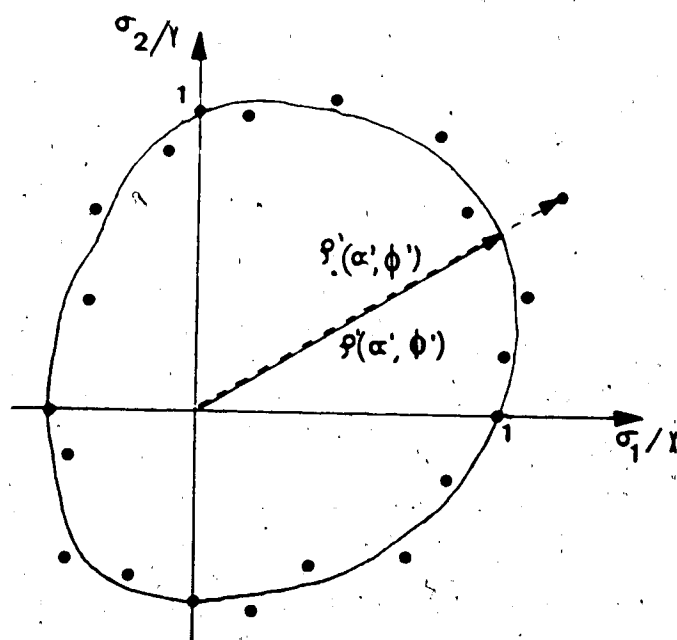
$$G_{12} = 5\,500 \text{ MPa}$$

$$S_{11} = 8.196 \times 10^{-6} \text{ MPa}^{-1}$$

$$S_{22} = 1.094 \times 10^{-4} \text{ MPa}^{-1}$$

$$S_{12} = -3.258 \times 10^{-6} \text{ MPa}^{-1}$$

$$S_{66} = 1.818 \times 10^{-4} \text{ MPa}^{-1}$$

A - SYSTEM OF AXIS  $\sigma_1 - \sigma_2 - \tau_{12}$ 

B - NORMALIZED SYSTEM OF AXIS

FIGURE 5-1 EXPERIMENTAL THEORETICAL CORRELATION

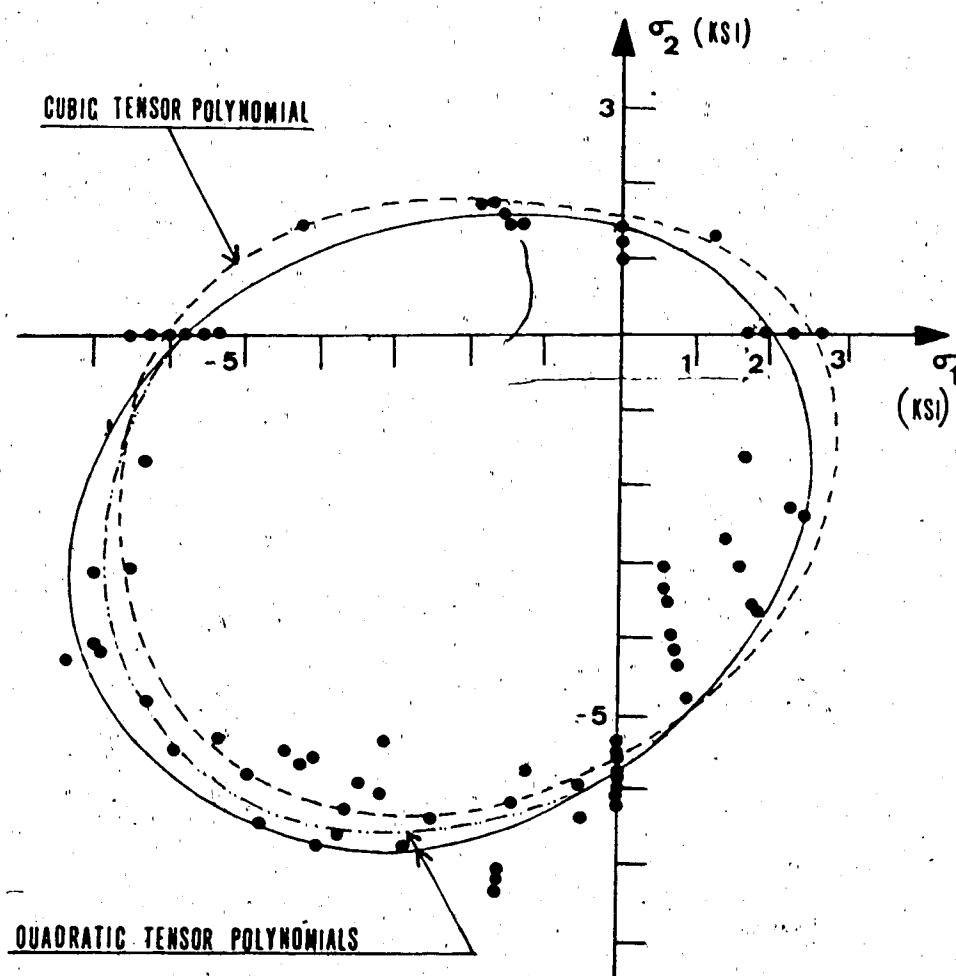


FIGURE 5-2 EXAMPLE 1: BIAXIAL STRESSES IN GRAPHITE

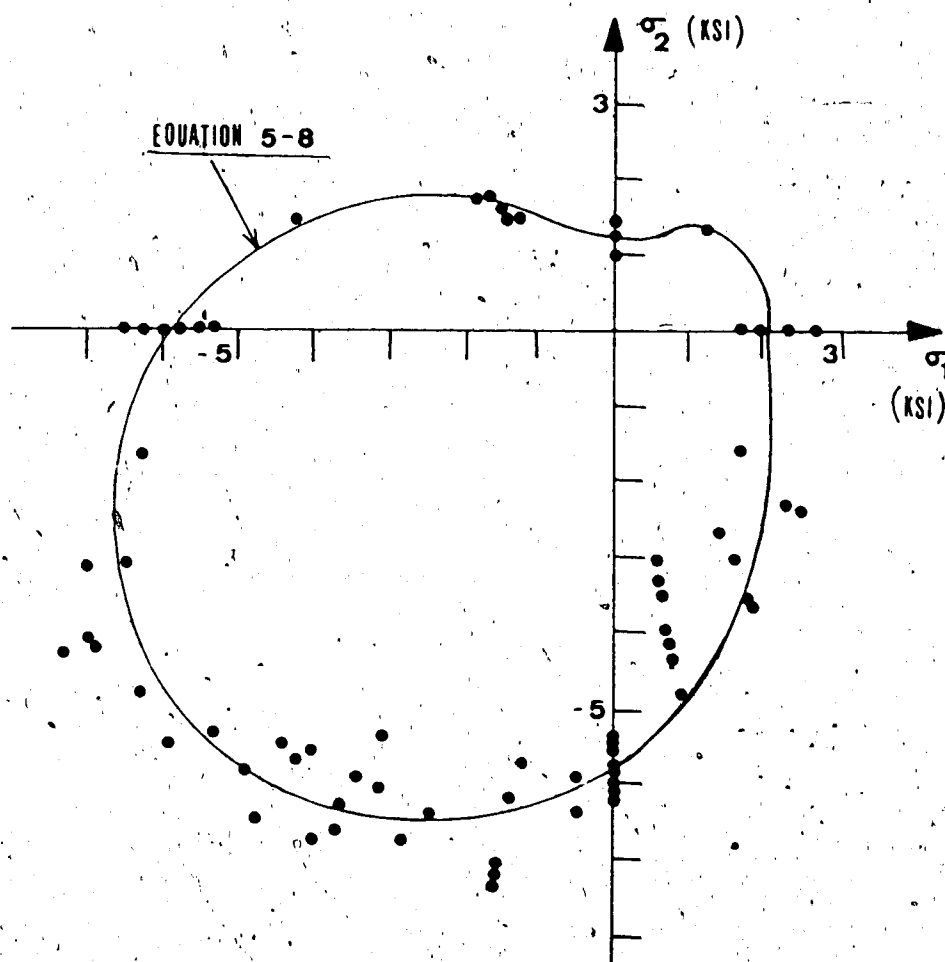


FIGURE 5-3 EXAMPLE 1: FIRST PARAMETRIC SOLUTION



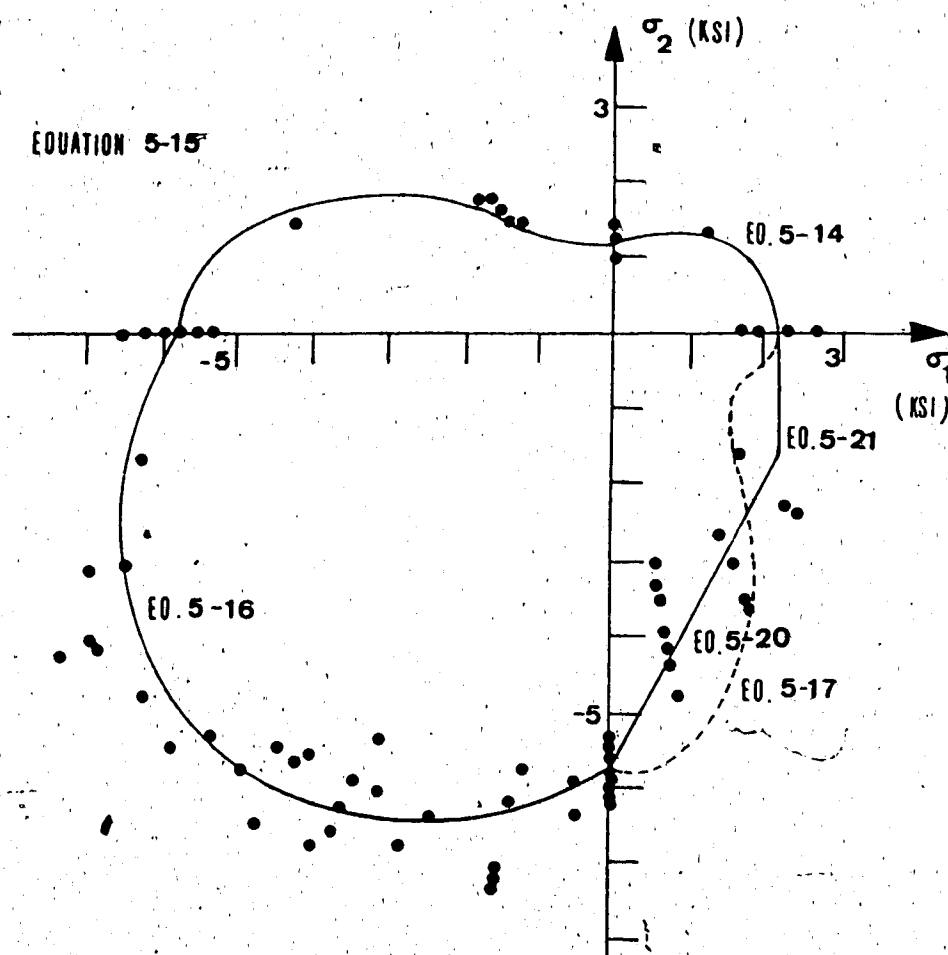


FIGURE 5-4 EXAMPLE 1: SECOND PARAMETRIC SOLUTION

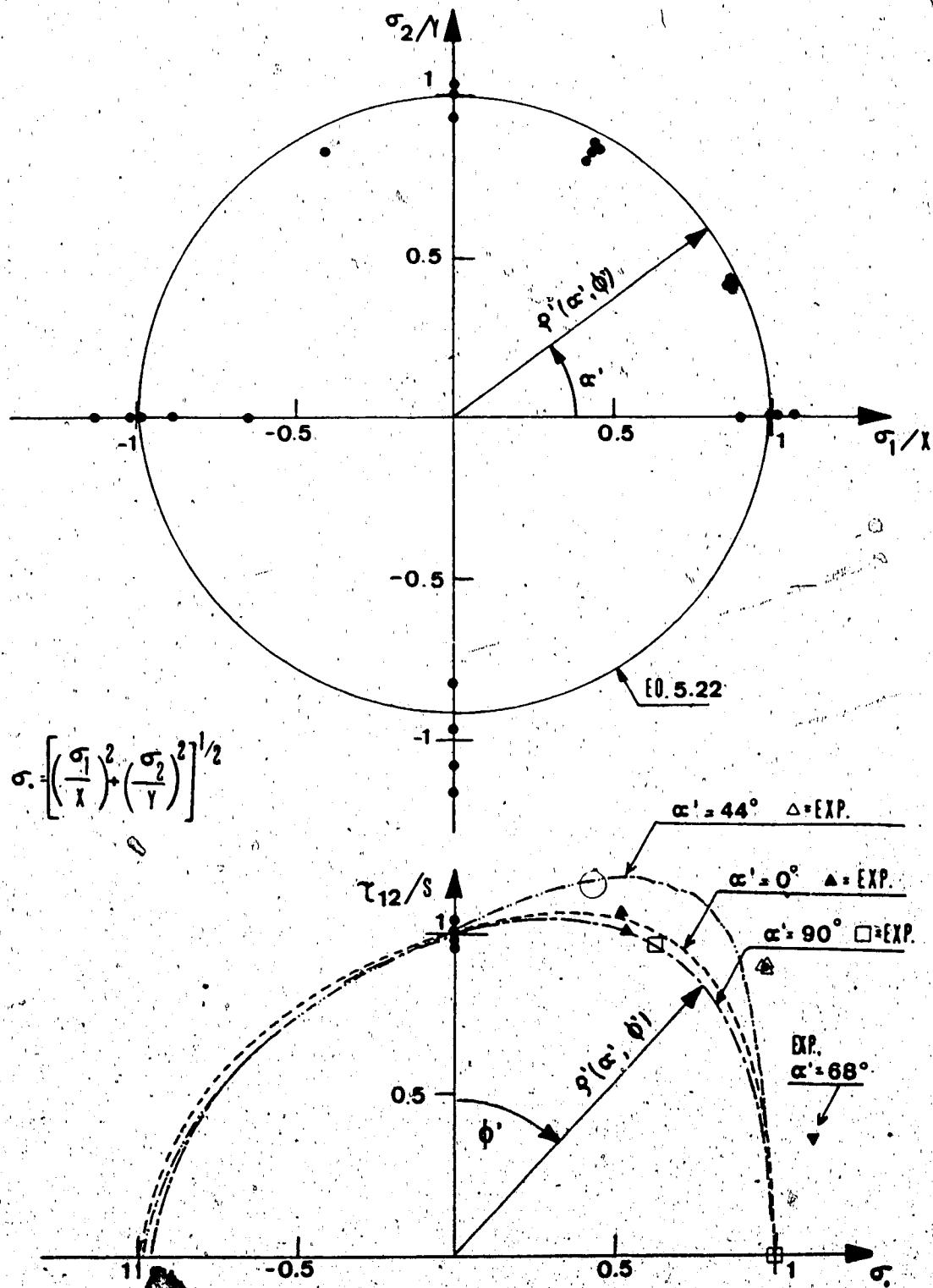


FIGURE 5-5 EXAMPLE 2. BIAxIAL STRESSES IN GRAPHITE EPOXY FABRIC.

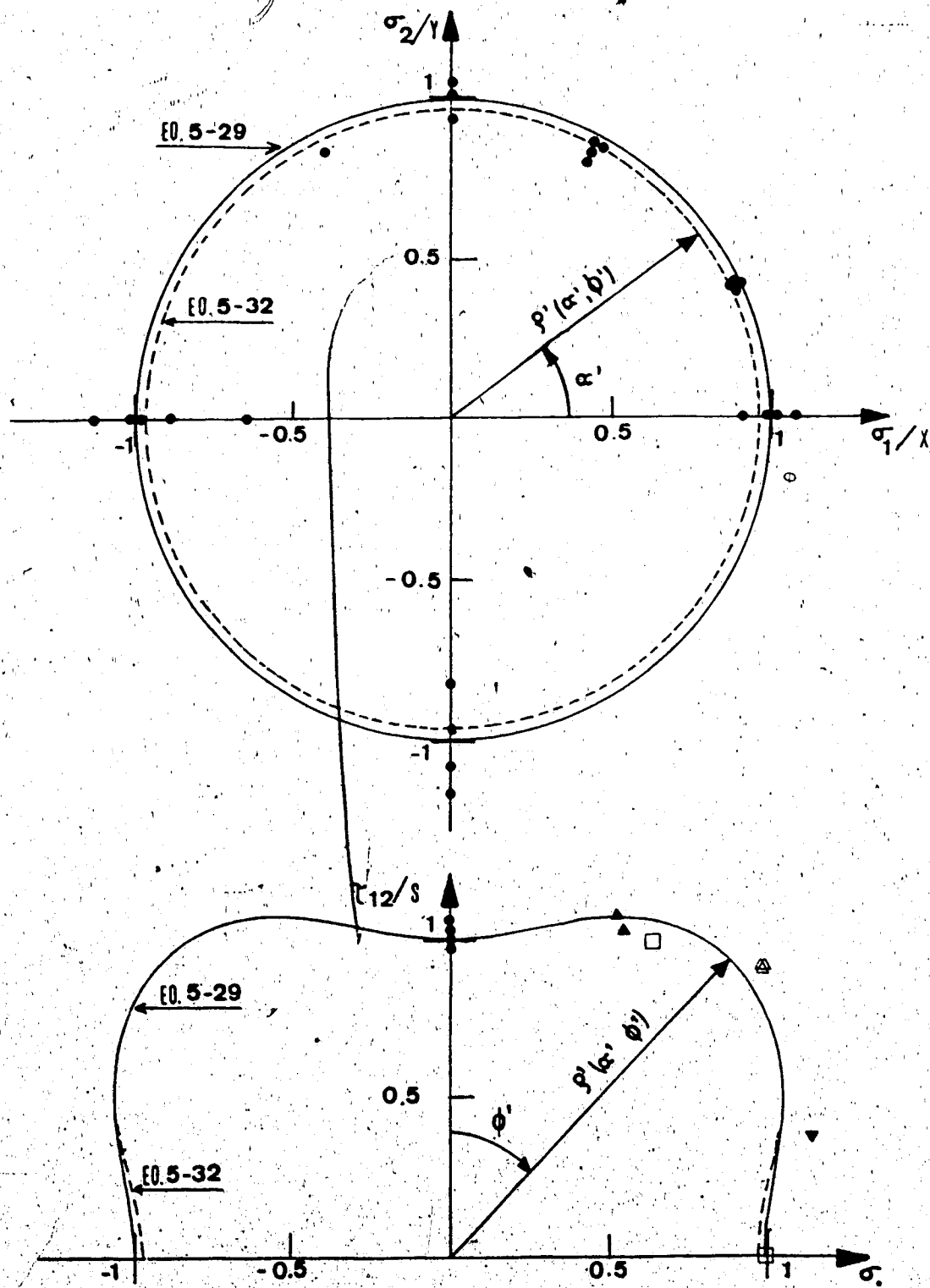


FIGURE 5-6 EXAMPLE 2: FIRST PARAMETRIC SOLUTION

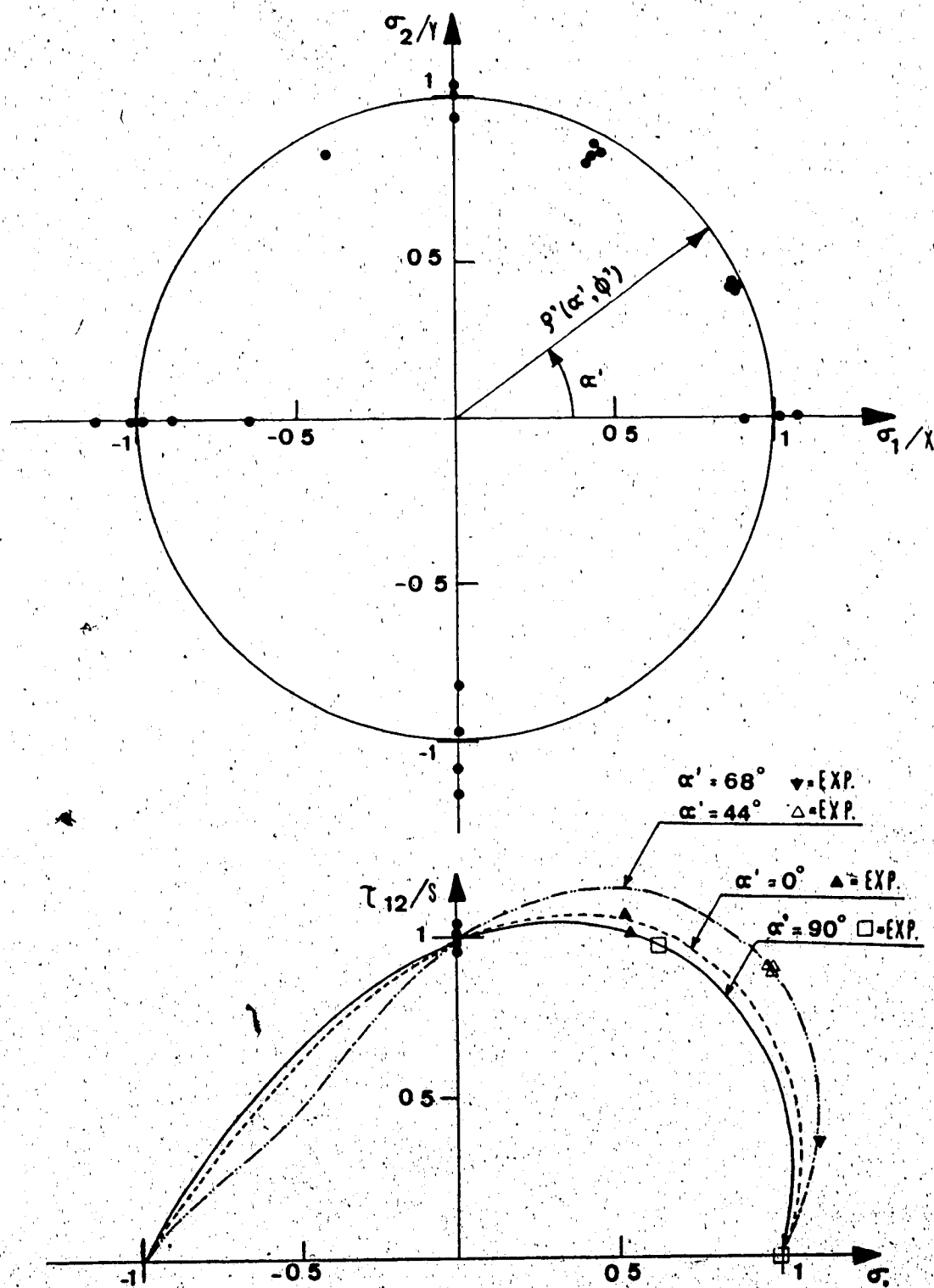


FIGURE 5-7 EXAMPLE 2: SECOND PARAMETRIC SOLUTION

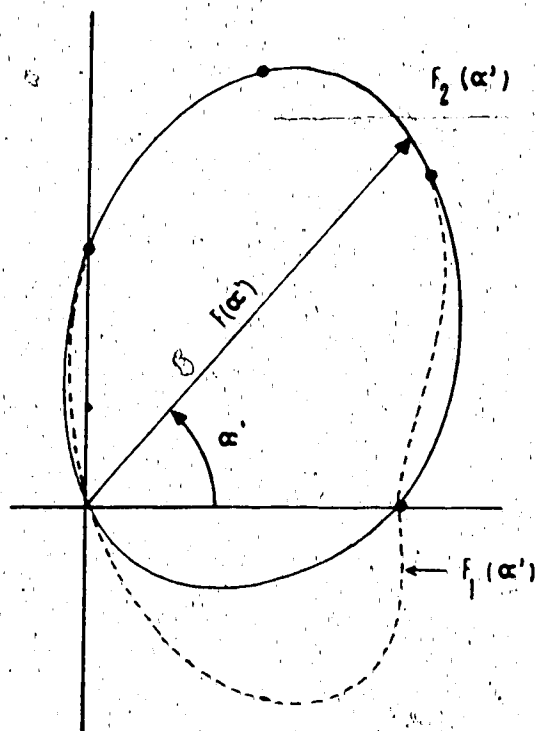


FIGURE 5-8 EXAMPLE 2: FITTING OF THE SECOND  
PARAMETRIC SOLUTION

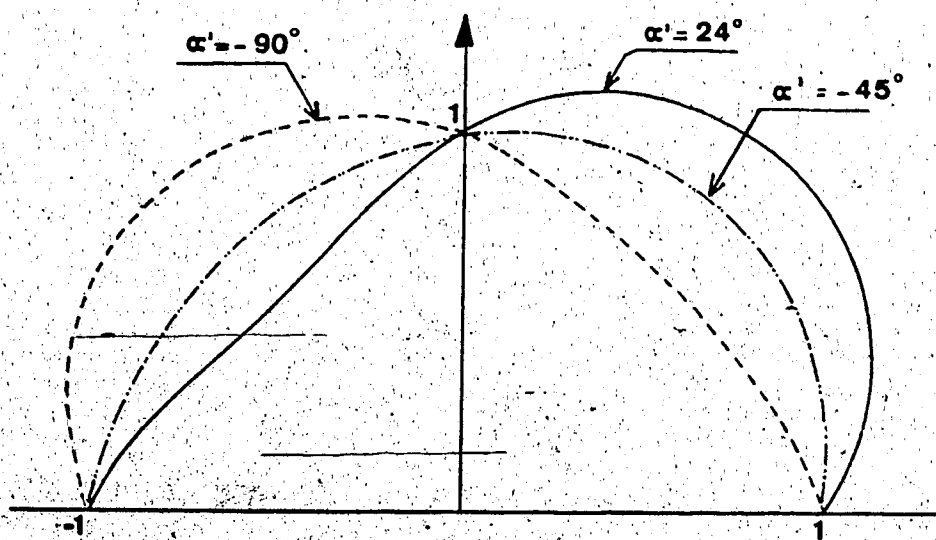


FIGURE 5-9 EXAMPLE 2: ADDITIONAL SECTIONS OF THE SECOND  
PARAMETRIC SOLUTION

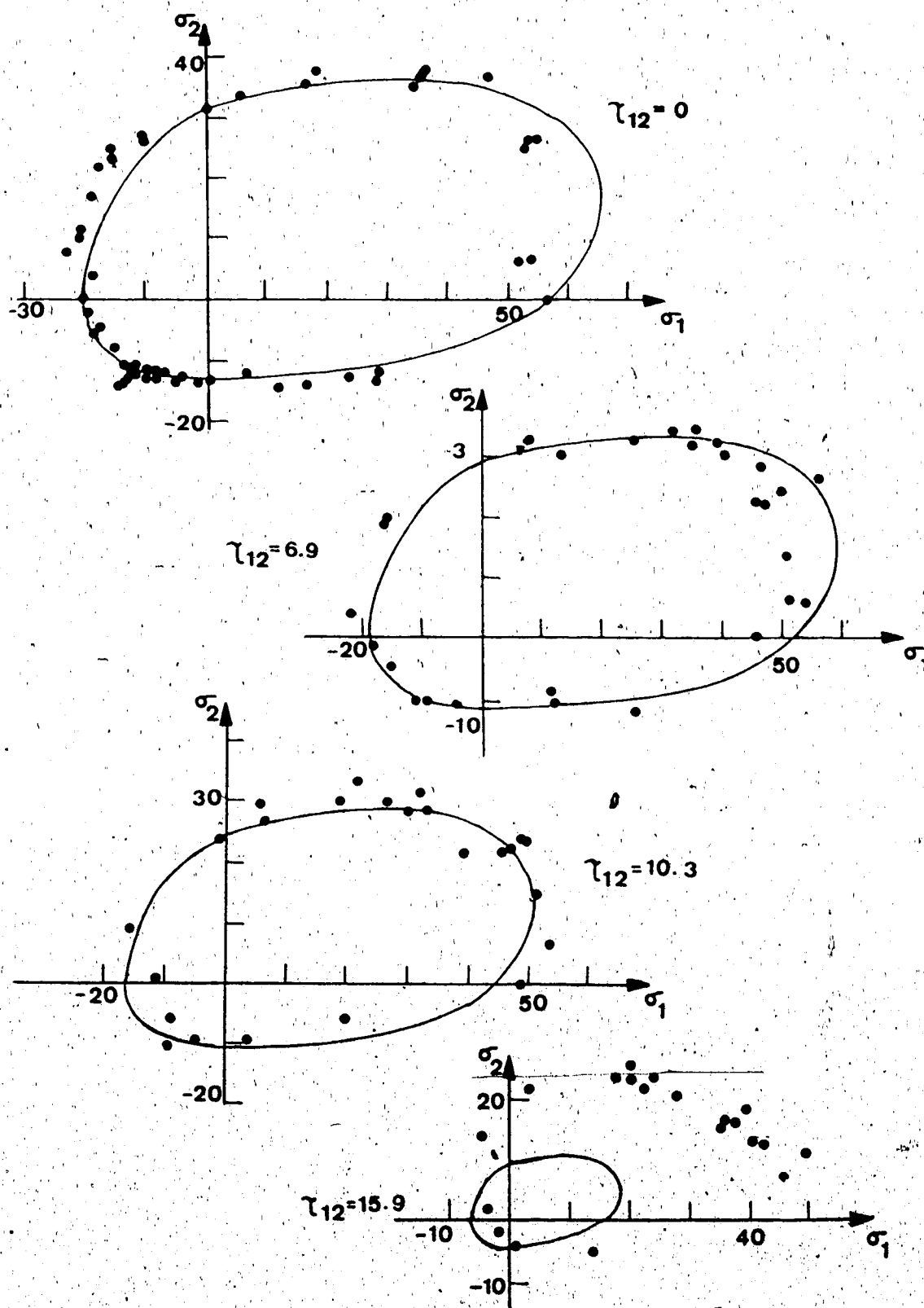


FIGURE 5-10 EXAMPLE 3 BIAxIAL STRESSES IN PAPERBOARD (ALL UNITS MPa)

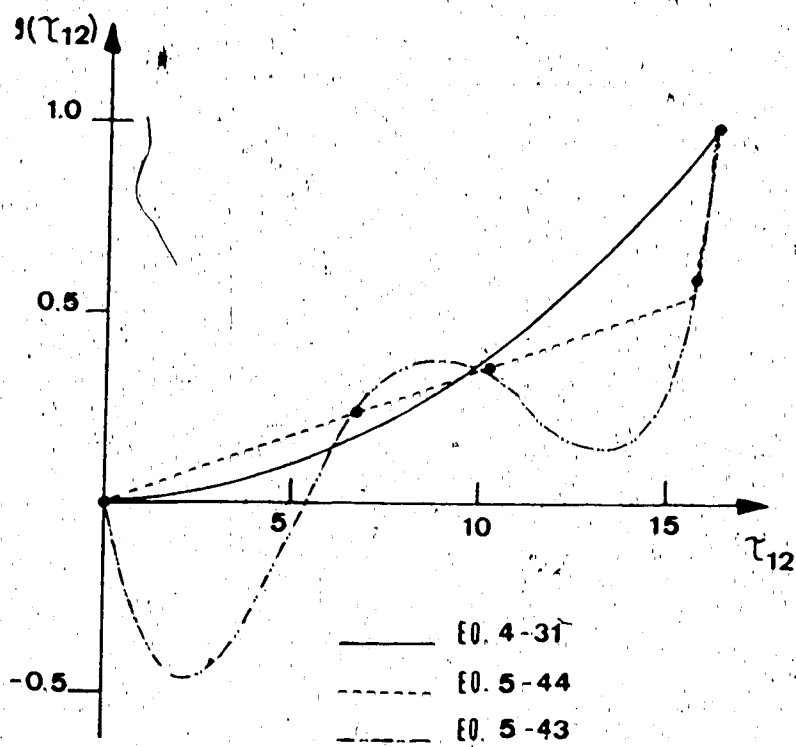


FIGURE 5-11 EXAMPLE 3: FITTING OF THE FAILURE FUNCTION

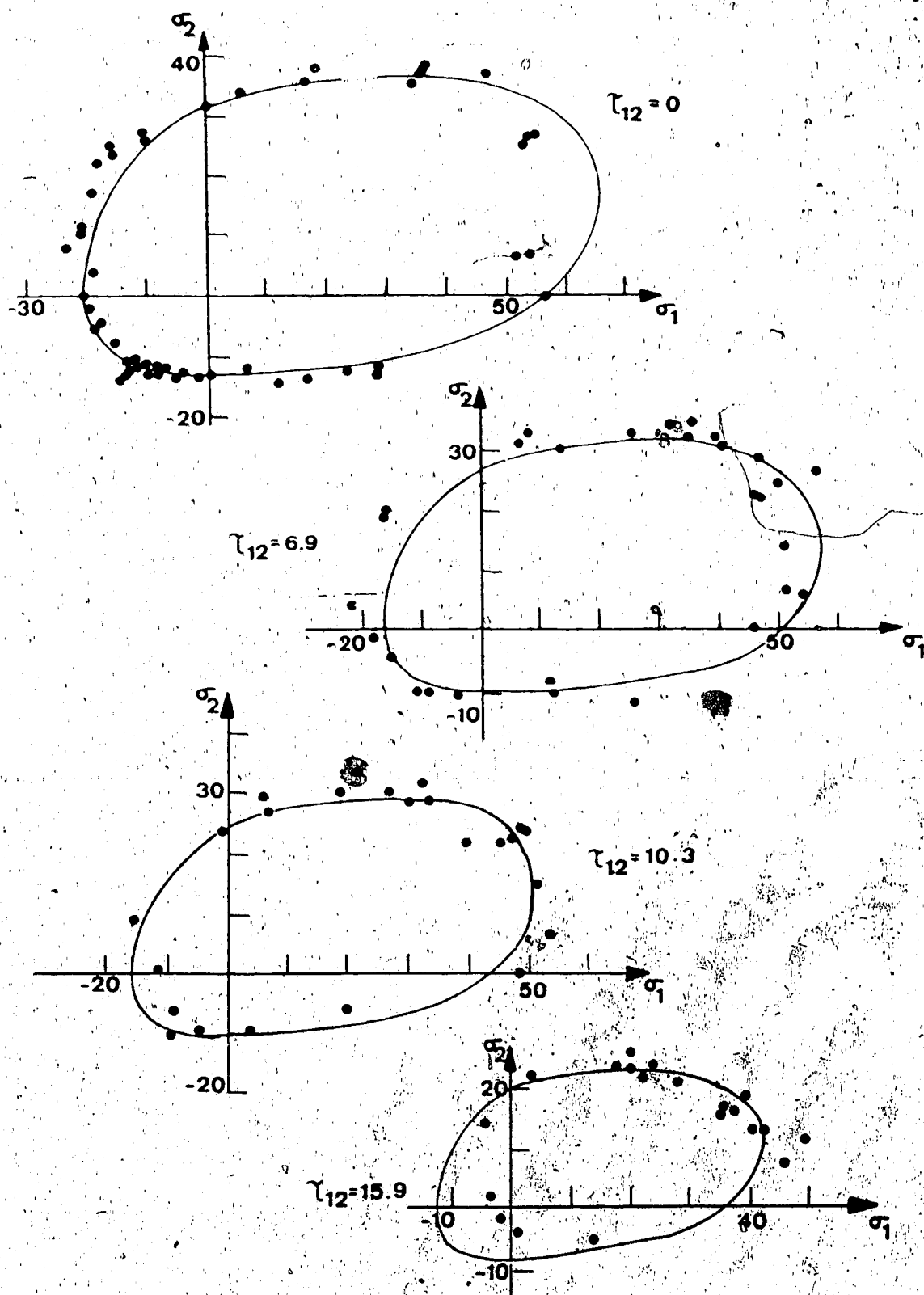


FIGURE 5-12 EXAMPLE 3: MODIFIED NORRIS CRITERION (ALL UNITS MPa)



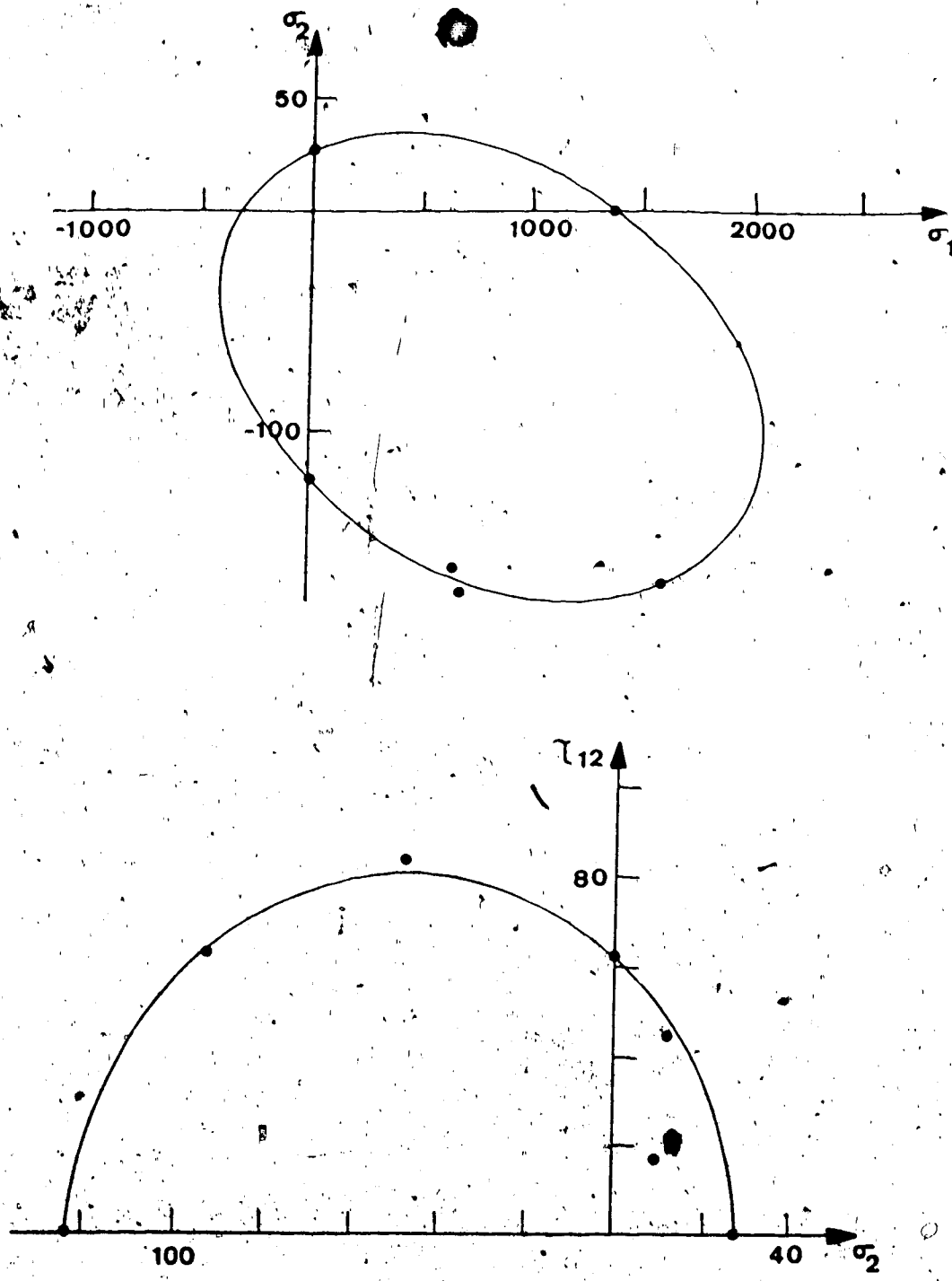


FIGURE 5-13 EXAMPLE 4: BIAxIAL STRESSES IN CARBON EPOXY

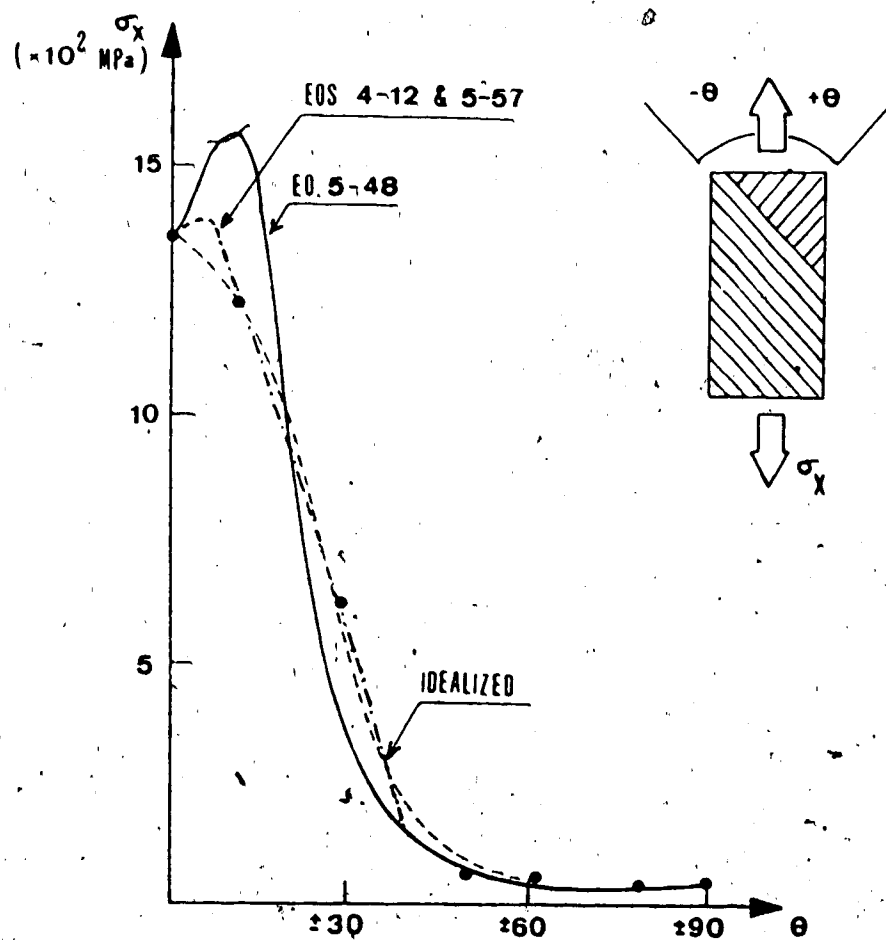


FIGURE 5-14 EXAMPLE 4: ANGLE PLY LAMINATES STRESSES.

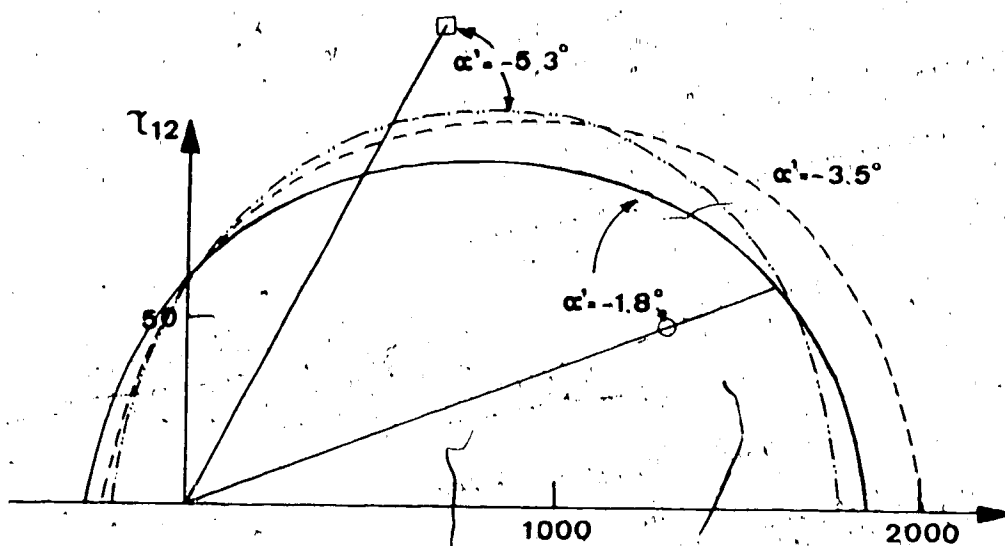


FIGURE 5-15 EXAMPLE 4: QUADRATIC TENSOR POLYNOMIAL

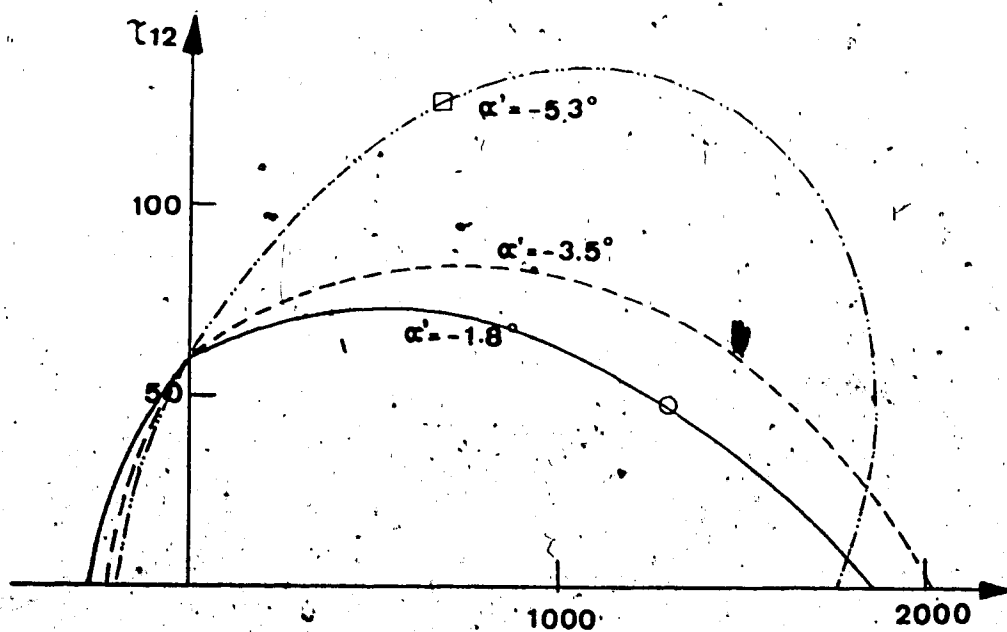


FIGURE 5-16 EXAMPLE 4: PARAMETRIC FAILURE ENVELOPE

## CHAPTER 6

## CONCLUSION

## CHAPTER 6

## CONCLUSION

The topic of this thesis is the failure prediction of fibre-reinforced composite materials. In the first chapter, the basic assumptions made in order to analyze these materials were introduced. Despite the complexity of observed failure modes, the hypotheses of homogeneity and orthotropy are retained for the analysis of unidirectional or bi-directional laminae. The corresponding equations of elasticity were presented in the second chapter.

Over the last twenty years, many failure criteria have been proposed for composite materials. A review of these theories was presented in Chapter 3. Among them, a survey has shown that the maximum stress and maximum strain theories are the most widely employed in practice, although they are generally viewed as conservative. Other criteria have been obtained by modifying the well-known Hill theory of plastic yielding for anisotropic materials. The tensor polynomial theory, first proposed in the 1970's, is now the most discussed among researchers. It is attractive for many reasons: it encompasses every criterion proposed previously, it is a single continuous function, and the rules of transformation are well known for tensors. The quadratic tensor polynomial is now the most popular. However, this failure envelope is always an ellipsoid and does not provide an accurate representation of failure data for all composites. Some researchers have recently advocated the use of third-order tensor polynomials. This causes an increase in the number of strength parameters. One disadvantage is that the closure of

the failure envelope cannot always be guaranteed. Also, to find the failure stresses under any loading condition, one has to solve for the roots of a cubic equation.

With the discussion still underway on the merits of the tensor polynomial theory, and with this approach becoming increasingly complicated, it seemed timely to investigate new techniques to predict failure of fibre-reinforced materials in plane stress. In Chapter 4, a method which was recently brought forward by Budiansky to predict plastic yielding in sheet materials was introduced. Then, a generalization of this method to predict the failure of fibre-reinforced materials in plane stress was proposed. Although the failure surface to be defined is in the  $\sigma_1 - \sigma_2 - \tau_{12}$  space, the new criterion is not written directly in terms of these stresses. It is rather suggested that a parametric equation of the failure surface can be written as  $\rho = \rho(\alpha, \phi)$ , where  $\rho$  is the length of the vector going from (0, 0, 0) to the failure point for a proportionate stress path. The values  $\alpha$  and  $\phi$  depend on the loading orientation.

The following characteristics of the parametric criterion were discussed. First, it was shown that the tensor polynomial theory was a special case of the new parametric criterion. It follows that all existing criteria could be written in parametric form. Second, the failure surface can always be closed if appropriate functions of the angles  $\alpha$  and  $\phi$  are selected. There is no need for additional conditions to ensure closure of the failure envelope. Third, it is possible to define failure surfaces with shapes much more complicated than ellipsoids without using more parameters. Among the possibilities investigated

were: use of high order equations, use of non-integer exponents, fitting of different portions of the failure surface with different equations. The major advantage of this approach is therefore its flexibility. This was demonstrated through the examples of Chapter 5. Finally, it should be pointed out that, in applying the parametric criterion, it is a simple task to identify the failure strength for any proportional loading path. One only needs to insert the appropriate values of the angles  $\alpha$  and  $\phi$  in the failure equation.

A disadvantage with the new parametric criterion at this time is that it does not yet provide a single equation that would apply to all fibre-reinforced materials. A new equation  $\rho = \rho(\alpha, \phi)$  has to be written for each material, depending on the available experimental data. When only the uniaxial strengths in the axes of material symmetry are known, it is still appropriate to write the quadratic tensor polynomial equation, because all experimental data are then well reproduced. However, when additional results are available that cannot be satisfied with this criterion, the expansion of the tensor equation to include third-order terms may not always be the best solution. The parametric failure criterion can be a useful alternative solution.

Eventually, different failure equations in parametric coordinates could be generated for different materials. A question that can be raised at this point is the possibility that a general parametric equation be developed for all fibre-reinforced laminae. This question was not investigated in detail here, but it was shown that a series of trigonometric functions could represent all failure surfaces satisfying the conditions of Chapter 4. Additional investigations should be pursued in this area in the future.

No experimental work has been performed in this investigation; only experimental results available in the literature have been used to demonstrate the flexibility of this new approach. A further step would now be to measure experimental data in order to use the criterion as efficiently as possible, that is along planes of constant  $\alpha$  and  $\phi$ . A chart identifying the tests lying on these planes was provided in Chapter 4. With that technique, it would be easier to write a failure function because only one term varies at a time.

Another area where complementary research should also be done concerns the influence of the loading path on the shape of the failure envelope. All failure theories developed so far are for proportionate loading paths. However, it is now well known that the loading path has a significant effect on the failure strength of fibre-reinforced laminae. When this is observed, the areas affected should be identified and this effect taken into account in the failure equation. This can possibly be achieved by writing different equations for different loading paths. A better understanding of the loading path influence on failure surfaces for laminae would certainly improve the accuracy of laminate analyses.



## REFERENCES

## REFERENCES

- ASHKENAZI, E.K. (1966), "Problems of the Anisotropy of Strength," *Polymer Mechanics*, 69-72.
- ASHTON, J.E., HALPIN, J.C., PETIT, P.H. (1969), Primer on Composite Materials: Analysis, Technomic Publishing Company, Stamford, CT.
- AZZI, V.D., TSAI, S.W. (1965), "Anisotropic Strength of Composites," *Experimental Mechanics* 5, 283-288.
- BORESI, A.P., SIDEBOTTOM, O.M. (1985), Advanced Mechanics of Materials, John Wiley and Sons, New York, NY.
- BUDIANSKY, B. (1984), Anisotropic Plasticity of Plane-Isotropic Sheets, in *Mechanics of Material Behavior*, Elsevier Science Publishers, Amsterdam.
- CHAMIS, C.C. (1969), "Failure Criteria for Filamentary Composites," *Composite Materials: Testing and Design*, ASTM STP460, 336-351.
- CHOO, Y.S.C. (1985), "Effect of Loading Path on the Failure of Fibre-Reinforced Composite Tubes," *Journal of Composite Materials* 19, 526-532.
- COWIN, S.C. (1979), "On the Strength Anisotropy of Bone and Wood," *Trans. ASME Journal of Applied Mechanics* 46, 832-836.
- DE RUVO, R., CARLSSON, L., FELLERS, C. (1980), "The Biaxial Strength of Paper," *TAPPI* 63, 133-136.
- FISHER, L. (1967), "Optimization of Orthotropic Laminates," *Trans. ASME Journal of Engineering for Industry* 89, Series B, 339-402.
- FRANCIS, P.H., WALRATH, D.E., WEED, D.N. (1979), "First-Ply-Failure of G/E Laminates Under Biaxial Loading," *Fibre Science and Technology* 12, 97-110.
- GOL'DENBLAT, I., KOPNOV, V.A. (1966), "Strength of Glass-Reinforced Plastics in the Complex Stress State," *Polymer Mechanics* 1, 54-59.
- GREENWOOD, J.H., "German Work on Grp Design," *Composites* 8, 175-184.
- GRIFFITH, J.E. BALDWIN, W.M. (1962), "Failure Theories for Generally Orthotropic Materials," in *Developments in Theoretical and Applied Mechanics*, Vol. 1, Plenum Press, New York, NY, 410-420.

- GUESS, T.P. (1980), "Biaxial Testing of Composite Cylinders: Experimental-Theoretical Comparison," *Composites* 11, 139-148.
- HÄHN, H.T., TSAI, S.W. (1974), "On the Behaviour of Composite Laminates After Initial Failure," *Journal of Composite Materials* 8, 288-305.
- HALPIN, J.C., PAGANO, N.J., WHITNEY, J.M., WU, E.M. (1969), "Characterization of Anisotropic Composite Materials," in *Composite Materials: Testing and Design*, ASTM STP460, 37-47.
- HASHIN, Z. (1980), "Failure Criteria for Unidirectional Fiber Composites," *Trans. ASME Journal of Applied Mechanics* 47, 329-334.
- HASHIN, Z. (1983), "Analysis of Composite Materials: A Survey," *Trans. ASME Journal of Applied Mechanics* 50, 481-505.
- HASHIN, Z., ROTEM, A. (1973), "A Fatigue Failure Criterion for Fibre-Reinforced Materials," *Journal of Composite Materials* 7, 448-464.
- HILL, R. (1956), The Mathematical Theory of Plasticity, Oxford University Press, London.
- HILL, R. (1979), "Theoretical Plasticity of Textured Aggregates," *Mathematical Proceedings of the Cambridge Philosophical Society* 85, 179-191.
- HOFFMAN, O. (1967), "The Brittle Strength of Orthotropic Materials," *Journal of Composite Materials* 1, 200-206.
- HUANG, C.L.D. (1985), "Cubic Strength Criteria for Transversely Isotropic Brittle Media," *Proceedings of the Tenth Canadian Congress of Applied Mechanics*, London, A45-46.
- HUTTER, U., SCHELLING, H., KRAUSS, H. (1974), "An Experimental Study to Determine Failure Envelope of Composite Tubular Specimens Under Combined Loads and Comparison with Classical Criteria," *Proc. of the NATO AGARD Meeting on Advanced Composites*, No. 163, Munich, Germany.
- IKEGAMI, K., NOSE, Y., YASUNAGA, T., SHIRATORI, E. (1982), "Failure Criterion of Angle-Ply Laminates of Fibre-Reinforced Plastics and Applications to Optimize the Strength," *Fibre Science and Technology* 16, 175-190.
- IKEGAMI, K., TAKAHASHI, T. (1983), "Failure Surfaces of Fibre-Reinforced Plastics and Optimal Fibre Orientations," *Proc. of the CNRS Colloquium #351, Grenoble, France, (in press)*.
- JONES, B.H. (1969), "Determination of Design Allowables for Composite Materials," in *Composite Materials: Testing and Design*, ASTM STP460, 285-306.

- JONES, E.R. (1969), "Strength of Glass Filament-Reinforced Plastics in Biaxial Loadings," *Journal of the Society of Plastics Engineers* 25, 50-53.
- JONES, R.M. (1975), *Mechanics of Composite Materials*, Scripta Book, Washington, D.C.
- LIEFMAN, J.M. (1975), "Non-Linear Matrix Failure Criterion for Fibre-Reinforced Composite Materials," *Composites Technology Review* 4, 78-83.
- MAKSIMOV, R.D., SOKOLOV, E.A., PLUME, E.Z. (1979), "Strength of an Organic/Glass Fibre-Reinforced Textolite in Plane Stress," *Mechanics of Composite Materials* 15, 702-709.
- MALMEISTER, A.K. (1966), "Geometry of Theories of Strength," *Polymer Mechanics* 2, 324-331.
- MARIN, J. (1957), "Theories of Strength for Combined Stresses and Non-Isotropic Materials," *Journal of the Aeronautical Sciences* 24, 265-268.
- MESHKOV, E.V., KULIK, V.I., UPITIS, Z.T., BUILIS, I.V. (1982), "Effect of Structural Parameters of Fiberglass on its Strength Under a Complex Stress State," *Mechanics of Composite Materials* 9, 299-302.
- NAYARANASWAMI, R., ADELMAN, H.M. (1977), "Evaluation of the Tensor Polynomial and Hoffman Strength Theories for Composite Materials," *Journal of Composite Materials* 11, 366-377.
- NORRIS, C.B. (1939), "The Elastic Theory of Wood Failure," *ASME Transactions* 61, 259-261.
- NORRIS, C.B. (1950), "Strength of Orthotropic Materials Subjected to Combined Stress," *U.S. Forest Products Laboratory Report* #1816.
- OWEN, M.J., GRIFFITHS, J.R. (1978), "Evaluation of Biaxial Stress Failure Surfaces for a Glass Fabric-Reinforced Polyester Resin Under Static and Fatigue Loading," *Journal of Materials Science* 13, 1521-1537.
- OWEN, M.J., RICE, D.J. (1981), "Biaxial Strength Behaviour of Glass Fabric-Reinforced Polyester Resins," *Composites* 12, 13-25.
- OWEN, M.J., RICE, D.J. (1982), "Biaxial Strength Behaviour of Glass-Reinforced Polyester Resins," *Composite Materials: Testing and Design*, ASTM STP787, 124-144.
- PABIOT, J. (1970), "Caractéristiques linéaires et non-linéaires d'un composite à renforcement unidirectionnel époxy-silice", *Proc. of the NATO AGARD Conference on Composite Materials* #63, Paris, France.

- PAGANO, N.J., PIPES, R.B. (1971), "Influence of Stacking Sequence on Laminate Strength," *Journal of Composite Materials* 5, 50-57.
- PETIT, P.H., WADDOUPS, M.E. (1969), "A Method of Predicting the Non-Linear Behaviour of Laminated Composites," *Journal of Composite Materials* 3, 2-17.
- PLUME, E.Z., MAKSIMOV, R.D. (1978), "Determining the Strength-Surface Tensor Components of Anisotropic Materials," *Polymer Mechanics* 14, 42-45.
- POPOV, E.P. (1976), *Mechanics of Materials*, Prentice-Hall, Englewood Cliffs, New Jersey.
- POPOV, E.P. (1968), *Introduction to Mechanics of Solids*, Prentice-Hall, Englewood Cliffs, New Jersey.
- PUCK, A., SCHNEIDER, W. (1969), "On Failure Mechanisms and Failure Criteria of Filament-Wound Glass-Fiber/Resin Composites," *Plastics and Polymers* 37, 33-44.
- PUPPO, A.H., EVENSEN, H.A. (1972), "Strength of Anisotropic Materials Under Combined Stresses," *AIAA Journal* 10, 468-474.
- RAGHAVA, R.S., CADDELL, R.M. (1974), "Yield Locus of Oriented Polycarbonates," *International Journal of Mechanical Sciences* 16, 789-799.
- ROWLANDS, R.E. (1975), "Flow and Failure of Biaxially Loaded Composites: Experimental-Theoretical Correlation," in *Proceedings of the ASME Winter Annual Meeting of the Applied Mechanics Division*, 97-126.
- ROWLANDS, R.E. (1985), "Strength (Failure) Theories and their Experimental Correlation," in *Handbook of Composites, Vol. 3: Failure Mechanics of Composites*, Elsevier Science Publishers, Amsterdam, 71-125.
- ROWLANDS, R.E., GUNDERSON, D.E., SUHLING, J.C., JOHNSON, M.W. (1985), "Biaxial Strength of Paperboard Predicted by Hill-Type Theories," *Journal of Strain Analysis* 20, 121-127.
- SANDHU, R.S. (1974), "Nonlinear Response of Unidirectional and Angle-Ply Laminates," *AIAA-ASME Structural, Structural Dynamics and Materials Conference*, Las Vegas, Nevada.
- SENDECKYJ, G.P. (1972), "A Brief Survey of Empirical Multiaxial Strength Criteria for Composites," in *Composite Materials: Testing and Design*, ASTM STP497, 41-51.
- SKUDRA, A.M., BULAVS, F. Ya. (1982), "Generalized Structural Criteria of Strength for Reinforced Plastics in Plane Stress State," *Mechanics of Composite Materials* 4, 428-434.

- SOKOLNIKOV, I.S. (1946), Mathematical Theory of Elasticity, R.E. Kriger Publishing Company, Malabar, Florida, (reprint edition 1983).
- SOKOLOV, E.A. (1979), "Experimental Evaluation of the Strength Anisotropy of a Unidirectionally Reinforced Organic Fiber-Reinforced Plastics," *Mechanics of Composite Materials* 15, 520-523.
- SOKOLOV, E.A., KREGER, A.F., MAKSIMOV, R.D. (1978), "Comparative Analysis of the Strength Anisotropy of Glass and Organic Fiber Plastic Laminates," *Polymer Mechanics* 14, 676-681.
- SONI, R.S. (1983), "A Comparative Study of Failure Envelopes in Composite Laminates," *Journal of Reinforced Plastics and Composites* 1, 34-42.
- STANOVSKY, J. (1985), "A Criterion for Ascertaining the Strength of Composite Materials," *Computers and Structures* 20, 387-390.
- SUHLING, J.C., ROWLANDS, R.E., JOHNSON, M.W., GUNDERSON, D.E. (1985), "Tensorial Strength Analysis of Paperboard," *Experimental Mechanics* 25, 75-84.
- TENNYSON, R.C. (1981), "Application of the Cubic Strength Criterion to the Failure Analysis of Composite Structures," NASA Contractor Report #165 712.
- TENNYSON, R.C., MACDONALD, D., NANYARO, A.P. (1978), "Evaluation of the Tensor Polynomial Failure Criterion for Composite Materials," *Journal of Composite Materials* 12, 63-75.
- TENNYSON, R.C., WHARRAM, G.E. (1985), "Evaluation of Failure Criterion for Graphite/Epoxy Fabric Laminates," NASA Contractor Report #172547.
- TSAI, S.W. (1965), "Strength Characteristics of Composite Materials," NASA Contractor Report #24.
- TSAI, S.W. (1983), "A Survey of Macroscopic Failure Criteria for Composite Materials," *Proc. of the CNRS Colloquium #351, Grenoble, France, (in press).*
- TSAI, S.W., HAHN, H.T. (1980), Introduction to Composite Materials, Technomic Publishing Co., Westport, Connecticut.
- TSAI, S.W., WU, E.M. (1971), "A General Theory of Strength for Anisotropic Materials," *Journal of Composite Materials* 5, 58-80.
- VOLOSHIN, A., ARCAN, M. (1980), "Failure of Unidirectional Fiber-Reinforced Materials: New Methodology and Results," *Experimental Mechanics* 20, 280-284.

- WENG, T.L. (1968), "Biaxial Fracture Strength and Mechanical Properties of Graphite-Base Refractory Composites," AIAA-ASME Structural Dynamics and Materials Conference, Palm Springs, California.
- WHITNEY, J.M., DANIEL, J.M., PIPES, R.B. (1982), "Experimental Mechanics of Fibre-Reinforced Composite Materials," Society for Experimental Stress Analysis, Brockfield Center, Connecticut.
- WU, E.M. (1974a), "Phenomenological Anisotropic Failure Criterion," in Composite Materials, Vol. 2: Mechanics of Composite Materials, Academic Press, New York, New York.
- WU, E.M. (1974b), "Failure Criteria to Fracture Mode Analysis of Composite Laminates," Proc. of the NATO AGARD Conference on Failure Modes of Composite Materials, #163, Munich, Germany.
- WU, E.M., SCHEUBLEIN, J.K. (1974), "Laminate Strength: A Direct Characterization Procedure," Composite Materials: Testing and Design, ASTM STP 546, 188-206.
- WU, R.Y., STACHURSKI, Z. (1984), "Evaluation of the Normal Stress Interaction Parameter in the Tensor Polynomial Theory for Anisotropic Materials," Journal of Composite Materials 18, 456-463.

## APPENDICES



APPENDIX I  
LIST OF TESTED MATERIALS  
IN THE LITERATURE

TYPE OF MATERIAL	IDENTIFICATION	REFERENCE
GLASS- EPOXY	glass epoxy AVCO 5505 glass epoxy glass epoxy glass epoxy glass-reinforced-plastic (grp). glass-reinforced-plastic (grp). glass-epoxy glass-plastic glass-plastic glass-textile glass-epoxy	Tennyson et al (1978) Hashin (1980) Hashin (1980) Azzl and Tsai (1965) Ikegami et al (1982) Hütter et al (1974) Greenwood Meshkov et al (1982) Skudra and Bulavs (1982) Jones (1969) Maksimov et al (1979) Puck and Schneider (1969)
GRAPHITE- EPOXY	graphite epoxy AS/3501-5A Morganite II graphite-epoxy graphite-epoxy SP-288T300 (3M) CFRP graphite + thornel graphite epoxy T300/1034 graphite epoxy fabric NARMCO 5208-WT300	Kim Wu (1974a) Tsai-Wu (1971) Tennyson et al (1978, 1981) Ikegami et al (1983) Guess (1980) Francis et al (1979) Tennyson and Wharram (1985)
KEVLAR	kevlar-reinforced plastic kevlar + organic fibre	Ikegami et al (1983) Guess (1980)
ORGANIC	organic fibre + textile hybrid glass + organic fibre and textile	Maksimov et al (1979) Sokolov (1979)
SILICIUM- EPOXY	silicium-epoxy	Pabiot (1970)

## LIST OF TESTED MATERIALS IN THE LITERATURE (CONT'D)

TYPE OF MATERIAL	IDENTIFICATION	REFERENCE
WOOD	pine paperboard paper	Cowin (1979) Suhling et al (1985) de Ruvo et al (1980)
POLY-CARBONATE	polycarbonate	Raghava (1974)
BONES	bones	Cowin (1979)
GRAPHITE	graphite AGOT type G graphite	Huang (1985) Franklin (1968)
PARTICULATE	graphite particulate JT-50	Wang (1968) Chamis (1969)
WOVEN FABRIC	fabric (weave + woven) + polyester resin woven fiberglass fiberglass cloth + epoxy	Owen and Rice (1981) Owen and Griffiths (1978) Plume and Maksimov (1978) Sokolov et al (1978) Griffith and Baldwin (1962)

## APPENDIX II.

MATHEMATICAL RELATIONSHIPS BETWEEN BUDIANSKY'S  
CRITERION AND THE NEW PARAMETRIC FAILURE CRITERION

From the strength of materials stress transformation laws, it is known (Popov, 1976) that the principal stresses of a plane stress system are given by

$$\begin{aligned}\sigma_p &= \frac{\sigma_1 + \sigma_2}{2} + \left[ \left( \frac{\sigma_1 - \sigma_2}{2} \right)^2 + \tau_{12}^2 \right]^{\frac{1}{2}} \\ \sigma_q &= \frac{\sigma_1 + \sigma_2}{2} - \left[ \left( \frac{\sigma_1 - \sigma_2}{2} \right)^2 + \tau_{12}^2 \right]^{\frac{1}{2}}\end{aligned}\quad (II-1)$$

The values of the stresses  $\sigma_1$ ,  $\sigma_2$ ,  $\tau_{12}$  can be expressed as a function of the new three-dimensional parametric failure equation

$$\begin{aligned}\sigma_1 &= \rho(\alpha, \phi) \cos \alpha \sin \phi \\ \sigma_2 &= \rho(\alpha, \phi) \sin \alpha \sin \phi \\ \tau_{12} &= \rho(\alpha, \phi) \cos \phi\end{aligned}\quad (4-3)$$

Substituting Equations (4-3) and (II-1) into Budiansky's criterion, Equations (4-1), it is found that

$$\begin{aligned}g(\beta) \cos \beta &= \frac{\rho(\alpha, \phi) \sin \phi (\cos \alpha + \sin \alpha)}{2 \sigma_{bt}} \\ g(\beta) \sin \beta &= - \frac{\rho(\alpha, \phi)}{\sigma_s} \sqrt{\frac{\sin^2 \phi (\cos \alpha - \sin \alpha)^2}{4} + \cos^2 \phi}\end{aligned}\quad (II-2)$$

Consequently, it can be shown that any isotropic function  $g(\beta)$  can be transformed into a  $\rho(\alpha, \phi)$  function. The transformation law is given by

$$\rho(\alpha, \phi) = g(\beta) \left[ \frac{\sin^2 \phi (\sin \alpha + \cos \alpha)^2}{4 \sigma_{bt}^2} + \frac{\sin^2 \phi (\cos \alpha - \sin \alpha)^2}{4 \sigma_s^2} + \frac{\cos^2 \phi}{\sigma_s^2} \right]^{-\frac{1}{2}}\quad (II-3)$$

where the value of the angle  $\beta$  is

$$\beta = \arctan \left( -\frac{\sigma_{bt}}{2\sigma_s} \right) \sqrt{\frac{\sin^2 \phi (\cos \alpha - \sin \alpha)^2 + 4 \cos^2 \phi}{\sin^2 \phi (\cos \alpha + \sin \alpha)^2}} \quad (II-4)$$

For example, the von Mises criterion can be written under Budiansky's parametric formulation as

$$\begin{aligned} g(\beta) &= 1 \\ \sigma_{bt} &= \chi \\ \sigma_s &= \chi/\sqrt{3} \end{aligned} \quad (II-5)$$

Substituting these values into (II-4), the von Mises criterion can now be written in the stress space  $\sigma_1 - \sigma_2 - \tau_{12}$  using the new failure criterion. This gives

$$\rho(\alpha, \phi) = \left[ \frac{\sin^2 \phi}{\chi^2} (1 - \sin \alpha \cos \alpha) + \frac{3 \cos^2 \phi}{\chi^2} \right]^{-\frac{1}{2}} \quad (II-6)$$

It was shown above that any function  $g(\beta)$  can be transformed into a function  $\rho(\alpha, \phi)$ . Any function  $\rho(\alpha, \phi)$  showing symmetry with respect to the planes  $\alpha = 45^\circ$  and  $\alpha = -45^\circ$  can in reverse be written into the form  $g(\beta)$  using the following transformation:

$$g(\beta) = \rho(\alpha, \phi) \left[ \frac{\sin^2 \phi (\sin \alpha + \cos \alpha)^2}{4 \sigma_{bt}^2} + \frac{\sin^2 \phi (\cos \alpha - \sin \alpha)^2}{4 \sigma_s^2} + \frac{\cos^2 \phi}{\sigma_s^2} \right]^{\frac{1}{2}} \quad (II-7)$$

$$\begin{aligned} \text{where } \sigma_{bt} &= \rho(45, 90) \\ \sigma_s &= \rho(-45, 90) \end{aligned} \quad (II-8)$$

# APPENDIX III

## SUMMARY OF EXAMPLES

### EXAMPLE 1

- Graphite Grade AGOT
- Ref.: Huang (1985)
- Original solution: Gol'denblat and Kopnov (Eq.(3-34), Fig. 5.2)
- Results in plane  $\tau_{12} = 0$  only (Table 5.1)

#### First Parametric Solution (Fig. 5.3)

##### Hypothesis:

- a) With data in plane  $\tau_{12} = 0$  only, use Eq. (4-23) with  $\Gamma(0) = 1$
- b) Use a function of  $\sin \alpha$ ,  $\cos \alpha$ , ..., etc.
- c) Fit the points  $X, X', Y, Y'$
- d) Fit the curve at  $\rho(-45, 90)$

##### Parametric failure envelope

(Eq. (5-6)):

$$\begin{aligned} \psi(\alpha) = & P_1 \cos \alpha + P_2 \sin \alpha \\ & + P_3 \cos^2 \alpha + P_4 \sin^2 \alpha \\ & + P_5 \sin \alpha \cos \alpha \end{aligned}$$

#### Second Parametric Solution (Fig. 5.4)

##### Hypothesis: (a), (b), (c) above

- d) Fit each quadrant with a different function  $\psi(\alpha)$

##### Parametric failure envelope

(Eq. (5-9)):

$$\psi(\alpha) = P |\cos \alpha|^{\xi} + R |\sin \alpha|^{\xi}$$

---

**EXAMPLE 2**


---

- Graphite epoxy fabric

- Ref.: Tennyson

and Wharram (1985)

- Original solution: Cubic tensor polynomial (Eq.(3-53), Fig. 5.5)

- Results: (Table 5.2)

First Parametric Solution (Fig. 5.6)

Hypothesis:

a) With  $X = X'$  and  $Y = Y'$ , use normalized coordinate systems

b) One failure point per shear level, then assume a circular failure envelope centered on  $\tau_{12}$ -axis at each shear level. Use cylindrical coordinate (Eq.(4-23)).

c) Use Eq.(5-27), special case of Eq.(5-23)

$$T(\alpha, \tau_{12}/S) = \psi(\alpha') \Gamma(\phi')$$

$$\psi(\alpha') = 1.0 \quad \text{for a circle}$$

$$\Gamma(0^\circ) = 1.0$$

$$\Gamma(90^\circ) = 1.0$$

$$\Gamma(\phi') > 1.0 \quad \text{to fit all data}$$

d) Write eq. symmetrical w.r. to

$$\tau_{12} = 0 \text{ plane}$$

Parametric failure envelope

(Eq.(5-29))

$$\Gamma(\phi') = 1.0 + P(\sin \phi' \cos \phi')^2$$

with  $P$  = best-fit value of data.

---

Second Parametric Solution (Fig. 5.7)

Hypothesis: (a) above

b) Use spherical coordinate

Equation (4-15)

$$c) \rho'(\alpha', 90) = \rho'(\alpha', 0) = 1.0$$

Parametric failure envelope

Equation (5-41)

$$\rho'(\alpha', \phi') = 1.0 + f(\alpha') \sin \phi' |\cos \phi'|$$

with  $f(\alpha')$  an equation to fit experimental data (see Eq.(5-36) to (5-40) for development)

EXAMPLE 3

- Paperboard
- Ref.: Rowlands et al. (1985)
- Original solutions: Quadratic tensor polynomial (Eq.(3-39)), Norris theory (Eq.(3-15)), Tsai-Hill theory (Eq.(3-14))
- Results in four  $\tau_{12}$  planes (Table 5.3)

Parametric Solution (Fig. 5.12)

Hypothesis:

a) Same shape of failure surface at all shear levels, then use cylindrical coordinates, Equation (4-20)

b) Norris failure criterion = good at  $\tau_{12} = 0$ 

c) Use Equation (4-30)

$$\tau_{12}(\alpha, \tau_{12}) = \psi(\alpha) \Gamma(\tau_{12})$$

with  $\psi(\alpha)$  = Norris criterion at  $\tau_{12} = 0$   
and  $\Gamma(\tau_{12})$  = linear equation to best-fit experimental results (see Eq.(5-43) to (5-46) for development)

Parametric failure envelope:  
(see Eq.(5-47))

---

**EXAMPLE 4**


---

- Carbon-epoxy
- Ref.: Ikegami and Takahashi (1983)
- Original solutions: Quadratic tensor polynomial (Eq.(3-39)), Hoffman's theory (Eq.(3-23))
- Results in Tables 5.9 and 5.10 include angle-ply laminates in uniaxial tension

Parametric Solution (Fig. 5.16)
Hypothesis:

- a) Keep quadratic tensor polynomial in planes  $\tau_{12} = 0$ ,  $\sigma_1 = 0$ ,  $\sigma_2 = 0$
- b) Modify tensor polynomial where needed ( $-14^\circ < \alpha < 0^\circ$ ) for improved correlation.

Add  $f(\alpha, \phi)$  to  $f_2(\alpha, \phi)$  in Eq.(4-12)

- c)  $f(0^\circ, \phi) = f(90^\circ, \phi) = f(\alpha, 90^\circ) = f(-14^\circ, \phi) = 0$

Parametric failure envelope: as in

$$(b) \text{ with } f(\alpha, \phi) = g(\alpha, \phi) \cos \alpha \sin \alpha \cdot \cos \phi \sin \phi$$

$$\text{where } g(\alpha, \phi) = A \cos^2 \alpha + B \sin^2 \alpha + C \sin \alpha \cos \alpha$$

and A, B, C are chosen to fit experimental data.

---



## APPENDIX IV

## DEVELOPMENT OF EQUATION (5-58)

Assuming that a general failure surface satisfying all conditions in Chapter 4 is given by the following

$$\rho(\alpha, \phi) = \sum_{m,n} B_{mn} f(n\alpha) g(m\phi) \quad (IV-1)$$

the equations  $f(n\alpha)$  and  $g(m\phi)$  must be found. One of Equations (4-7) requires that

$$\rho(\alpha, 180^\circ) = \rho(\alpha, \phi) \quad (4-7)$$

to provide symmetry with respect to the plane  $\tau_{12} = 0$ . Substituting in Equation (IV-1), the following is found:

$$g(\phi) = g(180^\circ - \phi) \quad (IV-2)$$

Possible functions satisfying this equality are

$$g(\phi) = \sin (2m-1) \phi \quad m > 1 \quad (IV-3)$$

$$g(\phi) = \cos^{2m} m\phi \quad m > 1 \quad (IV-4)$$

Of these, only Equation (IV-3) satisfies the condition that

$$g(\phi) \neq g(-\phi) \quad (IV-5)$$

The second of Equations (4-7) now has to be satisfied

$$\rho(\alpha+180^\circ, -\phi) = \rho(\alpha, \phi) \quad (4-7)$$

Combining this with Equations (IV-1) and (IV-3), it is found that

$$f(\alpha) = -f(\alpha+180^\circ)$$

$$(IV-6)$$

The following equation satisfies this requirement

$$f(\alpha) = \sin (2n-1) \alpha \quad n > 1 \quad (IV-7)$$

Equation (IV-1) then becomes

$$\rho(\alpha, \phi) = \sum_m \sum_n B_{mn} \sin [(2n-1)\alpha] \sin [(2m-1)\phi] \quad (5-58)$$